UC SESM 71-22

STRUCTURES AND MATERIALS RESEARCH
DEPARTMENT OF CIVIL ENGINEERING

LARGE DISPLACEMENT ANALYSIS OF SHELLS OF REVOLUTION INCLUDING CREEP, PLASTICITY AND VISCOELASTICITY

by

PER K. LARSEN

Report to:

Royal Norwegian Council for Scientific and Industrial Research

DECEMBER 1971

STRUCTURAL ENGINEERING LABORATORY
UNIVERSITY OF CALIFORNIA
BERKELEY CALIFORNIA

STRUCTURES AND MATERIAL RESEARCH
DEPARTMENT OF CIVIL ENGINEERING

REPORT NO. UCSESM 71-22

LARGE DISPLACEMENT ANALYSIS OF SHELLS OF REVOLUTION, INCLUDING CREEP, PLASTICITY AND VISCOELASTICITY

By

Per K. Larsen

Dissertation Committee:

E. P. Popov
E. L. Wilson
Professors of Civil Engineering

I. Finnie
Professor of Mechanical Engineering

Report To

Royal Norwegian Council for Scientific and Industrial Research

STRUCTURAL ENGINEERING LABORATORY
UNIVERSITY OF CALIFORNIA
BERKELEY, CALIFORNIA

December 1971

ABSTRACT

An incremental variational formulation for the nonlinear finite element analysis of time dependent deformations in solids is developed. Both material and geometrical nonlinearities are considered. The material nonlinearities are due to creep and plasticity, and the geometrical one is caused by large displacements resulting from finite rotations. The time dependence is due to creep in metals and viscoelasticity in polymeric materials.

The incremental equilibrium equations are derived in the Lagrangian mode of description using the virtual work principle. The resulting equations are linearized and solved by a step-forward integration procedure. For added accuracy an equilibrium check is made at each step, and the unbalanced force is added to the next load increment. Based on monitoring of the positive definiteness of the system stiffness matrix, a capability of postbuckling analysis of shells is developed.

Basic constitutive relations for creep and plasticity are reviewed, and the theory of viscoplasticity is extended to the case of large displacements in order to account for the effect of creep deformations on the strain hardening. In the plastic range the appropriate load criterion is obtained using von Mises yield condition assuming isotropic hardening. In the theory of finite linear viscoelasticity an approximate solution is formulated using Prony series expansion for the relaxation modulus.

Based on this formulation a finite element program was written for the analysis of large axisymmetric deformations of shells of revolution. Shell elements including shear deformations were used, which makes the program applicable to the analysis of both thin and moderately thick shells. Several numerical examples are presented to show the capabilities and accuracy of the formulation. The examples include the snap-through analysis of shallow elastic shells, and large displacement analyses of torispherical pressure vessels subjected to creep and plasticity. Creep buckling of columns and shallow shells, as well as viscoelastic buckling of shells, is investigated.

ACKNOWLEDGEMENTS

I wish to express my deepest gratitude to my research advisor, Professor E. P. Popov, for his supervision and continuous encouragement throughout the course of this work. I am also very grateful to the other members of my thesis committee, Professors E. L. Wilson and I. Finnie, for interesting discussions and for reading the manuscript. In addition, I will acknowledge the advice from Professor R. L. Taylor, Drs. S. Yaghmai, P. Sharifi, and P. Bergan.

The study leading to this work was supported by a NATO Science Fellowship, and a fellowship from the Royal Norwegian Council for Scientific and Industrial Research. The computer time and facilities were provided by the Computer Center of the University of California, Berkeley.

The work described here would not have been possible without the support of my wife Eva and daughter Tone. Their continued encouragement and cheer are gratefully acknowledged.

TABLE OF CONTENTS

ABSTRACT i

ACKNOWLEDGEMENTS iii

TABLE OF CONTENTS iv

NOMENCLATURE vii

1. INTRODUCTION 1

1.1 General Remarks 1
1.2 Survey of Existing Literature 2
1.3 Objective of Present Study 5

2. LARGE DEFORMATION OF CONTINUA 7

2.1 Description of Motion 7
2.2 Kinematics of Deformation 8
2.3 Stress Measures 15
2.4 Stress and Strain Rates 19
2.5 Virtual Work in Finite Deformations 20
2.6 Traction Boundary Conditions 27

2.6.1 Conservative Loading 28
2.6.2 Nonconservative Loading 29
2.6.3 Residual Load Method 31

2.7 Incremental Constitutive Relations in Elasticity. 33
2.8 Variational Methods and Virtual Work in the Theory of Creep and Plasticity 35

2.8.1 Review 35
2.8.2 Modification of the Incremental Equilibrium Equations 38

3. CONSTITUTIVE RELATIONS FOR CREEP AND PLASTICITY IN METALS 41

3.1 Introduction 41
3.2 Kinematic Decomposition of Finite Inelastic Deformations 44
3.3 Uniaxial Creep Theories 48
3.4 Flow Theory for Creep and Plasticity 50
3.5 Yield Function and Loading Criterion 56
3.6 Incremental Stress-Strain Relations 59
3.7 Odquist's Creep Theory 63
3.8 Generalized Plane Stress 66
3.9 Some Remarks on the Creep-Plasticity Interaction. 67

TABLE OF CONTENTS (CONTINUED)

4. AN APPROXIMATE SOLUTION TO PROBLEMS IN FINITE LINEAR VISCOELASTICITY 71

4.1 Constitutive Relations for Linear and Finite Linear Viscoelasticity 71
4.2 Method of Solution 76
4.3 Some Remarks on the Sources of Errors in the Solution 82

5. ANALYSIS OF NONLINEAR PROBLEMS 85

5.1 Characterization of the Nonlinear Problem 85
5.2 Numerical Solution Methods for Nonlinear Systems . 86
5.3 Postbuckling Analysis of Structures 93
5.4 Determination of Step Size for Time Integration . 98
5.5 Linearized Incremental Equilibrium Equations . . . 100
5.6 Numerical Examples of Solution Method 104
5.7 Some Comments on the Residual Load Method 106

6. FINITE ELEMENT FORMULATION OF THE NONLINEAR PROBLEM . . 112

6.1 Isoparametric Finite Elements 113
6.2 Degenerate Isoparametric Shell Elements 116

6.2.1 Geometric Representation 117
6.2.2 Displacement Field 118

6.3 Strain-Displacement Relations 121
6.4 Element Stiffness Matrices 126

6.4.1 Incremental Element Stiffness Matrix . . . 127
6.4.2 Geometric Stiffness Matrix 128

6.5 Consistent Nodal Forces 130

6.5.1 Equilibrium Nodal Forces 130
6.5.2 Creep Pseudo Loading 130
6.5.3 Traction Type Loading 131

7. NUMERICAL EXAMPLES 134

7.1 Description of Computer Programs 134
7.2 Finite Displacements of Elastic Structures 137

7.2.1 External Pressure on Torus 137
7.2.2 Postbuckling Behavior of Shallow Spherical Shell 138

7.3 Large Creep Deformations in Pressure Vessel . . . 145
7.4 Elastic-Plastic Analysis of Pressure Vessel . . . 152

TABLE OF CONTENTS (CONTINUED)

7.5 Creep Buckling Problems 154

7.5.1 Creep Buckling of Imperfect Column 154
7.5.2 Creep Buckling of Shallow Spherical Shell . 160

7.6 Viscoelastic Problems 164

7.6.1 Identification of Material Parameters . . . 164
7.6.2 Viscoelastic Creep Buckling of Shallow Spherical Shell 168

8. SUMMARY AND CONCLUSIONS 174

9. REFERENCES 178

APPENDIX A: INTERPOLATION POLYNOMIALS 188

APPENDIX B: DERIVATION OF DISPLACEMENT GRADIENTS 189

NOMENCLATURE

All symbols are defined when they first appear. The symbols that are introduced in some sections but which are not referred to later are not included. Some symbols may have two meanings in different sections; these are clearly defined when used. Both Greek and Latin indices range from 1 to 3, unless otherwise noted.

In Chapter 2, $\underset{\sim}{F}$ and $\underset{\sim}{u}$ represent the complete tensor and vector, with base vectors included. In other chapters the same symbol is used to denote the matrix or vector of tensor and vector components.

${}^1A$	Stored energy per unit mass in $\mathcal{B}_1$
A_{IJKL}	Strain transformation matrix, Eq. (3.53)
dA, da, $d\bar{a}$	Infinitesimal areas in $\mathcal{B}_0, \mathcal{B}_1$ and $\mathcal{B}_2$ respectively
$\mathcal{B}_0$ $\mathcal{B}_1$ $\mathcal{B}_2$	Initial configuration, and configuration 1 and 2 respectively.
$\partial\mathcal{B}_0$ $\partial\mathcal{B}_1$ $\partial\mathcal{B}_2$	Areas of $\mathcal{B}_0, \mathcal{B}_1, \mathcal{B}_2$ with prescribed tractions
C_{IJKL}, C^{IJKL}	Stress-strain transformation tensor.
$\underset{\sim}{C}$	Right Cauchy-Green deformation tensor.
${}^1\underset{\sim}{D}$	Rate-of-deformation tensor in $\mathcal{B}_1$
$\underset{\sim}{D}^E$, $\underset{\sim}{D}^I$	Elastic and inelastic part of $\underset{\sim}{D}$, see Eq. (3.6).
E, E_t	Young's modulus and tangent modulus
E_{IJKL}	Components of Hooke's generalized law
${}^1E_{IJ}$, ${}^2E_{IJ}$, E_{IJ}	Lagrangian strain in $\mathcal{B}_1, \mathcal{B}_2$ and increment of Lagrangian strain between $\mathcal{B}_1$ and $\mathcal{B}_2$ respectively.
${}^1\dot{E}_{IJ}$, ${}^2\dot{E}_{IJ}$	Lagrangian strain rates in $\mathcal{B}_1$ and $\mathcal{B}_2$

$^{1}\dot{E}^{E}_{IJ}$, $^{1}\dot{E}^{P}_{IJ}$, $^{1}\dot{E}^{C}_{IJ}$	Elastic, plastic and creep strain rates in $\mathcal{B}_1$
E^{IC}_{IJ}	Instantaneous creep strain increment, Eq. (3.64)
E^{TC}_{IJ}	Transient creep strain increment, Eq. (3.65)
e_{IJ}	Linear part of E_{IJ}
$\hat{e}_{IJ}$, $\hat{\hat{e}}_{IJ}$	Components of e_{IJ}, Eq. (2.50b)
$^{1}F^{i}_{.I}$, $F^{\alpha}_{.i}$	Deformation gradient in $\mathcal{B}_1$, and in $\mathcal{B}_2$ relative to $\mathcal{B}_1$, respectively.
$\underset{\sim}{F}^{E}$, $\underset{\sim}{F}^{I}$	Elastic and inelastic part of $\underset{\sim}{F}$, respectively Eq. (3.4).
F_{IJKL}	Strain transformation tensor, Eq. (3.54).
$^{1}\underset{\sim}{f}$, $^{2}\underset{\sim}{f}$	Body force vectors in $\mathcal{B}_1$ and $\mathcal{B}_2$ respectively.
f	Yield surface
G	Shear modulus
G_1, G_2	Shear and bulk relaxation modulus, respectively
G^{i}_{1}, G^{i}_{2}	Discrete relaxation moduli
G_{ijkl}, G_{IJKL}	Integrating (relaxation) functions
$\underset{\sim}{G}_I$, $\underset{\sim}{g}_i$, $\underset{\sim}{\bar{g}}_\alpha$	Base vectors in $\mathcal{B}_0$, $\mathcal{B}_1$ and $\mathcal{B}_2$, respectively
g	Plastic potential
g_i	As defined in section 4.2.
H_{IJKL}	Stress-strain transformation tensor, Eq. (3.57)
H_c, H_p	Creep and plastic hardening functions.
h	As defined in section 3.6.
h_i	Shell thickness at node i; and as defined in section 4.2.

$\underset{\sim}{N}$, $\underset{\sim}{n}$, $\underset{\sim}{\bar{n}}$	Normal vector in $\mathcal{B}_0$, $\mathcal{B}_1$ and $\mathcal{B}_2$, respectively.
${}^1p$, ${}^2p$, p	Normal pressure in $\mathcal{B}_1$ and $\mathcal{B}_2$, and incremental pressure between $\mathcal{B}_1$ and $\mathcal{B}_2$.
q_i	Internal variables.
$\underset{\sim}{R}$	Rotation tensor
R	Generalized load
r	Generalized displacement; and radius
s	Local curvelinear coordinate
${}^1S^{IJ}$, ${}^2S^{IJ}$, S^{IJ}	2nd Piola-Kirchhoff stress tensor in $\mathcal{B}_1$ and $\mathcal{B}_2$, and increment between $\mathcal{B}_1$ and $\mathcal{B}_2$, respectively.
${}^1\dot{S}^{IJ}$, ${}^2\dot{S}^{IJ}$	Rates of 2nd P-K stress in $\mathcal{B}_1$ and $\mathcal{B}_2$
S_C^{IC}, S_{IJ}^{C}	Delayed (creep) increment of P-K stress between $\mathcal{B}_1$ and $\mathcal{B}_2$
$\bar{S}^{IJ}$	Deviatoric component of S^{IJ}
${}^1T^{ij}$, ${}^2T^{\alpha\beta}$	Cauchy stress in $\mathcal{B}_1$ and $\mathcal{B}_2$, respectively.
${}^0\underset{\sim}{t}$, ${}^1\underset{\sim}{t}$, ${}^2\underset{\sim}{t}$	Traction vectors in $\mathcal{B}_0$, $\mathcal{B}_1$ and $\mathcal{B}_2$
t	Local coordinate; time
$\underset{\sim}{U}$	Stretch tensor
${}^1\underset{\sim}{u}$, ${}^2\underset{\sim}{u}$, $\underset{\sim}{u}$	Displacement vector to $\mathcal{B}_1$ and $\mathcal{B}_2$ from $\mathcal{B}_0$, and from $\mathcal{B}_1$ to $\mathcal{B}_2$, Fig. 2.1.
$\underset{\sim}{u}^E$, $\underset{\sim}{u}^I$	Elastic and inelastic displacement vector, Fig. 3.2.
u_i	Horizontal displacement at node i
δW_1, δW_2	Virtual work in $\mathcal{B}_1$ and $\mathcal{B}_2$
W_c, W_p	Creep and plastic work

w_i	Vertical displacement at node i
X^I, x^i, $\bar{x}^\alpha$	Coordinates of material point in $\mathcal{B}_0, \mathcal{B}_1, \mathcal{B}_2$
α_i	Rotation of normal at node i
β	Defined in Section 6.2.2.
δ	Virtual variation
δ^I_J, δ^i_j	Kronecker delta
$\partial_{\underset{\sim}{X}}\cdot$, $\cdot\partial_{\underset{\sim}{X}}$	Right and left divergence operator
ϵ_{ij}	Eulerian strain in $\mathcal{B}_1$
$\bar{\epsilon}$, $\bar{\epsilon}_p$, ϵ_c	Equivalent strain; equivalent plastic and creep strain.
ξ	Defined in section 3.6.
η	Local coordinate, Fig. 6.3.
η_{IJ}	Nonlinear part of E_{IJ}
θ	Circumferential coordinate for shell
θ_i	Angle at node i, see Fig. 6.3.
κ_c, κ_p	Creep and plastic hardening parameter
$\mathcal{H}$	Hardening parameter
λ	Lame constant
$\dot{\lambda}$, $d\lambda$	Proportionality factors in Chapter 3.
λ_i	Discrete relaxation time in Chapter 4.
μ	Lame constant
ν	Poisson's ratio
ξ	Local coordinate, Fig. 6.3.
$\rho_0, \rho, \bar{\rho}$	Mass density in $\mathcal{B}_0, \mathcal{B}_1$ and $\mathcal{B}_2$
ρ	Load proportionality factor in Chapter 5.
$\bar{\sigma}$	Equivalent stress

ϕ_i	Meridional angle at node i, Fig. 6.3.
Φ	Creep potential
$\varphi_i(\xi,\eta), \varphi_i(\xi)$	Interpolation polynomials
ψ_{ij}, ψ_{IJ}	Tensor valued functional
[ ]	Matrix
{ }	Column vector
< >	Row vector
[B]	Transformation matrix between displacement gradients and displacements.
$[B_1]$, $[B_2]$	Components of [B]
$\langle b_i \rangle_j$	Row vector of $[B_1]$ or $[B_2]$
[D]	Transformed stress-strain matrix
$[D_1]$, $[D_2]$, $[D_3]$	Integrated forms of [D]
$[H_{ij}]$	Defined in section 6.4.2.
[J]	Jacobian matrix; Appendix B
[K]	Stiffness matrix
$[K_A]$	Augmented stiffness matrix
$[K_o]$	Incremental stiffness matrix
$[K_1]$, $[K_2]$	Nonlinear stiffness matrices
$[K_3]$	Stiffness matrix due to nonconservative loading
$[K_G]$	Geometric stiffness matrix
$\{M_0\}, \{M_1\}, \{M_2\}$	As defined in Eq. (6.29)
$\{N_0\}, \{N_1\}$	As defined in section 6.5.
$\{Q_0\}, \{Q_1\}$	As defined in section 6.5.
{r}	Vector of nodal point global coordinates; and vector of generalized displacements.

$\{u\}$	Vector of radial displacements
$\{u_\partial\}$	Vector of displacement gradients
$\{w\}$	Vector of vertical displacements
$\{z\}$	Vector of nodal point global coordinates
$[\Gamma_{jk}]_i$	As defined in section 6.3.
$[\Lambda]$	Transformation matrix defined by Eq. (6.15)
$[\pi_{jk}]_i$	As defined in section 6.3.
$[\varphi]$, $[\varphi_u]$	Matrices of interpolation polynomials, see Chapter 6.
$[\Omega_{jk}]_i$	As defined in section 6.3.

1. INTRODUCTION

1.1 General Remarks

Shells of revolution play an important role in numerous technical and industrial applications. Structural components of this type can be found in aerospace structures, deep-submersible vessels, piping systems and as superstructures in the building industry. In recent years their use in nuclear power plants has become increasingly important, and they have found wide use as containers for transport of liquefied gasses, etc.

New design philosophies have emerged over the last decades employing design concepts based on ultimate strength, shake-down loads, and factors of safety. This trend together with the increased requirements for economic and optimum design necessitate the consideration of both geometrical and physical nonlinearities in the analysis procedures. The ever increasing stress levels in modern structures, and the more severe environment in which they serve impose greater challenges on the analyst.

High temperature creep and elastic-plastic deformations are of major importance in pressure vessels for nuclear power generators, and creep problem may become even more important in future fusion-type reactors. Creep must also be considered in certain aerospace applications. The introduction of new and exotic materials and the increasing use of high polymers as structural materials necessitate that creep problems be considered also at moderate stress levels and temperatures.

Recent advances in continuum mechanics and the development of powerful computer methods make the analysis of this class of problems feasible, and extensive research is being done in this area.

1.2 Survey of Existing Literature

The classical field theories for nonlinear problems have been formulated by Green et al [1, 2] and Truesdell et al [3, 4]. However, the complexity of these theories is such that only some very simple cases can be solved in closed form. The use of the computer and the new numerical methods allows a wider class of problems to be analyzed.

At first, researchers were mostly concerned with the solution of the governing differential equations by finite difference methods. The development of the finite element method, however, provided the analysts with a new and efficient tool for solving nonlinear boundary value problems. Variational methods have been the basis for a great number of papers on nonlinear problems over the last fifteen years.

In the following a brief survey of some of the literature in this field is made. This survey is not intended to be all inclusive, and only a few of the most important references are included in the compilation.

The first attempt at solving nonlinear problems by the finite element method was made by Turner et al [5]. The terms geometric stiffness or initial stress stiffness were introduced to account for the geometric effects. Martin [6] and Gallagher and Padlog [7] studied stability problems for beam columns. Argyris considered linearized stability problems and large

displacement problems [8-11]. The nonlinear behavior of structural members such as truss bars, beams, frames, plates and shells were investigated in a number of studies [12-20]. Energy principles and concepts from continuum mechanics were used by Oden [21-25]. Conjugate stress and strain measures were employed by Felippa [30] and Marcal [26-29], and a very rigorous treatment of the incremental equilibrium equations was given by Yaghmai [31].

The energy methods are not restricted to finite element formulations, and have been applied to finite difference solutions for nonlinear shell problems by Bushnell and Almroth [32].

The finite element method was used extensively in the analysis of inelastic problems during the same period. Important contributions were made by Argyris [8], Popov et al [33], Khojasteh-Bakht [34], Marcal [35] and Zienkiewicz [36]. Combined geometrical and material nonlinearities were considered by Marcal [27], Yaghmai [31], Armen et al [37] and Zudans [38].

Classical closed form solutions for infinitesimal creep problems are given by Odquist and Hult [39], Finnie and Heller [40], Hult [41] and Rabotnov [42]. Constitutive relations for creep and creep rupture are discussed in reference [43]. Numerical solutions for more complicated creep problems were introduced by Wahl [44], Mendelson et al [45] and Lin [46].

Early applications of the finite element method to creep problems were given by King [47] and Selna [48] for concrete dams and frames respectively. Linear viscoelastic problems have later been investigated by a number of authors [49-51], and

creep in metal structures are considered in references [52, 53].

When considering creep in structures with large displacements distinction must be made between stability problems and buckling problems. In stability problems the structure is perturbed from a stable configuration, and is then considered unstable if the perturbation increases with time. The buckling problem, however, is concerned with structures with initial displacements or external loads. The former approach has been used extensively by Rabotnov and Shesterikov [54], and the latter one by Hoff [55, 56]. Solutions to the creep buckling problem in columns and flat arches are given in references [57, 58, 59].

Creep buckling of shells subjected to primary or steady state creep has been studied by a number of investigators. Hoff, Jashman and Nachbar [60] studied steady state creep of cylindrical shells, discretizing the shell by the double membrane (or sandwich) model. Creep buckling of cylinders under bending was treated by a semiempirical method by Mathauser and Berkovits [61], and Stricklin, Hsu and Pian [62] studied the snap-through buckling of a shallow arch under a point load subjected to creep. Sander's variational principle and the finite difference method were used by Grigoliuk and Lipovtsev [63] for the analysis of shells of revolution with initial imperfections. The double membrane model was also used by Samuelson [64] in his study of cylinders with initial imperfections.

Creep buckling and large displacement analysis of shells and plates of linearly viscoelastic materials have received less attention. Using the Galerkin method Bychawski [65] obtained a

solution for cylindrical and spherical panels. Huang [66] applied the correspondence principle to the snap-through analysis of shallow spherical shells using finite differences to solve the governing equations. Finally an investigation of circular plates subjected to in-plane forces was made by DeLeeuw [67].

1.3 Objective of Present Study

The objective of the present investigation was the study of geometrical and material nonlinearities in shells of revolution under axisymmetric loads. More specifically this includes:

(i) Large displacement and postbuckling analysis of elastic and elastic-plastic shells.

(ii) Large displacement analysis of shells subjected to time-dependent effects, such as nonlinear creep and linear viscoelasticity.

(iii) Development of a constitutive theory capable of describing the coupling between nonlinear creep and instantaneous plasticity.

The study is restricted to quasi-static problems, and is based on the use of virtual work principles to obtain the total and incremental equilibrium equations. A Lagrangian formulation is used throughout the study.

By introducing the plane strain or the plane stress condition both axisymmetric shells and arches may be studied.

The discretized equilibrium equations are obtained using the finite element methods. Shear deformations are included through the use of the "degenerate" isoparametric family of elements.

2. LARGE DEFORMATION OF CONTINUA

2.1 Description of Motion

The motion of a body in general can be defined as a continuous sequence of configurations in Euclidean space and time. This motion can be described in a variety of modes, depending on which Euclidean space is chosen as a reference. The most common modes and their characteristics are [68].

i. Material description

ii. Reference description

iii. Spatial description

iv. Relative description (or current configuration as reference)

v. Convected description

Mode (i) uses the material particle in the body as the primitive quantity, while (ii) takes the material coordinates in a reference configuration as the primitive quantities. In most applications no distinction is made between the two, and they are both commonly denoted as the Lagrangian description. The spatial description, also called the Eulerian description, takes a point in space and time as primitives and observes material particles that pass through this point. The relative mode is a special variant of (ii), while the convected mode assigns fixed coordinates for the material points and describes the motion in terms of the deformation of the "body space".

The choice of mode of description for a particular problem is determined from a number of considerations. The most important

ones are the computational method used for solving the nonlinear field equations, and the constitutive theory describing the material. Modes (i), (ii) or (v) are the natural choice when dealing with elastic bodies, since the initial configuration is here of special importance. The relative mode has also been used for such problems, but is disadvantageous from a computational point of view. In problems associated with fluid flow, the spatial description is most commonly used.

For problems associated with plastic flow, creep flow, viscoelasticity, etc., the choice of mode of description is far from obvious. This is due to the variety of constitutive theories used for such problems. It should, however, be noted that the nonlinear equilibrium equations are most efficiently formulated and solved in the Lagrangian description. Even though the constitutive relations might be best formulated in an Eulerian description, the extra computational effort needed to transform these to a Lagrangian description is offset by the savings in formation and solution of the field equations.

In the present study, the Lagrangian description is chosen. In addition, an auxiliary convected coordinate system is introduced in order to facilitate certain coordinate transformations.

2.2 Kinematics of Deformation

In order to describe the kinematics of the system three configurations will be introduced. $\mathcal{B}_0$ denotes the initial configuration, $\mathcal{B}_1$ the current configuration, and $\mathcal{B}_2$ a neighboring configuration to $\mathcal{B}_1$, Fig. 2.1. Associated with $\mathcal{B}_0$ is given a fixed, orthogonal curvilinear coordinate system with coordinates

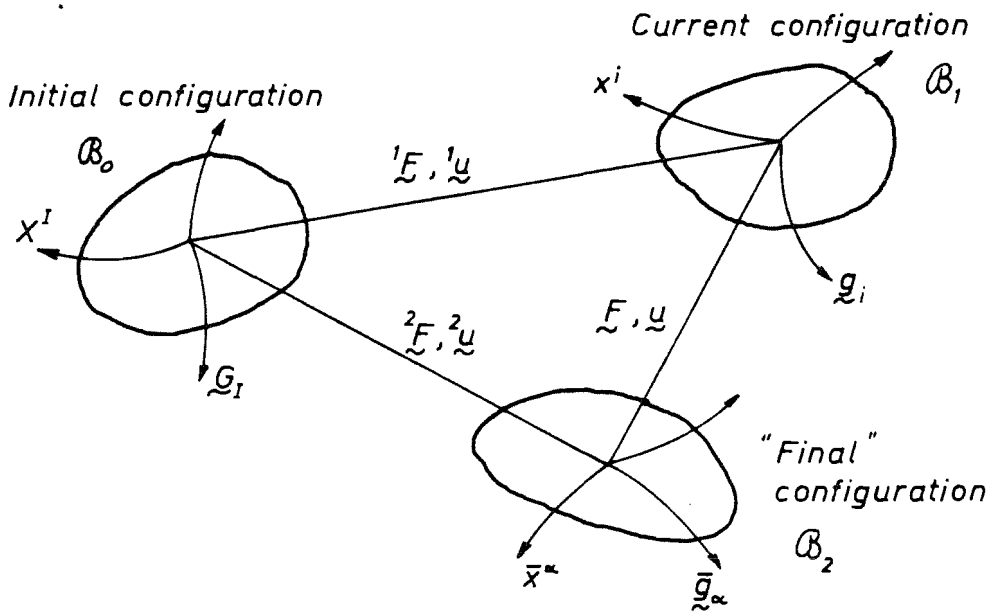

FIG. 2.1 DESCRIPTION OF MOTION.

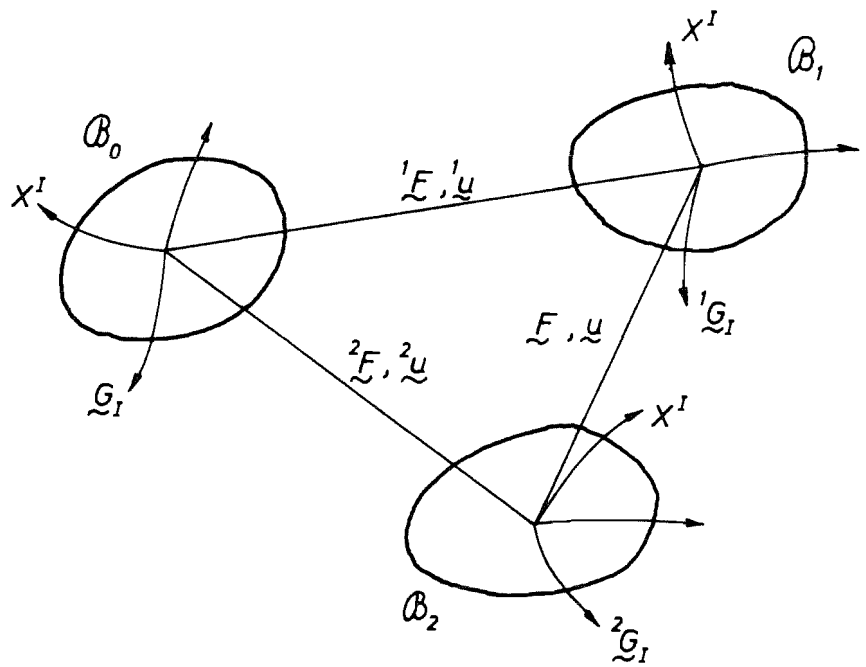

FIG. 2.2 CONVECTED COORDINATES.

$\bar{X}^I$ and base vectors $\underset{\sim}{G}_I$. Configuration $\mathcal{B}_1$ is described by the coordinates x^i and base vectors $\underset{\sim}{g}_i$, and $\mathcal{B}_2$ by $\bar{x}^\alpha$ and $\underset{\sim}{\bar{g}}_\alpha$. (All indecies have the range 1 to 3). The coordinates $\bar{X}^I$ will be assumed to be a global system in which the motion is described.

The motion of a particle with material coordinates $\bar{X}^I$ is given by:

$$x^i = \chi^i(\bar{X}^I, t) \tag{2.1}$$

where $\underset{\sim}{\chi}$ is a mapping function from $\mathcal{B}_0$, and the parameter t is time. This mapping function will take the value x^i in $\mathcal{B}_1$, and $\bar{x}^\alpha$ in $\mathcal{B}_2$, with reference to the base vectors in the respective spaces.

The structure of this mapping is given by

$$x^i = \chi^i(\bar{X}^I, t_1) = G^i_I \bar{X}^I + {}^1u^i = G^i_I(\bar{X}^I + {}^1u^I) \tag{2.2a}$$

$$\begin{aligned}\bar{x}^\alpha = \chi^\alpha(\bar{X}^I, t_2) &= G^\alpha_I \bar{X}^I + {}^2u^\alpha = G^\alpha_I(\bar{X}^I + {}^2u^I) \\ &= G^\alpha_I(\bar{X}^I + {}^1u^I + u^I) = g^\alpha_i x^i + u^\alpha\end{aligned} \tag{2.2b}$$

where the shifters are given by:

$$\begin{aligned}G^i_I &= \underset{\sim}{g}^i \cdot \underset{\sim}{G}_I \\ G^\alpha_I &= \underset{\sim}{\bar{g}}^\alpha \cdot \underset{\sim}{G}_I \\ g^\alpha_i &= \underset{\sim}{\bar{g}}^\alpha \cdot \underset{\sim}{g}_i\end{aligned} \tag{2.3}$$

In addition, an auxiliary convected coordinate system is introduced, Fig. 2.2. This system is defined such that it initially coincides with fixed system $\bar{X}^I$ and $\underset{\sim}{G}_I$. The coordinates

will remain X^I in both configuration $\mathcal{B}_1$ and $\mathcal{B}_2$, but the base vectors will be ${}^1\underset{\sim}{G}_I$ and ${}^2\underset{\sim}{G}_I$ in $\mathcal{B}_1$ and $\mathcal{B}_2$ respectively. This auxiliary system will simplify certain coordinate transformations, but it will not be used in the description of motion. The reason for this is that rate expressions become complicated in convected coordinates.

The relationship between the base vectors can be obtained by chain-rule of differentiation [69]

$$\begin{aligned} \underset{\sim}{G}_I &= \underset{\sim}{g}_i \, {}^1F^i_{\cdot I} \\ \underset{\sim}{G}_I &= \underset{\sim}{\bar{g}}_\alpha \, {}^2F^\alpha_{\cdot I} = \underset{\sim}{\bar{g}}_\alpha \, F^\alpha_{\cdot i} \, {}^1F^i_{\cdot I} \\ \underset{\sim}{g}_i &= \underset{\sim}{\bar{g}}_\alpha \, F^\alpha_{\cdot i} \end{aligned} \tag{2.4}$$

where ${}^2\underset{\sim}{F}$, ${}^1\underset{\sim}{F}$ and $\underset{\sim}{F}$ are the deformation gradient tensors between $\mathcal{B}_0$ and $\mathcal{B}_2$, $\mathcal{B}_0$ and $\mathcal{B}_1$, and $\mathcal{B}_1$ and $\mathcal{B}_2$ respectively, Fig. 2.1(*). The components of these two-point tensors are given by

$$\begin{aligned} {}^2F^\alpha_{\cdot I} &= \bar{x}^\alpha{}_{/I} = \bar{x}^\alpha{}_{/i} \, x^i{}_{/I} \\ {}^1F^i_{\cdot I} &= x^i{}_{/I} \\ F^\alpha_{\cdot i} &= \bar{x}^\alpha{}_{/i} \end{aligned} \tag{2.5}$$

The square of the length of a line element in the three configurations is

$$\begin{aligned} ({}^0ds)^2 &= G_{IJ} \, dX^I dX^J \\ ({}^1ds)^2 &= g_{ij} \, dx^i dx^j = {}^1G_{IJ} \, dX^I dX^J \\ ({}^2ds)^2 &= \bar{g}_{\alpha\beta} \, d\bar{x}^\alpha d\bar{x}^\beta = {}^2G_{IJ} \, dX^I dX^J \end{aligned} \tag{2.6}$$

(*) The complete tensor (including the base vectors) is denoted by $\underset{\sim}{F}$ while the matrix of the tensor components is written $[F]$. Similarly for vectors, $\underset{\sim}{x}$ and $\{x\}$.

Using Eqs. (2.6) the Green strain tensor is defined by

$$
\begin{aligned}
2\,{}^{2}E_{IJ} &= \bar{g}_{\alpha\beta}\,{}^{2}F^{\alpha}_{\cdot I}\,{}^{2}F^{\beta}_{\cdot J} - G_{IJ} = {}^{2}G_{IJ} - G_{IJ} \\
2\,{}^{1}E_{IJ} &= g_{ij}\,{}^{1}F^{i}_{\cdot I}\,{}^{1}F^{j}_{\cdot J} - G_{IJ} = {}^{1}G_{IJ} - G_{IJ} \\
2\,E_{IJ} &= \bar{g}_{\alpha\beta}\,{}^{2}F^{\alpha}_{\cdot I}\,{}^{2}F^{\beta}_{\cdot J} - g_{ij}\,{}^{1}F^{i}_{\cdot I}\,{}^{1}F^{j}_{\cdot J} = {}^{2}G_{IJ} - {}^{1}G_{IJ}
\end{aligned}
\tag{2.7}
$$

Here ${}^{2}E_{IJ}$, ${}^{1}E_{IJ}$ and E_{IJ} are the components of Green strain between $\mathcal{B}_0$ and $\mathcal{B}_2$, $\mathcal{B}_0$ and $\mathcal{B}_1$, and $\mathcal{B}_1$ and $\mathcal{B}_2$ respectively. All components are referred to base vectors in $\mathcal{B}_0$.

Note that the strain increment ϵ_{ij} between $\mathcal{B}_1$ and $\mathcal{B}_2$ referred to $\mathcal{B}_1$ is different from E_{IJ}

$$
\epsilon_{ij} = \bar{g}_{\alpha\beta}\,F^{\alpha}_{\cdot i}\,F^{\beta}_{\cdot j} - g_{ij} \tag{2.8}
$$

Noting that

$${}^{2}F^{\alpha}_{\cdot I} = F^{\alpha}_{\cdot i}\,{}^{1}F^{i}_{\cdot I}$$

one gets from Eq. (2.7c)

$$
E_{IJ} = {}^{1}F^{i}_{\cdot I}\,{}^{1}F^{j}_{\cdot J}\,\epsilon_{ij} \tag{2.9}
$$

or in rectangular Cartesian coordinates:

$$
E_{IJ} = \frac{\partial x_i}{\partial X_I}\,\frac{\partial x_j}{\partial X_J}\,\epsilon_{ij}
$$

In terms of the displacement increment $\underset{\sim}{u}$, the increment in Green strain is obtained from Eqs. (2.7a, b)

$$
2\,E_{IJ} = {}^{1}F^{K}_{\cdot I}\,u_{K|J} + {}^{1}F^{K}_{\cdot J}\,u_{K|I} + u^{K}{}_{|I}\,u_{K|J} \tag{2.10}
$$

When adding strain during the deformation one has the relationships

$$ {}^{2}E_{IJ} = {}^{1}E_{IJ} + E_{IJ} \tag{2.11} $$

or

$$ {}^{2}E_{IJ} = {}^{1}E_{IJ} + {}^{1}F^{i}_{\cdot I}\,{}^{1}F^{j}_{\cdot J}\,\epsilon_{ij} \tag{2.12} $$

For later use the physical components of the deformation gradient tensors in convected coordinates are given

$$ ({}^{1}F^{i}_{\cdot J})^{*} = \sqrt{\frac{g_{ii}}{G_{JJ}}}\,\frac{\partial x^{i}}{\partial X^{J}} = \sqrt{\frac{g_{ii}}{G_{JJ}}}\,\delta^{i}_{J} = \sqrt{{}^{1}G_{II}\,G^{JJ}} \tag{2.13} $$

where $( )^{*}$ indicates physical components. No sum implied.

In the discussion of constitutive theory the rate-of-deformation tensor $\underset{\sim}{D}$ will be needed. The distinction between the rate-of-deformation and Green strain rate arises from the fact that the former is referred to base vectors in the current configuration $\mathcal{B}_1$, while the latter is given relative to $\mathcal{B}_0$.

The velocity vector in Lagrangian description is

$$ \underset{\sim}{v} = \frac{d}{dt}\,\underset{\sim}{\chi}(\underset{\sim}{X}, t)\Big|_{\underset{\sim}{X}=\text{const.}} $$

In the spatial (Eulerian) description, the velocity is a primitive, and the spatial velocity gradient is given by [70]

$$ d\underset{\sim}{v} = {}^{1}\underset{\sim}{L}\cdot d\underset{\sim}{x} \tag{2.14} $$

or

$$dv^i = {}^1v^i{}_{/j}\, dx^j \tag{2.15}$$

where ${}^1\underset{\sim}{L}$ is the velocity gradient in configuration $\mathcal{B}_1$.

The non-symmetric velocity gradient can be decomposed into the symmetric rate-of-deformation tensor $\underset{\sim}{D}$ and the skew-symmetric spin tensor $\underset{\sim}{W}$

$$\begin{aligned} {}^1\underset{\sim}{D} &= \tfrac{1}{2}\left({}^1\underset{\sim}{L} + {}^1\underset{\sim}{L}^T\right) \\ {}^1\underset{\sim}{W} &= \tfrac{1}{2}\left({}^1\underset{\sim}{L} - {}^1\underset{\sim}{L}^T\right) \end{aligned} \tag{2.16}$$

The components of ${}^1\underset{\sim}{D}$ are given by

$${}^1D_{ij} = \tfrac{1}{2}\left({}^1v_{i/j} + {}^1v_{j/i}\right) = \tfrac{1}{2}\left({}^1u_{i/j} + {}^1u_{j/i}\right) \tag{2.17}$$

Following Malvern [69], it is found that

$$\frac{d}{dt}\left({}^1ds\right)^2 = 2\, d\underset{\sim}{x}\cdot{}^1\underset{\sim}{D}\cdot d\underset{\sim}{x} = 2\,{}^1D_{ij}\, dx^i dx^j \tag{2.18}$$

Using the definition of Green strain, one also has

$$\frac{d}{dt}\left({}^1ds^2 - {}^0ds^2\right) = \frac{d}{dt}\left({}^1ds^2\right) = 2\, d\underset{\sim}{X}\cdot{}^1\dot{\underset{\sim}{E}}\cdot d\underset{\sim}{X} \tag{2.19}$$

By further recalling the definition of the deformation gradient

$${}^1\dot{\underset{\sim}{E}} = {}^1\underset{\sim}{F}^T\cdot{}^1\underset{\sim}{D}\cdot{}^1\underset{\sim}{F}$$

or

$${}^1\dot{E}_{IJ} = {}^1F^i{}_I\,{}^1F^j{}_J\,{}^1D_{ij} \tag{2.20}$$

By restricting both the displacement increment $\underset{\sim}{u}$ and the time increment dt to be infinitesimal

$$\underset{\sim}{E} = {}^{1}\dot{\underset{\sim}{E}}\, dt = {}^{1}\underset{\sim}{F}^{T} \cdot ({}^{1}\underset{\sim}{D}\, dt) \cdot {}^{1}\underset{\sim}{F} \tag{2.21}$$

As can clearly be seen, the strain rate and the rate-of-deformation tensor coincide only when the displacement gradients are small compared to unity, i.e. ${}^{1}\underset{\sim}{F} \doteq \underset{\sim}{I}$. For finite deformation this is obviously not the case. In infinitesimal theory, however, this distinction is lost.

2.3 Stress Measures

The equilibrium equations in finite deformation are in general formulated in the deformed configuration. However, since the Green strain tensor is used to describe the kinematics of the system, a conjugate stress measure must be used. For this purpose the 2nd Piola-Kirchhoff stress tensor is introduced.

In configuration $\mathcal{B}_1$ the following definitions are used:

- ${}^{1}\underset{\sim}{T}$: Cauchy stress tensor in configuration $\mathcal{B}_1$. The components ${}^{1}T^{ij}$ are defined as force per unit area of the deformed configuration and referred to orthogonal base vectors in $\mathcal{B}_1$.
- ${}^{1}\underset{\sim}{S}$: Piola-Kirchhoff stress tensor in configuration $\mathcal{B}_1$. The components ${}^{1}S^{IJ}$ are defined as force in $\mathcal{B}_1$ per unit area in the reference configuration $\mathcal{B}_0$, and referred to base vectors in $\mathcal{B}_0$.

Note that the choice of $\mathcal{B}_0$ as a reference configuration is quite arbitrary, except for the fact that $\mathcal{B}_0$ is the basis for the Green strain tensor.

The Cauchy components ${}^1T^{ij}$ can be interpreted physically as the force acting on a unit area normal to base vector $\underset{\sim}{g}_i$ and in the direction of base vector $\underset{\sim}{g}_j$. For the components of ${}^1\underset{\sim}{S}$, however, no such interpretation is possible. They are merely defined by the fact that they are conjugate to the component of the Green strain tensor in an energy sense.

Using Cauchy's theorem, the stress tractions ${}^0\underset{\sim}{t}$ and ${}^1\underset{\sim}{t}$ in $\mathcal{B}_0$ and $\mathcal{B}_1$ respectively are given by, Fig. 2.3

$$ {}^0\underset{\sim}{t} = {}^1\underset{\sim}{S} \cdot \underset{\sim}{N} \tag{2.22} $$

$$ {}^1\underset{\sim}{t} = {}^1\underset{\sim}{T} \cdot \underset{\sim}{n} \tag{2.23} $$

where

$$ \begin{aligned} {}^1\underset{\sim}{S} &= {}^1S^{IJ}\,\underset{\sim}{G}_I\,\underset{\sim}{G}_J \\ {}^1\underset{\sim}{T} &= {}^1T^{ij}\,\underset{\sim}{g}_i\,\underset{\sim}{g}_j \\ \underset{\sim}{N} &= N_K\,\underset{\sim}{G}^K \\ \underset{\sim}{n} &= n_k\,\underset{\sim}{g}^k \end{aligned} \tag{2.24} $$

The 2nd Piola-Kirchhoff stress tensor can now be defined using the relationship

$$ {}^1\underset{\sim}{t}\,da = \underset{\sim}{F} \cdot {}^0\underset{\sim}{t}\,dA \tag{2.25} $$

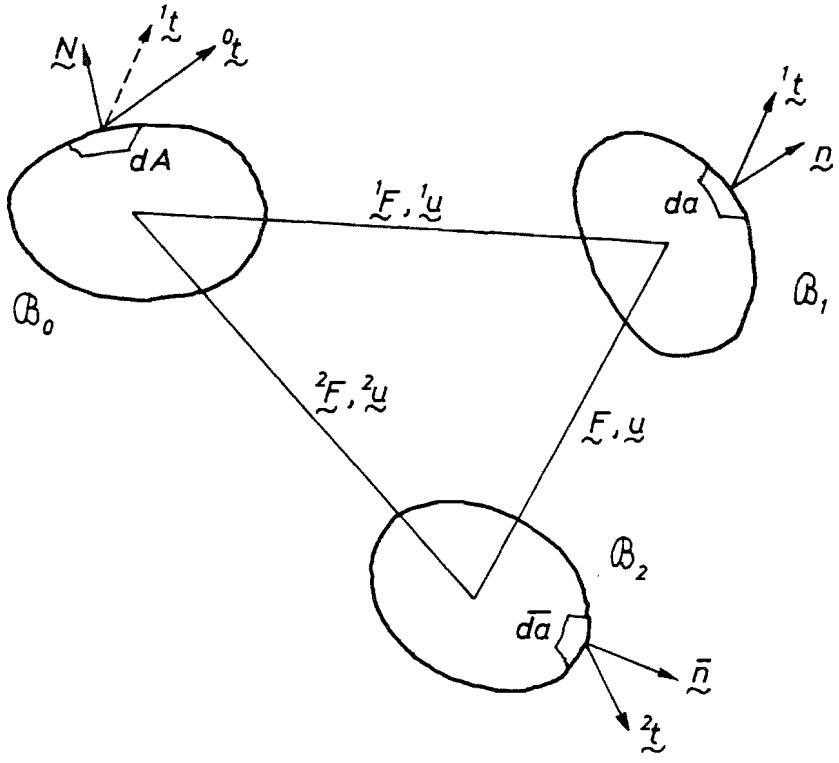

FIG. 2.3 TRACTION VECTORS AND NORMALS.

and introducing Nanson's formula [69]

$$\underset{\sim}{n}\, da = \frac{\rho_0}{\rho} ({}^1\underset{\sim}{F}^{-1})^T \cdot \underset{\sim}{N}\, dA \tag{2.26}$$

which when combined give

$${}^1\underset{\sim}{t}\, da = {}^1\underset{\sim}{T} \cdot \underset{\sim}{n}\, da = {}^1\underset{\sim}{T} \frac{\rho_0}{\rho} ({}^1\underset{\sim}{F}^{-1})^T \cdot \underset{\sim}{N}\, dA = {}^1\underset{\sim}{F} \cdot {}^1\underset{\sim}{t}\, dA = {}^1\underset{\sim}{F} \cdot {}^1\underset{\sim}{S} \cdot \underset{\sim}{N}\, dA$$

Comparing terms, one gets

$${}^1\underset{\sim}{T} = \frac{\rho}{\rho_0} {}^1\underset{\sim}{F} \cdot {}^1\underset{\sim}{S} \cdot {}^1\underset{\sim}{F}^T \tag{2.27}$$

or on component form

$${}^1T^{ij} = \frac{\rho}{\rho_0} {}^1F^i_{\ I}\, {}^1F^j_{\ J}\, {}^1S^{IJ} \tag{2.28}$$

In Cartesian coordinates this simplifies to

$${}^1T_{ij} = \frac{\rho}{\rho_0} \frac{\partial x_i}{\partial X_I} \frac{\partial x_j}{\partial X_J} {}^1S_{IJ}$$

The Piola-Kirchhoff tensor is symmetric whenever the Cauchy stress is symmetric

$${}^1S^{IJ} = {}^1S^{JI}$$

The question of representation of the Piola-Kirchhoff stress tensor has occasionally arisen. Yaghmai [31] attempted to write the tensor in terms of the base vectors in the deformed configuration

$${}^1\underset{\sim}{S} = {}^1\bar{S}^{ij}\, \underset{\sim}{g}_i \underset{\sim}{g}_j$$

The relationship between the components is obtained by a simple coordinate transformation

$$ {}^{1}S^{IJ} = {}^{1}\bar{S}^{ij}\,{}^{1}F^{I}_{\cdot i}\,{}^{1}F^{J}_{\cdot j} \tag{2.29} $$

where ${}^{1}F^{I}_{\cdot i}$ are the component of the tensor ${}^{1}\underset{\sim}{F}^{-1}$

Combining Eqs. (2.29) and (2.28) the following equation is obtained:

$$ {}^{1}\bar{S}^{ij} = \frac{\rho_o}{\rho}\,{}^{1}\tau^{ij} \tag{2.30} $$

This is the form used by Lee [71] in his work on finite plastic deformation.

2.4 Stress and Strain Rates

The constitutive relations for nonlinear materials are frequently expressed in terms of stress and strain rates. For Piola-Kirchhoff stress and Green strain tensors

$$ {}^{1}\dot{\underset{\sim}{E}} = \frac{d}{dt}\left({}^{1}E_{IJ}\,\underset{\sim}{G}^{I}\underset{\sim}{G}^{J}\right) = {}^{1}\dot{E}_{IJ}\,\underset{\sim}{G}^{I}\underset{\sim}{G}^{J} \tag{2.31} $$

$$ {}^{1}\dot{\underset{\sim}{S}} = \frac{d}{dt}\left({}^{1}S^{IJ}\,\underset{\sim}{G}_{I}\underset{\sim}{G}_{J}\right) = {}^{1}\dot{S}^{IJ}\underset{\sim}{G}_{I}\underset{\sim}{G}_{J} \tag{2.32} $$

since $\underset{\sim}{G}_{I}$ and $\underset{\sim}{G}^{I}$ are fixed base vectors in $\mathcal{B}_o$, and are independent of time

Define:

$$ {}^{1}\dot{E}_{IJ} = \lim_{\Delta t\to 0}\frac{{}^{2}E_{IJ} - {}^{1}E_{IJ}}{\Delta t} = \lim_{\Delta t\to 0}\frac{E_{IJ}}{\Delta t} \tag{2.33} $$

$$ {}^{1}\dot{S}^{IJ} = \lim_{\Delta t\to 0}\frac{{}^{2}S^{IJ} - {}^{1}S^{IJ}}{\Delta t} = \lim_{\Delta t\to 0}\frac{S^{IJ}}{\Delta t} \tag{2.34} $$

Using the above definitions, the stress and strain tensors in $\mathcal{B}_2$, ${}^2\underset{\sim}{S}$ and ${}^2\underset{\sim}{E}$, can be found by Taylor series expansion around $\mathcal{B}_1$. For a sufficiently small time increment only the linear terms are needed, and the increments are given by

$$E_{IJ} = {}^1\dot{E}_{IJ}\, dt \tag{2.35}$$

$$S^{IJ} = {}^1\dot{S}^{IJ}\, dt \tag{2.36}$$

referred to base vectors in $\mathcal{B}_0$.

The time rate of the Cauchy stress tensor is, on the other hand, given by

$${}^1\dot{\underset{\sim}{T}} = {}^1\dot{T}^{ij}\, \underset{\sim}{g}_i\, \underset{\sim}{g}_j + {}^1T^{ij}\, \dot{\underset{\sim}{g}}_i\, \underset{\sim}{g}_j + {}^1T^{ij}\, \underset{\sim}{g}_i\, \dot{\underset{\sim}{g}}_j$$

where the time derivative of the base vectors does not vanish.

2.5 Virtual Work in Finite Deformations

In this section an incremental equilibrium equation will be derived for a body subjected to initial stresses and strains. This will be done by writing virtual work expressions in two neighboring configurations, and by proper identification of stresses and strain obtain the desired incremental equation. This approach was first proposed by Yaghmai [31].

The following derivation is independent of the constitutive theory used, but will later be specialized to the case of plasticity

and creep problems.

The body during deformation will describe a motion from an initial configuration $\mathcal{B}_0$ to the final one $\mathcal{B}$. An arbitrary configuration in this deformation space will be denoted $\mathcal{B}_1$ and its neighboring one $\mathcal{B}_2$. Each configuration can be described relative to some Eucledian space. The choice of this space is quite arbitrary, but for the present the configuration $\mathcal{B}_i$ is described relative to the space $\mathcal{B}_i$. This duplicity in notation should not lead to problems, since its meaning should be clear from the context.

The virtual work done by the external forces in $\mathcal{B}_2$ under an infinitesimal virtual displacement is given by

$$\delta W_2 = \int_{\partial\mathcal{B}_2} \delta\underset{\sim}{u} \cdot \overset{2}{\underset{\sim}{t}}\, d\bar{a} + \int_{\mathcal{B}_2} \bar{\rho}\, \delta\underset{\sim}{u} \cdot \overset{2}{\underset{\sim}{f}}\, d\bar{v} \tag{2.37}$$

where $\overset{2}{\underset{\sim}{t}}$ is the surface traction vector per unit area in $\mathcal{B}_2$ and $\overset{2}{\underset{\sim}{f}}$ is the body force vector per unit mass. $\bar{\rho}$ is the mass density and $\partial\mathcal{B}_2$ is the surface of $\mathcal{B}_2$ where tractions are prescribed.

Similarly the virtual work expression in $\mathcal{B}_1$ is given by

$$\delta W_1 = \int_{\partial\mathcal{B}_1} \delta\underset{\sim}{u} \cdot \overset{1}{\underset{\sim}{t}}\, da + \int_{\mathcal{B}_1} \rho\, \delta\underset{\sim}{u} \cdot \overset{1}{\underset{\sim}{f}}\, dv \tag{2.38}$$

At this stage it should be noted that Eqs. (2.37) and (2.38) are given relative to the spaces $\mathcal{B}_2$ and $\mathcal{B}_1$ respectively. Before they can be subtracted they must be transformed to a common space. This common space may be any one of

i) Initial space $\mathcal{B}_0$

ii) Current space $\mathcal{B}_1$

iii) "Final" space $\mathcal{B}_2$

Alternative (iii) leads to a spatial (or Eulerial) description, (ii) to a relative description and (i) to the Lagrangian description. According to our previous discussion the latter alternative is chosen. Yaghmai [31] used (ii) in his treatment of elastic-plastic deformation.

It should be noted that the transformation of the integrals over $\mathcal{B}_1$ and $\mathcal{B}_2$ to integrals over $\mathcal{B}_0$ is purely kinematical. The choice of constitutive theory is therefore immaterial to this transformation.

By Cauchy's principle

$$\delta W_2 = \int_{\partial\mathcal{B}_2} \delta\underset{\sim}{u}\cdot {}^2\underset{\sim}{T}\cdot\bar{\underset{\sim}{n}}\, d\bar{a} + \int_{\mathcal{B}_2} \bar{\rho}\,\delta\underset{\sim}{u}\cdot {}^2\underset{\sim}{f}\, d\bar{v} \tag{2.39}$$

$$\delta W_1 = \int_{\partial\mathcal{B}_1} \delta\underset{\sim}{u}\cdot {}^1\underset{\sim}{T}\cdot\underset{\sim}{n}\, da + \int_{\mathcal{B}_1} \rho\,\delta\underset{\sim}{u}\cdot {}^1\underset{\sim}{f}\, dv \tag{2.40}$$

Using Nanson's formula, Eq. (2.26), the following relations are established

$$\begin{aligned}
\underset{\sim}{n}\, da &= \frac{\rho_0}{\rho}\,({}^1\underset{\sim}{F}^{-1})^T\cdot\underset{\sim}{N}\, dA \\
\bar{\underset{\sim}{n}}\, d\bar{a} &= \frac{\rho_0}{\bar{\rho}}\,({}^2\underset{\sim}{F}^{-1})^T\cdot\underset{\sim}{N}\, dA \\
\bar{\underset{\sim}{n}}\, d\bar{a} &= \frac{\rho}{\bar{\rho}}\,(\underset{\sim}{F}^{-1})^T\cdot\underset{\sim}{n}\, da
\end{aligned} \tag{2.41}$$

By substituting (2.41a, b) into the virtual work expression the Lagrangian formulation is obtained. Eq. (2.41c) combined with

(2.39, 40) gives the relative formulation, and the inverse of (2.41c) leads to the Eulerian formulation. The correct form of the incremental equilibrium equations can therefore be obtained simply by using the appropriate combination of Eq. (2.41).

From the definition of the 2nd Piola-Kirchhoff stress tensor, (2.27) one has

$$
\begin{aligned}
{}^{2}\underset{\sim}{T} &= \frac{\bar{\rho}}{\rho_0}\, {}^{2}\underset{\sim}{F}\cdot{}^{2}\underset{\sim}{S}\cdot{}^{2}\underset{\sim}{F}^{T} \\
{}^{1}\underset{\sim}{T} &= \frac{\rho}{\rho_0}\, {}^{1}\underset{\sim}{F}\cdot{}^{1}\underset{\sim}{S}\cdot{}^{1}\underset{\sim}{F}^{T}
\end{aligned}
\tag{2.27}
$$

Combining Eqs. (2.27, 41, 40, 39) the virtual work expressions become

$$
\delta W_2 = \int_{\partial \mathcal{B}_0} \delta\underset{\sim}{u}\cdot({}^{2}\underset{\sim}{F}\cdot{}^{2}\underset{\sim}{S})\cdot\underset{\sim}{N}\, dA + \int_{\mathcal{B}_0} \rho_0\, \delta\underset{\sim}{u}\cdot{}^{2}\underset{\sim}{f}\, dV
$$

$$
\delta W_1 = \int_{\partial \mathcal{B}_0} \delta\underset{\sim}{u}\cdot({}^{1}\underset{\sim}{F}\cdot{}^{1}\underset{\sim}{S})\cdot\underset{\sim}{N}\, dA + \int_{\mathcal{B}_0} \rho_0\, \delta\underset{\sim}{u}\cdot{}^{1}\underset{\sim}{f}\, dV
$$

The surface integrals are transformed to volume integrals by the Green-Gauss theorem

$$
\delta W_2 = \int_{\mathcal{B}_0} \left((\partial_{\underset{\sim}{X}}\cdot\delta\underset{\sim}{u})\cdot({}^{2}\underset{\sim}{F}\cdot{}^{2}\underset{\sim}{S}) + \delta\underset{\sim}{u}\cdot({}^{2}\underset{\sim}{F}\cdot{}^{2}\underset{\sim}{S} + \rho_0\, {}^{2}\underset{\sim}{f})\cdot\partial_{\underset{\sim}{X}} \right) dV
$$

$$
\delta W_1 = \int_{\mathcal{B}_0} \left((\partial_{\underset{\sim}{X}}\cdot\delta\underset{\sim}{u})\cdot({}^{1}\underset{\sim}{F}\cdot{}^{1}\underset{\sim}{S}) + \delta\underset{\sim}{u}\cdot({}^{1}\underset{\sim}{F}\cdot{}^{1}\underset{\sim}{S} + \rho_0\, {}^{1}\underset{\sim}{f})\cdot\partial_{\underset{\sim}{X}} \right) dV
$$

where $(\partial_{\underset{\sim}{X}}\cdot)$ and $(\cdot\partial_{\underset{\sim}{X}})$ are the left and right divergence operators respectively. The derivatives are taken with respect to $\mathcal{B}_0$. For vectors the two operators coincide. The last term in each integral is recognized as a statement of equilibrium of the body.

$$
\begin{aligned}
(\overset{2}{\underset{\sim}{F}}\cdot\overset{2}{\underset{\sim}{S}} + \rho_0\overset{2}{\underset{\sim}{f}})\cdot\partial_{\underset{\sim}{X}} &= 0 \\
(\overset{1}{\underset{\sim}{F}}\cdot\overset{1}{\underset{\sim}{S}} + \rho_0\overset{1}{\underset{\sim}{f}})\cdot\partial_{\underset{\sim}{X}} &= 0
\end{aligned}
\tag{2.42}
$$

The virtual work expressions can then be simplified to

$$\delta W_2 = \int_{\mathcal{B}_0} (\partial_{\underset{\sim}{X}}\cdot\delta\underset{\sim}{u})\cdot(\overset{2}{\underset{\sim}{F}}\cdot\overset{2}{\underset{\sim}{S}})\,dV \tag{2.43}$$

$$\delta W_1 = \int_{\mathcal{B}_0} (\partial_{\underset{\sim}{X}}\cdot\delta\underset{\sim}{u})\cdot(\overset{1}{\underset{\sim}{F}}\cdot\overset{1}{\underset{\sim}{S}})\,dV \tag{2.44}$$

At this stage the formal vector notation will be abandoned, and the equations will be written in component form.

$$\delta W_2 = \int_{\mathcal{B}_0} (\delta u_\alpha)|_K \, {}^2F^\alpha_{\cdot J} \, {}^2S^{JK}\,dV \tag{2.45}$$

$$\delta W_1 = \int_{\mathcal{B}_0} (\delta u_i)|_K \, {}^1F^i_{\cdot J} \, {}^1S^{JK}\,dV \tag{2.46}$$

$$\delta(u_\alpha) = \delta(G_\alpha{}^M u_M)$$

$$\delta(u_i) = \delta(G_i{}^N u_N)$$

Following Toupin [72] the shifters can be taken as constants during differentiation and variation

$$G_i{}^N|_K = G_i{}^N|_j = G_N{}^i|^K = G_M{}^i|^j \equiv 0$$

Hence

$$\delta(u_\alpha) = G_\alpha^{\ M}\,\delta u_M$$
$$\delta(u_i) = G_i^{\ N}\,\delta u_N \tag{2.47}$$

The motion is given by

$$\underset{\sim}{\bar{x}} = \underset{\sim}{x} + \underset{\sim}{u} = \underset{\sim}{X} + {}^1\underset{\sim}{u} + \underset{\sim}{u}$$

or

$$\bar{x}^\alpha = G_I^\alpha\,(X^I + {}^1u^I + u^I)$$

Hence:

$${}^2F^\alpha_{\ J} = G^\alpha_I\,(\delta^I_J + {}^1u^I/_J + u^I/_J)$$
$${}^1F^i_{\ J} = G^i_I\,(\delta^I_J + {}^1u^I/_J) \tag{2.48}$$

Combining Eqs. (2.47) and (2.48) with the virtual work expression (2.45) and (2.46) gives

$$\delta W_2 = \int_{\mathcal{B}_0} (\delta u_I)/_K\,(\delta^I_J + {}^1u^I/_J + u^I/_J)\,{}^2S^{JK}\,dV \tag{2.49}$$

$$\delta W_1 = \int_{\mathcal{B}_0} (\delta u_I)/_K\,(\delta^I_J + {}^1u^I/_J)\,{}^1S^{JK}\,dV \tag{2.50}$$

since

$$G_\alpha^{\ M} G^\alpha_I = G^M_{\ I} = \delta^M_{\ I} \quad \text{and} \quad G_i^{\ N} G^i_{\ I} = \delta^N_{\ I}$$

Due to the symmetry of the 2nd Piola-Kirchhoff stress tensor

$$(\delta u_I)/_K\,{}^2S^{IK} = \tfrac{1}{2}\,\delta\,(u_I/_K + u_K/_I)\,{}^2S^{IK} = {}^2S^{IK}\,\delta\hat{e}_{IK}$$

$$(\delta u_I)/_K\,u^I/_J\,{}^2S^{JK} = \tfrac{1}{2}\,\delta\,(u_I/_K\,u^I/_J)\,{}^2S^{JK} = {}^2S^{JK}\,\delta\eta_{JK}$$

$$(\delta u_I)/_K\,{}^1u^I/_J\,{}^2S^{JK} = \tfrac{1}{2}\,(\delta u_I/_K\,{}^1u^I/_J + \delta u_I/_J\,{}^1u^I/_K)\,{}^2S^{JK} = {}^2S^{JK}\,\delta\hat{e}_{JK}$$

where

$$E_{IJ} = e_{IJ} + \eta_{IJ} = \hat{e}_{IJ} + \hat{\hat{e}}_{IJ} + \eta_{IJ} \tag{2.50a}$$

Using Eq. (2.10) and introducing the displacement ${}^{1}\underset{\sim}{u}$, this gives

$$2 e_{IJ} = 2 \hat{e}_{IJ} + 2 \hat{\hat{e}}_{IJ} \tag{2.50b}$$

where

$$2 \hat{e}_{IJ} = u_{I/J} + u_{J/I} \tag{2.50c}$$

$$2 \hat{\hat{e}}_{IJ} = u_{K/I}\, {}^{1}u^{K}{}_{/J} + u_{K/J}\, {}^{1}u^{K}{}_{/I} \tag{2.50d}$$

$$2 \eta_{IJ} = u_{K/J}\, u^{K}{}_{/I} \tag{2.50e}$$

and η_{IJ} is the nonlinear part of the strain increment.

Since the Piola-Kirchhoff stress tensor is always referred to fixed base vectors in the initial configuration $\mathcal{B}_0$, the following additive decomposition can be used

$${}^{2}S^{IJ} = {}^{1}S^{IJ} + S^{IJ} \tag{2.50f}$$

Subtracting Eq. (2.50) from (2.49) and introducing the above relations gives

$$\delta W_2 - \delta W_1 = \int_{B_0} (S^{IJ} \delta E_{IJ} + {}^1S^{IJ} \delta \eta_{IJ}) dV \qquad (2.51)$$

Equation (2.51) is an incremental virtual work expression, or a statement of incremental equilibrium. In a displacement formulation for the finite element method it will give rise to the stiffness matrix of the structure.

2.6 Traction Boundary Conditions

In contrast to the displacement boundary conditions, the traction boundary conditions introduce further complications in a Lagrangian formulation of finite deformation. The latter has to be formulated in the deformed configuration, and will hence depend on the deformation itself. This problem has been discussed by Oden [25] who solved the problem by an iterative procedure.

In order to obtain a correct load term of the incremental equilibrium equations the external loading is divided into two groups

i) Conservative loading

ii) Nonconservative loading

The first group consists of forces that can be derived from a potential, such as gravitational and inertia forces. These forces do not change direction during deformation. The forces in the latter group, however, do change direction, and can be

represented by hydrostatic pressure and "follow-through" forces.

2.6.1 Conservative Loading

The traction vector ${}^{2}\underset{\sim}{t}$, ${}^{1}\underset{\sim}{t}$, ${}^{2}\underset{\sim}{f}$ and ${}^{1}\underset{\sim}{f}$ in Eqs. (2.37) and (2.38) do not change direction during the deformation.

Imposing the condition of conservation of mass

$$\rho\, dv = \bar{\rho}\, d\bar{v} = \rho_0\, dV$$

the volume integrals can be transformed to integrals over $\mathcal{B}_0$. In transforming the surface integrals to $\partial_{\mathcal{B}_0}$ the total load remains unchanged, but the load intensities will change according to the ratios da/dA and $d\bar{a}/dA$

Define

$${}^{2}\underset{\sim}{\bar{t}}\, dA = {}^{2}\underset{\sim}{t}\, d\bar{a}$$

$${}^{1}\underset{\sim}{\bar{t}}\, dA = {}^{1}\underset{\sim}{t}\, da$$

where ${}^{2}\underset{\sim}{\bar{t}}$ and ${}^{1}\underset{\sim}{\bar{t}}$ are the traction vectors in $\mathcal{B}_2$ and $\mathcal{B}_1$ respectively, measured per unit area in $\mathcal{B}_0$. For most structures this distinction is immaterial, but it may be important for instance in large deformations of rubberlike materials.

Subtraction of Eq. (2.38) from (2.37) using the above definitions gives

$$\delta W_2 - \delta W_1 = \int_{\partial\mathcal{B}_0} \delta\underset{\sim}{u} \cdot ({}^{2}\underset{\sim}{\bar{t}} - {}^{1}\underset{\sim}{\bar{t}})\, dA + \int_{\mathcal{B}_0} \rho_0\, \delta\underset{\sim}{u} \cdot ({}^{2}\underset{\sim}{f} - {}^{1}\underset{\sim}{f})\, dV$$

Defining the incremental traction and body forces by:

$$\underset{\sim}{f} = {}^{2}\underset{\sim}{f} - {}^{1}\underset{\sim}{f}$$

$$\underset{\sim}{\bar{t}} = {}^{2}\underset{\sim}{\bar{t}} - {}^{1}\underset{\sim}{\bar{t}}$$

the virtual work expression becomes

$$\delta W_2 - \delta W_1 = \int_{\partial \mathcal{B}_0} \delta \underset{\sim}{u} \cdot \bar{\underset{\sim}{t}}\, dA + \int_{\mathcal{B}_0} \rho_0\, \delta \underset{\sim}{u} \cdot \underset{\sim}{f}\, dV \tag{2.52}$$

2.6.2 Nonconservative Loading

Following Oden [25] the traction vectors can for a pressure type loading be written as

$$^2\underset{\sim}{t}\, d\bar{a} = -\,^2p\, \bar{\underset{\sim}{n}}\, d\bar{a}$$

$$^1\underset{\sim}{t}\, da = -\,^1p\, \underset{\sim}{n}\, da$$

where ^2p and ^1p are the pressures in $\mathcal{B}_2$ and $\mathcal{B}_1$, and $\bar{\underset{\sim}{n}}$ and $\underset{\sim}{n}$ are the unit outward normals respectively.

Using Nanson's formula, (2.41), this can be transformed to

$$^2\underset{\sim}{t}\, d\bar{a} = -\,^2p\, \frac{\rho_0}{\rho}\, (^2\underset{\sim}{F}^{-1})^T \cdot \underset{\sim}{N}\, dA$$

$$^1\underset{\sim}{t}\, da = -\,^1p\, \frac{\rho_0}{\rho}\, (^1\underset{\sim}{F}^{-1})^T \cdot \underset{\sim}{N}\, dA$$

Substitution into Eqs. (2.37) and (2.38) gives

$$\delta W_2 = \int_{\partial \mathcal{B}_0} -\,^2p\, \frac{\rho_0}{\rho}\, \delta \underset{\sim}{u} \cdot (^2\underset{\sim}{F}^{-1})^T \cdot \underset{\sim}{N}\, dA + \int_{\mathcal{B}_0} \rho_0\, \delta \underset{\sim}{u} \cdot {}^2\underset{\sim}{f}\, dV \tag{2.53}$$

$$\delta W_1 = \int_{\partial \mathcal{B}_0} -\,^1p\, \frac{\rho_0}{\rho}\, \delta \underset{\sim}{u} \cdot (^1\underset{\sim}{F}^{-1})^T \cdot \underset{\sim}{N}\, dA + \int_{\mathcal{B}_0} \rho_0\, \delta \underset{\sim}{u} \cdot {}^1\underset{\sim}{f}\, dV \tag{2.54}$$

Introducing the proper shifters the above equations can be written on component form

$$\delta W_2 = -\int_{\partial \mathcal{B}_0} {}^2p\, \frac{\rho_0}{\rho}\, \delta u_I\, (^2F^{-1})^I_{\ J}\, N^J\, dA + \int_{\mathcal{B}_0} \rho_0\, \delta u_I\, {}^2f^I\, dV$$

$$\delta W_1 = -\int_{\partial \mathcal{B}_0} {}^1p\, \frac{\rho_0}{\rho}\, \delta u_I\, (^1F^{-1})^I_{\ J}\, N^J\, dA + \int_{\mathcal{B}_0} \rho_0\, \delta u_I\, {}^1f^I\, dV$$

Defining the pressure increment p , the following decomposition cam be made

$$ {}^{2}p = {}^{1}p + p $$

Finally

$$ \delta W_2 - \delta W_1 = -\int_{\partial\mathcal{B}_o} p \frac{\rho_o}{\rho} \delta u_I \frac{\rho}{\bar{\rho}} ({}^{2}F^{-1})^{I}_{\cdot J} N^{J} dA + \int_{\mathcal{B}_o} \rho_o \delta u_I f^{I} dV - $$

$$ - \int_{\partial\mathcal{B}_o} {}^{1}p \frac{\rho_o}{\rho} \delta u_I \left(\frac{\rho}{\bar{\rho}} ({}^{2}F^{-1})^{I}_{\cdot J} - ({}^{1}F^{-1})^{I}_{\cdot J} \right) N^{J} dA \qquad (2.55) $$

Here the first integral gives rise to the conventional load term associated with the pressure increment p between $\mathcal{B}_1$ and $\mathcal{B}_2$ The second term is the effect of the increment in body force, and the last term gives the effect of the pressure ${}^{1}p$ during the deformation from $\mathcal{B}_1$ to $\mathcal{B}_2$.

So far no assumptions have been made regarding the magnitude of strains and rotations. However, in order to simplify Eq. (2.55) the following restrictions are imposed:

i) The displacement increment $\underset{\sim}{u}$ between $\mathcal{B}_1$ and $\mathcal{B}_2$ is small compared to, ${}^{1}\underset{\sim}{u}$.

ii) The rotations associated with $\underset{\sim}{u}$ are small compared to unity.

Mathematically this means

$$ \frac{\rho}{\bar{\rho}} \doteq 1 \qquad (2.56a) $$

$$ \frac{\partial}{\partial \bar{x}^{J}} \doteq \frac{\partial}{\partial x^{J}} \qquad (2.56b) $$

Using (2.56b) ${}^{2}\underset{\sim}{F}^{-1}$ can be written in rectangular Cartesian coordinates:

$$({}^{2}F^{-1})_{IJ} = \frac{\partial X_I}{\partial \bar{x}_J} = \frac{\partial X_I}{\partial x_K}\frac{\partial x_K}{\partial \bar{x}_J} = \frac{\partial X_I}{\partial x_K}\frac{\partial}{\partial \bar{x}_J}(\bar{x}_K - u_K)$$
$$= \frac{\partial X_I}{\partial x_K} - \frac{\partial X_I}{\partial x_K}\frac{\partial X_M}{\partial x_J}\frac{\partial u_K}{\partial X_M}$$

Introducing this into Eq. (2.55) gives in Cartesian components

$$\delta W_2 - \delta W_1 = -\int_{\partial B_0} p\,\frac{\rho_0}{\rho}\,\delta u_I\,\frac{\partial X_I}{\partial x_J}\,N_J\,dA + \int_{B_0}\rho_0\,\delta u_I\,f_I\,dV +$$
$$+\int_{\partial B_0}({}^{1}p + p)\,\frac{\rho_0}{\rho}\,\delta u_I\,\frac{\partial X_I}{\partial x_K}\,\frac{\partial X_M}{\partial x_J}\,\frac{\partial u_K}{\partial X_M}\,N_J\,dA \qquad (2.57)$$

The equivalent version in curvilinear coordinates can easily be obtained by taking the covariant derivatives with respect to the proper coordinate system.

Note that the last surface integral in (2.57) is linear in the displacement increment $\underset{\sim}{u}$, and has hence the form of a stiffness term. It should also be noted that this term is non-symmetric, as could be expected since it accounts for the non-conservative loading.

Equation (2.57) is equivalent to the load term derived by Marcal et. al. [28] using a different approach.

2.6.3 Residual Load Approach

The finite element method, or the Ritz method, are two of the most efficient methods for solving general boundary value problems. These methods ensure global force equilibrium of the system, but

do not guarantee that the local stress equilibrium equations are satisfied. Hence the internal stress field in a displacement formulation will not necessarily be in equilibrium with the applied external tractions.

This means that the surface traction ${}^1\underset{\sim}{t}$ is not in general in equilibrium with the stress fields ${}^1\underset{\sim}{T}$ or ${}^1\underset{\sim}{S}$. A residual traction vector ${}^1\underset{\sim}{R}$ can therefore be defined by

$$\int_{\partial B_1} \delta\underset{\sim}{u} \cdot {}^1\underset{\sim}{R}\, da = \int_{\partial B_1} \delta\underset{\sim}{u} \cdot ({}^1\underset{\sim}{T}\cdot\underset{\sim}{n} - {}^1\underset{\sim}{t})\, da \tag{2.58}$$

This residual traction vector is often called the "out-of-balance" force, and should be added to the incremental traction vector in (2.57).

Computationally it can be done by using (2.50) instead of (2.54) when deriving Eq. (2.55). By so doing a virtual work expression using the stress field is used instead of one using surface tractions. Introducing the approximations (2.56a, b) and (2.57) the incremental virtual work expression becomes

$$\begin{aligned}\delta W_2 - \delta W_1 = &-\int_{\partial B_0} p \frac{\rho_0}{\rho}\, \delta u_I\, X^I{}_{/J}\, N^J\, dA - \int_{\partial B_0} {}^2p \frac{\rho_0}{\rho}\, \delta u_I\, X^I{}_{/K}\, X^M{}_{/J}\, u^K{}_{/M}\, N^J dA \\ &- \int_{B_0} {}^1S^{IJ}(\delta\hat{e}_{IJ} + \delta\hat{\hat{e}}_{IJ})\, dV + \int_{B_0} \rho_0\, \delta u_I f^I dV\end{aligned} \tag{2.59}$$

where the deformation gradients are taken with respect to B_1 and the displacement gradient with respect to B_0.

The second surface integral is still linear in $\underset{\sim}{u}$, and is hence of the stiffness type. It is, as previously noted, also non-symmetric.

Equation (2.59) is valid for nonconservative loading. The equivalent expression for conservative loading is easily obtained

$$\delta W_2 - \delta W_1 = \int_{\partial B_o} \delta u_I \, {}^2\bar{t}^I \, dA + \int_{B_o} \rho_o \delta u_I f^I \, dV - \int_{B_o} {}^1S^{IJ} (\delta \hat{e}_{IJ} + \delta \hat{e}_{IJ}) \, dV \quad (2.60)$$

2.7 Incremental Constitutive Relations in Elasticity

In order to use the virtual work expression previously derived, an incremental constitutive relationship has to be obtained. The form of this relationship is highly dependent on the stress and strain measures used. When a spatial description and Cauchy stresses are used Biot [73] has shown that the initial stresses have to be introduced into the incremental constitutive equations. For hypoelastic materials this leads to a formulation in terms Jaumann's stress rate and the rate-of-deformation [74].

For a hyperelastic material, the strain energy function W exists. W is an analytic function of the Green strain tensor $\underset{\sim}{E}$, and is given per unit mass in the undeformed configuration. Following Fung [74]

$${}^2S^{IJ} = \rho_o \frac{\partial^2 W}{\partial^2 E_{IJ}} \quad (2.61)$$

and

$$ {}^{1}S^{IJ} = \rho_0 \frac{\partial {}^{1}W}{\partial {}^{1}E_{IJ}} \tag{2.62} $$

where ${}^{2}W$ is the strain energy in configuration $\mathcal{B}_2$, and ${}^{1}W$ is the strain energy in $\mathcal{B}_1$

For an isotropic body the strain energy function can be written as

$$ {}^{2}W = {}^{2}W\left({}^{2}I_1, {}^{2}I_2, {}^{2}I_3\right) \tag{2.63} $$

where ${}^{2}I_i$ are the principal invariants of the strain tensor ${}^{2}E_{IJ}$ Similarly an expression for ${}^{1}W$ may be written.

For a linearly elastic material Eq. (2.63) can be simplified, and

$$ \rho_0 {}^{2}W = C^{IJKL} {}^{2}E_{IJ} {}^{2}E_{KL} \tag{2.64} $$

$$ \rho_0 {}^{1}W = C^{IJKL} {}^{1}E_{IJ} {}^{1}E_{KL} \tag{2.65} $$

Substitution of (2.64) and (2.63) and subtracting the (2.62) from (2.61) gives

$$ {}^{2}S^{IJ} - {}^{1}S^{IJ} = C^{IJKL}\left({}^{2}E_{KL} - {}^{1}E_{KL}\right) \tag{2.66} $$

$$ \text{or} \quad S^{IJ} = C^{IJKL} E_{KL} $$

where

$$ C^{IJKL} = \mu\left(\delta^{IK}\delta^{JL} + \delta^{IL}\delta^{JK}\right) + \lambda \delta^{IJ}\delta^{KL} $$

and μ and λ are the Lamé constants:

$$\mu = \frac{E}{2(1+\nu)} \qquad \lambda = \frac{\nu E}{(1+\nu)(1-2\nu)}$$

2.8 Variational Methods and Virtual Work in the Theory of Creep and Plasticity

2.8.1 Review

Over the years a number of variational methods have been formulated in the theory of elasticity. Many of these are based on the existence of strain energy or complementary energy functions for the system at hand. In the theory of creep and plasticity, however, the stresses or strains cannot in general be derived from potentials. The variational methods that can be constructed for such problems are therefore more restricted.

The most extensive discussions of variational methods in creep and plasticity are given by Kachanov [75] and Rabotnov [42]. Extremum and variational principles for work hardening and rigid plastic materials are also presented by Hill [76]. In Washizu's presentation [77] distinction is also made between principles valid for the deformation theory of plasticity and those valid for flow theory. The form of the variational principles depend in general on the mathematical model used to describe the physical processes in creep and plasticity. This brings up the necessity to distinguish between steady state creep, transient creep, and deformation and flow theory of plasticity.

In steady state creep and deformation theory of plasticity the governing equations are similar to those of the nonlinear theory of elasticity, in that the creep and plastic strains can be derived from state functions. For infinitesimal deformations variational principles of the Lagrangian type can be used [42, 77], provided the concept of unloading is introduced for the plastic deformation. Kachanov's principles [75] can be applied to problems of transient creep and deformation type plasticity. However, they may be considered inconsistent since creep is described by a flow law while the deformation theory is used for plastic deformation.

When flow theory of plasticity is used, the variational principles have to be formulated in incremental form. One such principle is given by Wang and Prager [78] for infinitesimal deformations. Here the creep strain rate is assumed independent of the stress rate, which leads to an initial strain formulation. A variational principle of the Hellinger-Reissner type was derived by Sanders et al [79], and later discussed by Pian [80]. The assumptions of Wang and Prager were retained, but the inclusion of the effect of initial stresses in the deformed configuration makes the principle valid also for geometrically nonlinear problems. The principle is given in terms of the Cauchy-Green strain tensor in a Lagrangian description. In order to have a conjugate formulation the 2nd Piola-Kirchhoff stress tensor must therefore be used. This fact is not stated in reference [79] nor that volume and surface integrals must be taken over the undeformed configuration.

Sanders functional in rectangular Cartesian coordinates is given by

$$\mathcal{J} = \int_{\mathcal{B}_o} \left(\dot{E}_{IJ}\, \dot{S}_{IJ} + \tfrac{1}{2}\, \dot{u}_{K,I}\, \dot{u}_{K,J}\, S_{IJ} - \tfrac{1}{2} \left(\dot{E}^{i}_{IJ} + 2\dot{E}^{c}_{IJ} \right) \dot{S}_{IJ} \right) dV + \int_{\partial\mathcal{B}_o} \dot{\bar{t}}_I\, \dot{u}_I\, dA - \int_{\partial\mathcal{B}_o} \left(\dot{u}_I - \dot{\bar{u}}_I \right) \dot{t}_I\, dA \tag{2.67}$$

where $\dot{E}^{i}_{IJ}$ is the instantaneous strain rate, $\dot{E}^{c}_{IJ}$ the creep strain rate, and $\dot{\bar{t}}_I$ and $\dot{\bar{u}}_I$ the prescribed rate of traction and velocity respectively on the boundary.

Taking the variation of Eq. (2.67) with respect to the rate quantities gives

$$\delta \mathcal{J} = \int_{\mathcal{B}_o} \left(\left(\dot{E}_{IJ} - \dot{E}^{i}_{IJ} - \dot{E}^{c}_{IJ} \right) \delta \dot{S}_{IJ} - \delta \dot{u}_K \frac{d}{dt} \left({}^{1}F_{KI}\, S_{IJ} \right)_{,J} \right) dV + \int_{\partial\mathcal{B}_o} \left(\dot{t}_I - \dot{\bar{t}}_I \right) \delta \dot{u}_I\, dA - \int_{\partial\mathcal{B}_o} \left(\dot{u}_I - \dot{\bar{u}}_I \right) \delta \dot{t}_I\, dA \tag{2.68}$$

Here ${}^{1}F_{IJ}$ are the components of the deformation gradient tensor ${}^{1}\underset{\sim}{F}$ in the current configuration, $\mathcal{B}_1$.

It should be noted that Eq. (2.68) is only valid when the creep strain rate is derived from a state function. Since $\dot{E}^{c}_{IJ}$ is independent of the stress rate this implies that $\delta \dot{E}^{c}_{IJ} = 0$ As typical for variational principles of the Hellinger-Reissner type, the stress and strain rates may be expanded independently.

2.8.2 Modification of the Incremental Equilibrium Equations

The most general of the variational methods described previously was derived from virtual work expressions. The extension of Eq. (2.51) to creep problems should therefore be natural. Equation (2.51) was derived without any restrictions on the constitution of the material at hand. However, before creep problems can be considered, the following assumptions must be made:

i) Assuming the elastic, plastic and creep strain rates to be defined, the additive decomposition law is valid.

$$\dot{E}_{IJ} = \dot{E}^{E}_{IJ} + \dot{E}^{P}_{IJ} + \dot{E}^{C}_{IJ} = \dot{E}^{I}_{IJ} + \dot{E}^{C}_{IJ} \qquad (a)$$

where $\dot{E}^{I}_{IJ}$ is the instantaneous strain rate. For small enough time steps a similar equation can be written for the strain increments.

ii) There exists a linear relationship between the increment of P-K stress and the instantaneous strain increment (*)

$$S_{IJ} = C_{IJKL}\, E^{I}_{KL} \qquad (b)$$

It should be noted that Eq. (a) is not the only way of decomposing the kinematic variables, as will be discussed in section 3.2. Assumption (ii) is fundamental for any incremental formulation using the displacement method, and is used both in plasticity and viscoplasticity.

(*) Rectangular Cartesian coordinates are used in this section

For most metals subjected to creep the creep strain rate is independent of the stress rate. This implies that the increment E^c_{IJ} must be treated as an initial strain increment in the equilibrium equations.

Combining Eqs. (a) and (b) gives

$$S_{IJ} = C_{IJKL}\,(E_{KL} - E^c_{KL}) = S^I_{IJ} - S^c_{IJ} \tag{c}$$

where

$$S^I_{IJ} = C_{IJKL}\,E_{KL} \tag{d}$$

$$S^c_{IJ} = C_{IJKL}\,E^c_{KL} \tag{e}$$

Here S^I_{IJ} and S^c_{IJ} are defined as the "instantaneous" and "creep" stress increment respectively, and are assumed to have the same invariance properties as S_{IJ}.

Substituting Eq. (c) into Eq. (2.51) gives

$$\delta W_2 - \delta W_1 = \int_{\mathcal{B}_0} \left(S^I_{IJ}\,\delta e_{IJ} + (S_{IJ} - S^c_{IJ})\,\delta\eta_{IJ} - S^c_{IJ}\,\delta e_{IJ} \right) dV \tag{2.69}$$

Eq. (2.69)gives the incremental equilibrium equations for a body subjected to initial stresses and creep strains. The effect of the "creep" stress S^c_{IJ} is two-fold. One is the presence of the creep pseudo-loading given by the last term in Eq. (2.69). The other is the contribution to the geometrically nonlinear term.

From a computational point of view, Eq. (2.69) is in the most convenient form. The creep pseudo-loading can, however, be transformed further by the Green-Gauss theorem

$$\int_{\mathcal{B}_o} S^c_{IJ}\,\delta e_{IJ}\,dV = \int_{\mathcal{B}_o} S^c_{IJ}\,{}^1F_{KI}\,\delta u_{K,J}\,dV = \tag{2.70}$$

$$= \int_{\partial\mathcal{B}_o} S^c_{IJ}\,{}^1F_{KI}\,N_J\,\delta u_K\,dA - \int_{\mathcal{B}_o} \left(S^c_{IJ}\,{}^1F_{KI}\right)_{,J}\,\delta u_K\,dV$$

where the "fictitious" traction and body-force due to creep can be identified.

It can easily be shown that Eqs. (2.68) and (2.69) are equivalent if Eqs. (c, d, e) are substituted into Eq. (2.68).

3. CONSTITUTIVE RELATIONS FOR CREEP AND PLASTICITY IN METALS

3.1 Introduction

In general the term creep is associated with the time-dependent deformations in materials. For most metals creep is of importance only at elevated temperatures, but is observed at room temperature for materials like concrete and plastics.

The physical theory of creep can be described in terms of the micro-structure of the material [81]. For metals creep is caused by cross-slip and dislocation climb in the material lattice. Dislocation motion and vacancy migration are thermally activated, and are the dominant mechanisms at elevated temperatures. In polymers creep is due to stretching and distortion of the individual chain-molecules, and to large scale relative motion of the molecules. The importance of the physical theory of creep is that it provides important guidance for the formulation of the constitutive theory describing the phenomenon.

A phenomenological description of creep is provided by the uniaxial creep test under constant stress, Fig. 3.1. Here the commonly used terminology is defined. When loaded, the material exhibits an instantaneous response that may be elastic-plastic if the stress level is above the yield stress. The primary or transient creep is characterized by a decreasing strain rate, and is followed by the secondary or steady-state creep where the strain rate is constant. Finally, the tertiary state is reached that takes the material to rupture.

The steady-state period is dominant in most materials, but may be missing for some materials at given stress and temperature levels. The simple creep test is even today the basic source of information regarding creep behavior of materials.

The theory of plasticity is usually divided into two subclasses, the flow theory and the deformation theory. The deformation (or Hencky) theory gives a relationship between total stress and strain, where the total plastic strain components are functions of the current state of stress. This approach is similar to the treatment of nonlinear elasticity, except for the concept of unloading in plastic region. The flow theory, on the other hand, is an incremental theory that gives a relationship between increments of plastic strain and increments of stress. Whereas the former is independent of the loading path, the latter has to be integrated along the loading path in order to give total strains. For proportional or radial loading, i.e., where the ratios between the stress components are kept constant during loading, it can be shown that the two theories are equivalent. However, for nonradial loading the flow theory is considered the superior one, and is therefore chosen in this study.

In the flow theory of plasticity the behavior of a body is governed by three conditions:

i) The initial yield condition

ii) The flow rule

iii) The hardening rule

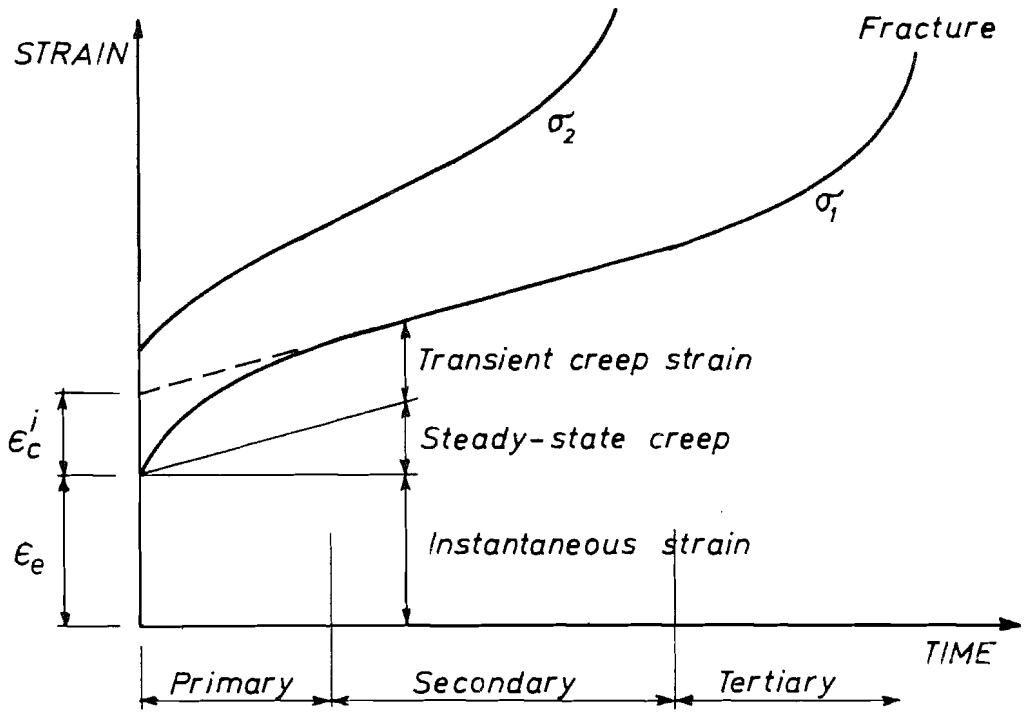

FIG. 3.1 TYPICAL CREEP CURVES.

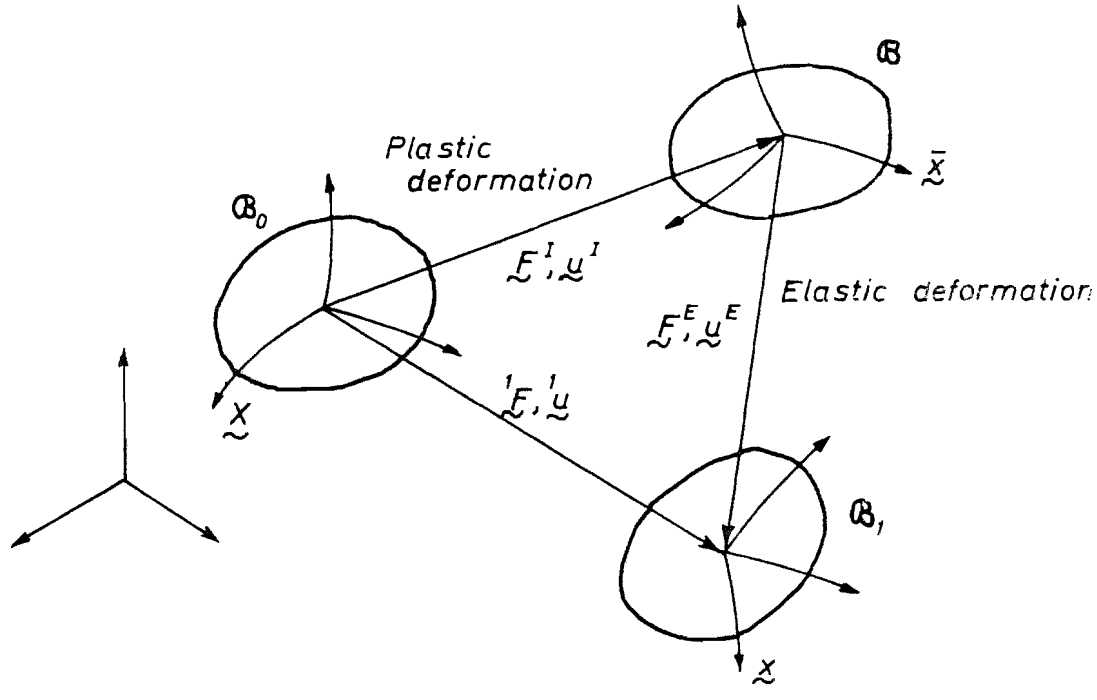

FIG. 3.2 INELASTIC KINEMATIC DECOMPOSITION

The flow rule and the hardening rule are also present in most creep theories, but the equivalent of the yield condition is not defined. The lack of the yield condition accounts for the problem of obtaining an incremental stress-strain relationship in creep, and ultimately for the necessity of using the initial strain method in solving creep problems.

3.2 Kinematic Decomposition of Finite Inelastic Deformation

In a general inelastic problem in continuum mechanics the total deformation of a stressed body is determined by a number of physical effects. When formulating a constitutive theory for a material these effects must be identified. The most common form of this identification is the decomposition of the kinematic variables.

For the problem at hand these effects are the deformation due to creep and plasticity. In the following, these two effects are lumped together and denoted inelastic effect.

During the deformation of an inelastic body three configurations can be defined, [82, 83, 71], Fig. 3.2. The initial configuration $\mathcal{B}_0$ is stress free, while the current configuration $\mathcal{B}_t$ has undergone the combined elastic-inelastic deformation. The intermediate configuration $\mathcal{B}$ is obtained when the stresses in $\mathcal{B}_t$ are conceptually released. It should be noted that $\mathcal{B}$ in general is non-Euclidean [71].

The Cauchy-Green strain tensor is given by

$$2\,{}^{t}\underset{\sim}{\epsilon} = {}^{t}\underset{\sim}{F}^{T} \cdot {}^{t}\underset{\sim}{F} - \underset{\sim}{I} \tag{3.1a}$$

or

$$2\,{}^{1}E_{IJ} = {}^{1}u_{I,J} + {}^{1}u_{J,I} + {}^{1}u_{K,I}\,{}^{1}u_{K,J} \quad (*) \tag{3.1b}$$

From Fig. 3.2 the total displacement field is given by

$${}^{1}\underset{\sim}{u} = \underset{\sim}{u}^{E} + \underset{\sim}{u}^{I} \tag{3.2}$$

Substitution of Eq. (3.2) into (3.1a) gives

$${}^{1}E_{IJ} = {}^{1}E^{E}_{IJ} + {}^{1}E^{I}_{IJ} + \tfrac{1}{2}\left(u^{I}_{K,I}\, u^{E}_{K,J} + u^{I}_{K,J}\, u^{E}_{K,I} \right) \tag{3.3}$$

where ${}^{1}\underset{\sim}{E}^{E}$ and ${}^{1}\underset{\sim}{E}^{I}$ are defined by Eq. (3.16) with $\underset{\sim}{u}^{E}$ and $\underset{\sim}{u}^{I}$ respectively substituted for $\underset{\sim}{u}$.

Eq. (3.3) clearly shows that the elastic and inelastic strains ${}^{1}\underset{\sim}{E}^{E}$ and ${}^{1}\underset{\sim}{E}^{I}$ are not in general additive during finite deformations. For infinitesimal deformation, however, the non-linear terms in the strain-displacement relationship are neglected, and Eq. (3.3) degenerates to the classical form. It should be noted that this derivation was based purely on kinematics, and the displacement fields $\underset{\sim}{u}^{E}$ and $\underset{\sim}{u}^{I}$ were assumed continuous and differentiable.

Green and Naghdi [84] retained the additive decomposition of the total elastic and inelastic strains. No kinematic interpretation of $\underset{\sim}{E}^{E}$ and $\underset{\sim}{E}^{I}$ is given, and they are determined from constitutive theory only. Furthermore, they are assumed to have the same invariance properties as ${}^{1}\underset{\sim}{E}$.

(*) Rectangular Cartesian coordinates are used in this Chapter.

The multiplicative decomposition was given by Lee [83, 71] in the form

$$ {}^{1}\underset{\sim}{F} = \underset{\sim}{F}^{E}\cdot\underset{\sim}{F}^{I} \tag{3.4} $$

where ${}^{1}\underset{\sim}{F}$ is the deformation gradient at $\mathcal{B}_1$ relative to $\mathcal{B}_0$. $\underset{\sim}{F}^{E}$ and $\underset{\sim}{F}^{I}$ are in general not deformation gradients, but linear transformations determined by the constitutive theory. For the case where the mapping between $\mathcal{B}_0$, $\mathcal{B}$ and $\mathcal{B}_1$ is continuous and differentiable, they are found by chain rule of differentiation.

Yaghmai has shown [31] that Green and Naghdi's and Lee's formulation are equivalent, provided the proper definitions are used for ${}^{1}\underset{\sim}{E}^{E}$ and ${}^{1}\underset{\sim}{E}^{I}$

$$ 2\,{}^{1}\underset{\sim}{E} - 2\,{}^{1}\underset{\sim}{E}^{I} + 2\,{}^{1}\underset{\sim}{E}^{E} = \left(\left(\underset{\sim}{F}^{I}\right)^{T}\underset{\sim}{F}^{I} - \underset{\sim}{I}\right) + \left(\underset{\sim}{F}^{I}\right)^{T}\left(\left(\underset{\sim}{F}^{E}\right)^{T}\underset{\sim}{F}^{E} - \underset{\sim}{I}\right)\underset{\sim}{F}^{I} \tag{3.5} $$

It is here quite clear that the "elastic" strain in general no longer can be determined from the generalized Hooke's law.

The complexity of both the additive and multiplicative decomposition render them rather unfeasible for practical applications at the moment. Green and Naghdi's formulation mainly because it requires the determination of Helmholtz free energy function.

A number of formulations have therefore been made that impose the additive decomposition of the kinematic rate quantities, since these are linear in the velocities.

Bodner [85] took the total rate of deformation in the form

$$ D_{ij} = D_{ij}^{E} + D_{ij}^{I} \tag{3.6} $$

This form is very convenient when the equilibrium equations are formulated in a relative description. In a Lagrangian formulation Eq. (3.6) must be transformed back to the reference configuration, $\mathcal{B}_o$. This transformation gives rise to the different interpretations.

Bodner gave the Lagrangian strain rates by

$$ {}^{1}\dot{\underset{\sim}{E}}^{E} = ({}^{1}\underset{\sim}{F}^{E})^{T} \cdot \underset{\sim}{D}^{E} \cdot {}^{1}\underset{\sim}{F}^{E} \tag{3.7a} $$

$$ {}^{1}\dot{E}^{I} = ({}^{1}\underset{\sim}{F}^{I})^{T} \cdot \underset{\sim}{D}^{I} \cdot {}^{1}\underset{\sim}{F}^{I} \tag{3.7b} $$

where $\underset{\sim}{F}^{E}$ and $\underset{\sim}{F}^{I}$ are defined by Eq. (3.4) and Fig. 3.2. Eqs. (3.7a, b) imply that the strain rates are no longer additive.

Yaghmai [31] assumed that the rate of deformations were additive, but gave them the same invariance properties as $\underset{\sim}{D}$, i.e. using the deformation gradient ${}^{1}\underset{\sim}{F}$ in Eqs. (3.7a, b).

Equations (3.7a, b) are based on an extension of the transformation from rate of deformation to Lagrangian strain rate, Eq. (2.20). This transformation is based on purely kinematic considerations, while $\underset{\sim}{D}^{I}$ and $\underset{\sim}{D}^{E}$ are determined from the constitutive relations and do not in general satisfy kinematics. They may even be discontinuous. It seems therefore inconsistent to use the transformations in Eqs. (3.7a, b). By giving $\underset{\sim}{D}^{E}$ and $\underset{\sim}{D}^{I}$ the same invariance properties as $\underset{\sim}{D}$ the additivity of strain rates are also ensured. The only consequence of this assumption is that the constitutive relations for $\underset{\sim}{D}^{I}$ and $\underset{\sim}{D}^{E}$ must be formulated as to satisfy the principles of thermodynamics.

In a Lagrangian formulation the decomposition is most conveniently given in terms of the Lagrangian strain rates directly

$$ {}^{t}\dot{\underset{\sim}{E}} = {}^{t}\dot{\underset{\sim}{E}}^{E} + {}^{t}\dot{\underset{\sim}{E}}^{P} + {}^{t}\dot{\underset{\sim}{E}}^{C} \tag{3.8} $$

where the elastic, plastic and creep strain rates have the same invariance properties as ${}^{t}\dot{\underset{\sim}{E}}$. This form is used in the following development.

3.3 Uniaxial Creep Theories

The constitutive equations for creep deformations in materials can in general be written either on integral or differential form. The former has been used mainly for polymers, fibers and biological tissues. The latter is most commonly used for metals, and will be discussed here.

An extensive discussion of uniaxial creep theories for constant stress can be found in the references by Odquist and Hult [39], Finnie and Heller [40], and Rabotnov [42]. See also a review paper by Finnie [86].

The earliest work on creep of metals was mostly concerned with the steady-state creep. A number of creep laws were proposed, like

Bailey-Norton: $$ \dot{\epsilon}_c = B\sigma^n \tag{3.9} $$

Ludvig $$ \dot{\epsilon}_c = C e^{\sigma/\sigma_0} \tag{3.10} $$

Nadai: $$ \dot{\epsilon}_c = D \sinh(\sigma/\sigma_1) \tag{3.11} $$

where $\dot{\epsilon}_c$ is the creep strain rate and σ the applied stress. B, C, D, n, σ_0 and σ_1 are constants that may be temperature dependent.

For short time tests where the transient creep is dominant, the following form is widely used

$$\epsilon_c = A e^{B\sigma} t^k \tag{3.12}$$

where t is time since loading.

Odquist [43] gave a simplified creep law that included both the transient creep and the steady state using the following decomposition

$$\epsilon_c = \epsilon_c^i + \epsilon_c^d \tag{3.13}$$

Here ϵ_c^d is given by the steady-state creep law, and ϵ_c^i is the intercept on the strain axis obtained by extending the steady-state line back to zero time, Fig. 3.1. The term ϵ_c^i includes both the "equivalent" transient creep and the instantaneous plastic strain, and is given by a power law

$$\epsilon_c^i = (\sigma/\sigma_o)^m \tag{3.14}$$

Since ϵ_c^i represents an irrecoverable strain, it is only included during loading.

The previous laws do not provide for the inelastic behavior. Marin and Pao [87] observed that part of the primary creep strain was recoverable, and modified the transient creep law to include this effect. However, this formulation introduces two additional creep constants to be determined experimentally, which is a great disadvantage.

The primary motivation for many of these creep laws was their ease in computational use. In numerical methods such considerations are of minor importance, and more complicated laws can be used.

For transient problems like creep buckling problems the stresses will vary considerably, and the constant stress assumption above is no longer satisfied. The effect of a sudden increase in stress, $\Delta\sigma$, is illustrated for Eq. (3.12) in Fig. 3.3. Differentiation of Eq. (3.12) with respect to time gives

$$\dot{\epsilon}_c = k A e^{B\sigma} t^{k-1} \tag{3.15}$$

Solving for t from Eq. (3.12) and substituting into Eq. (3.15) gives

$$\dot{\epsilon}_c = k (A e^{B\sigma})^{\frac{1}{k}} \epsilon_c^{1-\frac{1}{k}} \tag{3.16}$$

where ϵ_c is the total accumulated creep strain. The "time-hardening" law (3.15) and the "strain-hardening" law (3.16) are equivalent when the stress is kept constant. Eq. (3.16) has in general been shown to be in better agreement with experimental results, and will be used in later numerical examples.

3.4 Flow Theory for Creep and Plasticity

Based on the physical causes of creep and plasticity of metals, certain similarities in the constitutive relations for these effects may be expected. The most important of these similarities is the use of the flow rule.

Using a constitutive relation of differential form the creep strain rate is in general given by

$$\dot{\epsilon}^c_{IJ} = \alpha_{IJ}(q_i) \tag{3.17}$$

where α_{IJ} is a symmetric tensor-valued function in terms of the internal variables q_i . The functional structure of α_{IJ} and the

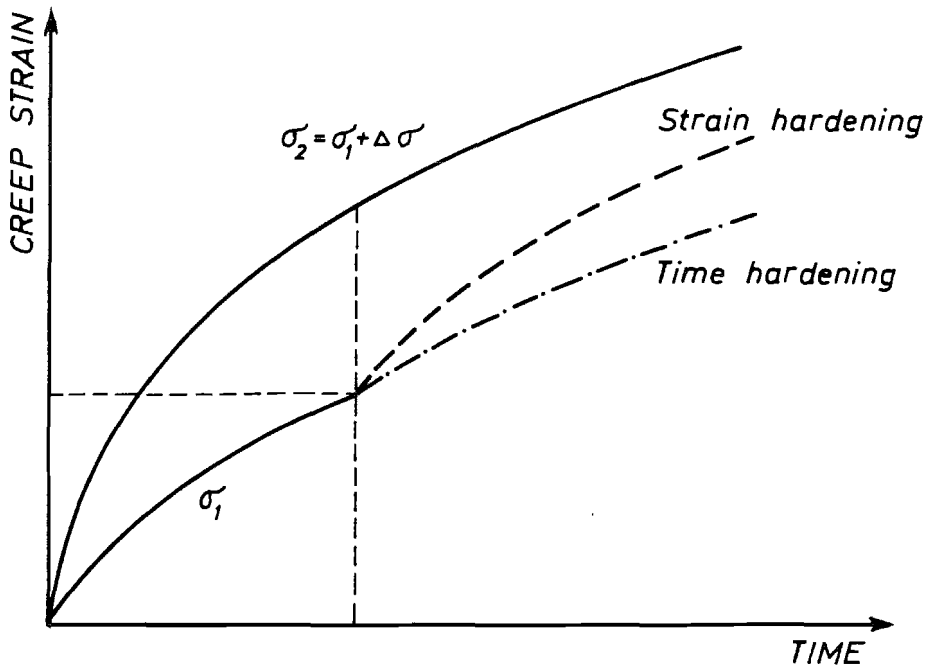

FIG. 3.3 TIME AND STRAIN HARDENING IN CREEP

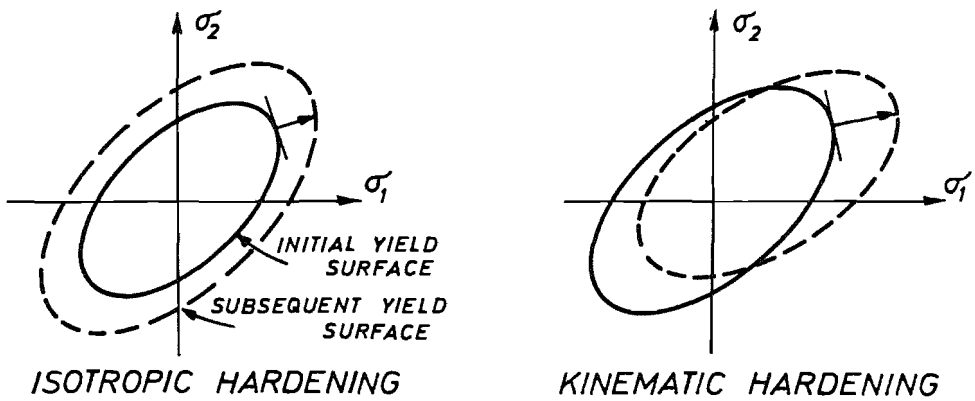

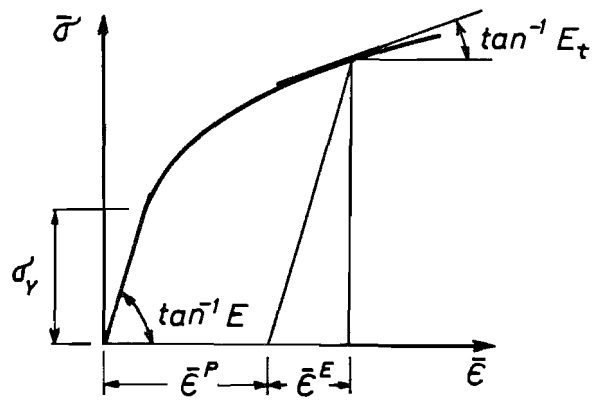

FIG. 3.4 HARDENING RULES IN PLASTICITY.

identification of the variables q_i may be quite general, but has to satisfy certain thermodynamical restrictions [84, 88].

Similarly the plastic strain rate is

$$ {}^1\dot{E}^P_{IJ} = \beta_{IJ}(P_i) \tag{3.18} $$

In the following a special case of the general theory will be considered, where

$$ \alpha_{IJ} = \frac{\partial \Phi}{\partial {}^1S_{IJ}} \tag{3.19} $$

$$ \beta_{IJ} = \dot{\lambda} \frac{\partial g}{\partial {}^1S_{IJ}} \tag{3.20} $$

Φ and g are the creep and plastic potentials, respectively, and $\dot{\lambda}$ is a non-negative scalar. Furthermore, the potentials are assumed to be convex, such that for uncoupled creep and plasticity effects

$$ ({}^1S_{IJ} - {}^1S^*_{IJ}) \frac{\partial \Phi}{\partial {}^1S_{IJ}} \geq 0 \tag{3.21} $$

$$ ({}^1S_{IJ} - {}^1S^*_{IJ}) \frac{\partial g}{\partial {}^1S_{IJ}} \geq 0 \tag{3.22} $$

for all points ${}^1S^*_{IJ}$ within or on the surfaces Φ and g in the 6-dimentional stress space. Eqs. (3.21) and (3.22) are merely restatements of Drucher's postulate, and are not a consequence of the thermodynamics of the process.

Following the infinitesimal theory of plasticity the plastic potential g is taken equal to the yield function f

$$ {}^1\dot{E}^P_{IJ} = \dot{\lambda} \frac{\partial f}{\partial {}^1S_{IJ}} \tag{3.23} $$

For steady state creep the potential Φ is only a function of the state of stress. During isotropic deformation Φ can furthermore be written in terms of the stress deviators.

$$\Phi = \Phi(J_2, J_3) \tag{3.24}$$

where

$$J_1 = {}^1\bar{S}_{II} \equiv 0$$
$$J_2 = \tfrac{1}{2}\,{}^1\bar{S}_{IJ}\,{}^1\bar{S}_{IJ} \tag{3.25}$$

and

$$J_3 = \tfrac{1}{3}\,{}^1\bar{S}_{IJ}\,{}^1\bar{S}_{JK}\,{}^1\bar{S}_{KI}$$

$${}^1\bar{S}_{IJ} = {}^1S_{IJ} - \delta_{IJ}\,{}^1S_{KK} \tag{3.26}$$

For many materials it is not necessary to allow for the influence of J_3 , and the von Mises theory of creep is obtained

$$\Phi = \Phi(\bar{\sigma}) \tag{3.27}$$

The equivalent stress $\bar{\sigma}$ is given by

$$\bar{\sigma} = \sqrt{3J_2} \tag{3.28}$$

Combining Eqs. (3.17), (3.19) and (3.27) gives

$${}^1\dot{E}^c_{IJ} = \frac{\partial \Phi}{\partial\, {}^1S_{IJ}} = \frac{\partial \Phi}{\partial \bar{\sigma}}\,\frac{3}{2\bar{\sigma}}\,{}^1\bar{S}_{IJ} \tag{3.29}$$

Eq. (3.29) gives the creep strain rate as a linear function of the stress deviator, and is equivalent to the Prandtl-Reuss equations.

For transient creep the more general form

$$\Phi = \Phi({}^1S_{IJ}, q_i) \tag{3.30}$$

should be used. This gives

$$ {}^{1}\dot{E}^{c}_{IJ} = \frac{\partial \Phi}{\partial {}^{1}S_{IJ}} + \frac{\partial \Phi}{\partial q_i}\frac{\partial q_i}{\partial {}^{1}S_{IJ}} \tag{3.31} $$

The two terms on the right side represent steady-state and transient creep respectively. Rabotnov [89] defined the internal variables through a linear differential equation

$$ dq_i = a_{iKL}\,{}^{1}E^{c}_{KL} + b_{iKL}\,{}^{1}S_{KL} + c_i\,t \tag{3.32} $$

where t is the time. According to the identification of the constants, time-hardening, strain-hardening or inelastic effects are obtained.

A special case is given by

$$ \Phi = \Phi({}^{1}S_{IJ}, {}^{1}E^{c}_{IJ}, {}^{1}E^{p}_{IJ}) \tag{3.33} $$

For isotropic deformations the invariants of stress and strain tensors are used. Following infinitesimal theory of plasticity two measures of hardening is possible.

The work-hardening parameter is given by

$$ K_c = K_c\left(\int_0^{{}^{1}E^{c}_{IJ}} dW_c\right) \tag{3.34} $$

$$ K_p = K_p\left(\int_0^{{}^{1}E^{p}_{IJ}} dW_p\right) \tag{3.35} $$

where the increment of creep and plastic work is given by

$$ dW_i = {}^{1}S_{IJ}\,{}^{1}\dot{E}^{i}_{IJ}\,dt = {}^{1}S_{IJ}\,E^{i}_{IJ} \tag{3.36} $$

with the superscript i indicating creep or plasticity.

The strain-hardening is similarly expressed by

$$K_c = K_c \left(\int_0^{{}^t\bar{\varepsilon}^c} d\bar{\varepsilon}^c \right) \tag{3.37}$$

$$K_p = K_p \left(\int_0^{{}^t\bar{\varepsilon}^p} d\bar{\varepsilon}^p \right) \tag{3.38}$$

with the equivalent creep and plastic strain defined as

$$d\bar{\varepsilon}^i = \left(\frac{2}{3} \dot{\varepsilon}^i_{IJ} \dot{\varepsilon}^i_{IJ} \right)^{1/2} \tag{3.39}$$

It should be noted that in the most general case a mixed invariant measure representing both creep and plasticity of the form $\varepsilon^p_{IJ} \varepsilon^c_{IJ}$ should be introduced.

The previous derivation was based on the existence of a creep potential Φ. A discussion of its existence based on micro- and macro-structural slip theory is given by Rice [90].

A more stringent constitutive equation for crystalline elastic-visco-plastic materials has been given by Kratochvil and Dillon [91] without using creep potential. This formulation utilizes thermodynamics with internal state variables related to crystal effects in the material. A similar formulation has also been proposed by Tseng [92]. However, at the present time these formulations are far too complex for use in analysis, and the material constants used in the constitutive equations are not available for most engineering materials.

3.5 Yield Function and Loading Criterion

The constitutive relations for viscoelastic/plastic solids have been discussed in detail by Naghdi and Murch [93], and Perzyna [94] for infinitesimal theory. These relationships will be extended here to the special case of small strains-large rotations. This extension is based on the use of the 2nd Piola-Kirchhoff (P-K) tensor, and the following postulate:

> The physical components of the Cauchy stress tensor in surface coordinates of the deformed shell are approximately equal to the components of the P-K tensor in the undeformed configuration.

The implication of this is that the mathematical representation of the yield function is the same in both the P-K and Cauchy stress space.

The yield function is given by a surface in the 6-dimensional stress space, and contains the origin. As in inviscid theory of plasticity this surface is convex [93, 94]. However, the plastic strain rate will only be normal to the instantaneous yield surface, which is determined from the time and path stress history.

During its path through the deformation space, the body is in configuration $\mathcal{B}_t$ at time t. In this configuration the yield function is given by

$$f({}^t S_{IJ}, {}^t E^P_{IJ}, {}^t E^C_{IJ}, \mathcal{H}) = 0 \tag{3.40}$$

where $\mathcal{H}$ is a hardening parameter that depends on the whole deformation history of the body. Contrary to the inviscid theory of plasticity f will vary with time even when the stress is kept constant. This is due to the dependence on time through the creep strain ${}'E^c_{IJ}$.

For initially isotropic materials with isotropic hardening Eq. (3.40) can be rewritten

$$f = F({}'s_{IJ}) - \mathcal{H}({}'E^c_{IJ}, {}'E^p_{IJ}) = 0 \tag{3.41}$$

Eq. (3.41) implies that the shape of the yield surface is retained but undergoes a uniform expansion in stress space, Fig. 3.4. This hardening rule, however, does not account for the Bauschinger effect.

Assuming that creep deformations do not alter the initial yield stress, the von Mises condition for initial yielding is

$$F({}'s_{IJ}) = J_2 = k^2 \tag{3.42}$$

where J_2 is given by Eq. (3.28) and k is the initial yield stress in pure shear.

The hardening parameter $\mathcal{H}$ may also be taken as

$$\mathcal{H}({}'E^c_{IJ}, {}'E^p_{IJ}) = \mathcal{H}(\kappa_c, \kappa_p) \tag{3.43}$$

where κ_c and κ_p are defined by Eqs. (3.34) to (3.38).

Following infinitesimal theory of inviscid plasticity [95], the following types of behavior can be defined

i) Loading

ii) Neutral loading

iii) Unloading

For an elastic state $f<0$, for a plastic state $f=0$, while $f>0$ constitutes an inadmissible state.

The time rate of f is given by

$$\dot{f} = \frac{\partial f}{\partial {}'S_{IJ}} {}'\dot{S}_{IJ} + \frac{\partial f}{\partial {}'E^{c}_{IJ}} {}'\dot{E}^{c}_{IJ} + \frac{\partial f}{\partial {}'E^{P}_{IJ}} {}'\dot{E}^{P}_{IJ} \tag{3.44}$$

Associated with the plastic state three paths of actions are possible.

Unloading is characterized by zero plastic strain rate, ${}'\dot{E}^{P}_{IJ} = 0$, and is characterized by $f=0$ and $\dot{f}<0$. From Eq. (3.44) the criterion for unloading is determined as

$$\frac{\partial f}{\partial {}'S_{IJ}} {}'\dot{S}_{IJ} + \frac{\partial f}{\partial {}'E^{c}_{IJ}} {}'\dot{E}^{c}_{IJ} < 0 \tag{3.45}$$

Neutral loading is a change from one plastic state to another without change in the plastic strain rate, i.e., $f=0$, $\dot{f}=0$

$$\frac{\partial f}{\partial {}'S_{IJ}} {}'\dot{S}_{IJ} + \frac{\partial f}{\partial {}'E^{c}_{IJ}} {}'\dot{E}^{c}_{IJ} = 0 \tag{3.46}$$

Loading is a change from one plastic state to another accompanied with strain hardening; $f=0$, $\dot{f}=0$

$$\frac{\partial f}{\partial {}'S_{IJ}} {}'\dot{S}_{IJ} + \frac{\partial f}{\partial {}'E^{c}_{IJ}} {}'\dot{E}^{c}_{IJ} > 0 \tag{3.47}$$

Note that in contrast to inviscid plasticity the time enters as a parameter in the loading criterion through the creep rate.

3.6 Incremental Stress-Strain Relationships

The plastic strain increment E^P_{IJ} is known as soon as the proportionality factor $\dot{\lambda}$ in Eq. (3.23) is determined

$$E^P_{IJ} = d(\,'E^P_{IJ}) = \dot{\lambda}\, dt\, \frac{\partial f}{\partial\, 'S_{IJ}} = d\lambda\, \frac{\partial f}{\partial\, 'S_{IJ}} \qquad \text{(a)}$$

In the plastic state $d\lambda$ can be determined by substituting Eq. (a) into Eq. (3.44), and setting the latter equal to zero. Replacing the rate quantities with the incremental variables gives

$$d\lambda = -\alpha \left(\frac{\partial f}{\partial\, 'S_{IJ}}\, S_{IJ} + \frac{\partial f}{\partial\, 'E^c_{IJ}}\, E^c_{IJ} \right) \qquad (3.48)$$

where

$$\alpha^{-1} = \frac{\partial f}{\partial\, 'E^P_{IJ}}\, \frac{\partial f}{\partial\, 'S_{IJ}}$$

Substituting Eq. (3.48) into Eq. (a) one gets

$$E^P_{IJ} = -\alpha\, \frac{\partial f}{\partial\, 'S_{IJ}} \left(\frac{\partial f}{\partial\, 'S_{KL}}\, S_{KL} + \frac{\partial f}{\partial\, 'E^c_{IJ}}\, E^c_{KL} \right) \qquad (3.49)$$

Eq. (3.49) gives the increment in plastic strain as a linear function of the increments in stress and creep strains.

In a displacement formulation the relationship between increments of stress and strain is needed. This may be obtained by inverting Eq. (3.49) numerically and combining the result with the generalized Hooke's law:

$$S_{IJ} = E_{IJKL} \left(E_{KL} - E^c_{KL} - E^P_{KL} \right) \qquad (3.50)$$

where

$$E_{IJKL} = \mu(\delta_{IK}\delta_{JL} + \delta_{IL}\delta_{JK}) + \lambda\,\delta_{IJ}\,\delta_{KL} \tag{3.51}$$

The Lamé constants μ and λ are given in section 2.7.

In the theory of plasticity the incremental stress-strain relationship may be obtained directly without numerical inversion. This is due to the restriction, $df = 0$, that is imposed on the yield function during plastic deformations.

$$df = \frac{\partial f}{\partial' s_{IJ}}\, s_{IJ} + \frac{\partial f}{\partial' E^c_{IJ}} E^c_{IJ} + \frac{\partial f}{\partial' E^p_{IJ}} E^p_{IJ} = 0 \tag{b}$$

Combining Eqs. (a), (b) and (3.50) one gets

$$d\lambda = h\left(\frac{\partial f}{\partial' s_{IJ}} E_{IJKL} E_{KL} + \left(\frac{\partial f}{\partial' E^c_{KL}} - \frac{\partial f}{\partial' s_{IJ}} E_{IJKL}\right) E^c_{KL}\right) \tag{c}$$

where

$$h^{-1} = \frac{\partial f}{\partial' s_{IJ}} \frac{\partial f}{\partial' s_{KL}} E_{IJKL} - \frac{\partial f}{\partial' s_{IJ}} \frac{\partial f}{\partial' E^p_{IJ}} \tag{d}$$

An alternative expression to Eq. (3.49) is now obtained by substitution of Eqs. (c) and (d) into Eq. (a).

$$E^p_{IJ} = A_{IJKL}\, E_{KL} + F_{IJKL}\, E^c_{KL} \tag{3.52}$$

where the following definitions are given

$$A_{IJKL} = h \frac{\partial f}{\partial' s_{IJ}} \frac{\partial f}{\partial' s_{MN}} E_{MNKL} \tag{3.53}$$

$$F_{IJKL} = h \frac{\partial f}{\partial' S_{IJ}} \frac{\partial f}{\partial' E^c_{KL}} - A_{IJKL} \tag{3.54}$$

The incremental stress-strain law is obtained by Eqs. (3.50), (3.52), (3.53), and (3.54) as

$$S_{IJ} = C_{IJKL} E_{KL} - H_{IJKL} E^c_{KL} \tag{3.55}$$

with

$$C_{IJKL} = E_{IJKL} - E_{IJMN} A_{MNKL} \tag{3.56}$$

and

$$H_{IJKL} = E_{IJMN} F_{MNKL} + E_{IJKL} \tag{3.57}$$

Note that in the case of elastic-creep deformations without plastic strains occurring

$$C_{IJKL} = H_{IJKL} \tag{3.58}$$

Using von Mises yield criterion and isotropic hardening the following relations hold

$$\begin{aligned} \frac{\partial f}{\partial' S_{IJ}} &= \frac{3}{2\bar{\sigma}} {}' S_{IJ} \\ \frac{\partial f}{\partial' E^P_{IJ}} &= \frac{\partial f}{\partial \bar{\epsilon}^P} \frac{\partial \bar{\epsilon}^P}{\partial W_P} \frac{\partial W_P}{\partial' E^P_{IJ}} = -\frac{1}{\bar{\sigma}} H' {}' S_{IJ} \\ \frac{\partial f}{\partial' E^c_{IJ}} &= \frac{\partial f}{\partial \bar{\epsilon}^c} \frac{\partial \bar{\epsilon}^c}{\partial W_c} \frac{\partial W_c}{\partial' E^c_{IJ}} = -\frac{1}{\bar{\sigma}} H'' {}' S_{IJ} \end{aligned} \tag{3.59}$$

where

$$H' = \frac{\partial f}{\partial \bar{\epsilon}^p} \quad \text{and} \quad H'' = \frac{\partial f}{\partial \bar{\epsilon}^c}$$

Here H' can be determined from a simple uniaxial tension test for a given amount of creep hardening

$$\frac{1}{H'} = \frac{1}{E} - \frac{1}{E_t} \tag{3.60}$$

where the tangent modulus E_t is given by $E_t = \frac{d\bar{\sigma}}{d\bar{\epsilon}}$

Similarly H'' can be determined from a plot of the hardening parameter versus the equivalent creep strain $\bar{\epsilon}^c$ when the plastic strain is kept constant.

$$\frac{1}{H''} = \frac{1}{E} - \frac{1}{E_t}$$

Since H' and H'' are strongly dependent on the accumulated creep and plastic hardening respectively, such tests are not readily available today.

Define

$$\eta = \frac{E_t}{E}$$

which gives

$$h = \frac{1}{3\mu + H'} = \frac{2(1+\nu)(1-\eta)}{E(3-\eta(1-2\nu))} \tag{3.61}$$

With this notation one gets

$$A_{IJKL} = \frac{9}{2}\mu h \, \frac{1}{\bar{\sigma}^2} \, {}'\bar{S}_{IJ} \, {}'\bar{S}_{KL} \tag{3.62}$$

$$C_{IJKL} = \mu(\delta_{IK}\delta_{JL} + \delta_{IL}\delta_{JK}) + \lambda \delta_{IJ}\delta_{KL} - 9\mu^2 h \, \frac{1}{\bar{\sigma}^2} \, {}'\bar{S}_{IJ} \, {}'\bar{S}_{KL} \tag{3.63}$$

Note that both A_{IJKL} and C_{IJKL} are functions of the total creep strain.

From Eqs. (3.54) and (3.57) one finally gets

$$F_{IJKL} = -\frac{3}{2\bar{\sigma}^2}\frac{1}{3\mu+H'}{}^1\bar{S}_{IJ}\left(H''\,{}^1S_{KL}+3\mu\,{}^1\bar{S}_{KL}\right) \tag{3.64}$$

$$H_{IJKL} = \mu\left(\delta_{IK}\delta_{JL}+\delta_{IL}\delta_{JK}\right)+\lambda\delta_{IJ}\delta_{KL} - \\ -\frac{3}{\bar{\sigma}^2}\frac{\mu}{3\mu+H'}{}^1\bar{S}_{IJ}\left(H''\,{}^1S_{KL}+3\mu\,{}^1\bar{S}_{KL}\right) \tag{3.65}$$

Finally, Eqs. (3.62) to (3.65) must be modified to the generalized plane stress state used in the shell application.

3.7 Odquist's Creep Theory

A less stringent method for treating the combined creep and plasticity problem was proposed by Odquist [43]. Considering the primary creep strain as an instantaneous irreversible deformation, he combines this with the instantaneous plastic deformation. However, no coupling between creep and plasticity was accounted for in the formulation of the yield criterion.

Using the Prandtl-Reuss equations, a linear relationship is assumed between the instantaneous inelastic strain increment E^{IC}_{IJ} and the deviator of the stress increment

$$E^{IC}_{IJ} = K\left(\frac{\bar{\sigma}}{\sigma_K}\right)^K \frac{3}{2\bar{\sigma}}\bar{S}_{IJ} \tag{3.66}$$

where

$$E^{IC}_{IJ} = E^{P}_{IJ} + E^{TC}_{IJ}$$

with E^{TC}_{IJ} being the increment of transient (primary) creep.

Since E_{IJ}^{IC} is considered to be irrecoverable, Eq. (3.66) is only applicable during loading. The loading criterion is here not based on the concept of a yield function, but was proposed by Odquist to be:

$$\begin{aligned} &\text{Loading :} \quad \bar{\sigma}\, d\bar{\sigma} > 0 \\ &\text{Unloading :} \quad \bar{\sigma}\, d\bar{\sigma} < 0 \end{aligned} \tag{3.67}$$

Taking the total differential of Eq. (3.28) one gets

$$d\bar{\sigma} = \frac{\partial \bar{\sigma}}{\partial' \bar{S}_{IJ}}\, \bar{S}_{IJ}$$

which transforms Eqs. (3.67) to

$$\bar{\sigma} d\bar{\sigma} = \frac{3}{2\bar{\sigma}}\, {}'\bar{S}_{IJ}\, \bar{S}_{IJ} \geq 0 \tag{3.68}$$

It should be noted that Eq. (3.68) is similar to the loading criterion used in the theory of inviscid plasticity. However, the concept of neutral loading and yielding has no meaning here. Even though plastic deformations strictly occur only when $f = 0$, the transient creep deformation takes place independently of the value of the yield function f. Eq. (3.66) is not capable of separating the two phenomena.

When using a displacement formulation the incremental form of the stress-strain relationship must be determined. In the theory of inviscid plasticity this relationship may be obtained directly through the use of the yield function. Such an approach, however, is not possible in Odquist's method unless additional postulates regarding the existence of a yield function are introduced. The incremental stress-strain relationship must therefore be obtained by numerical inversion of Eq. (3.66) and

the generalized Hooke's law:

$$E^{e}_{IJ} = \frac{1}{2G'}\left(S_{IJ} - \frac{\nu}{1+\nu}\,\delta_{IJ}\,S_{KK}\right)$$

where the shear modulus G' is given by

$$G' = \frac{E'}{2(1+\nu)}$$

The instantaneous tangent modulus E' is defined by [41]

$$E' = \frac{d\bar{\sigma}}{d\bar{\epsilon}_i} \tag{3.69}$$

where $\bar{\epsilon}_i$ is the instantaneous strain due to the elastic and primary creep response.

Defining

$$\eta = K\left(\frac{\bar{\sigma}}{\sigma_K}\right)^{r}\frac{3}{2\bar{\sigma}}$$

one gets

$$E_{IJ} = \frac{1}{2G'}\left(S_{IJ} - \frac{\nu}{1+\nu}\,\delta_{IJ}\,S_{KK}\right) + \eta\,\bar{S}_{IJ} + E^{c}_{IC}$$

where E^{c}_{IJ} is the steady state creep strain. This can be written as

$$E_{IJ} = G_{IJKL}\,S_{KL} + E^{c}_{IJ} \tag{3.70}$$

For axisymmetric deformations the strain-stress matrix G_{IJKL} is given by

$$[G]\begin{bmatrix} \left(\frac{1}{E'}+\frac{2}{3}\eta\right) & \left(-\frac{\nu}{E'}-\frac{1}{3}\eta\right) & \left(-\frac{\nu}{E'}-\frac{1}{3}\eta\right) & 0 \\ & \left(\frac{1}{E'}+\frac{2}{3}\eta\right) & \left(-\frac{\nu}{E'}-\frac{1}{3}\eta\right) & 0 \\ \text{Symmetric} & & \left(\frac{1}{E'}+\frac{2}{3}\eta\right) & 0 \\ & & & \left(\frac{1}{G'}+\eta\right) \end{bmatrix} \tag{3.71}$$

By inverting Eq. (3.71) the stress-strain relationship is obtained on the form

$$S_{IJ} = C_{IJKL} (E_{KL} - E^{c}_{KL}) \tag{3.72}$$

where

$$C_{IJKL} = G^{-1}_{IJKL} \tag{3.73}$$

3.8 Generalized Plane Stress

In thin shell and moderately thick shell applications the stress-strain relations in a state of generalized plane stress are needed.

For this purpose, Eqs. (3.56) or (3.65) must be modified.

For axisymmetric deformations we assume

$$^{1}S_{12} = {}^{1}S_{23} = {}^{1}S_{33} = 0$$

$$S_{12} = S_{23} = S_{33} = 0$$

$$E_{12} = E_{23} = 0$$

Hence

$$S_{IJ} = C_{IJKL} E_{KL} + C_{IJ33} E_{33} \tag{3.74}$$

and

$$S_{33} = C_{33KL} E_{KL} + C_{3333} E_{33} \tag{3.75}$$

Solving for E_{33} from Eq. (3.75) and substituting into Eq. (3.74) gives

$$S_{IJ} = \bar{C}_{IJKL} E_{KL} \tag{3.76}$$

with

$$\bar{C}_{IJKL} = C_{IJKL} - C_{IJ33} \frac{C_{33KL}}{C_{3333}} \tag{3.77}$$

In the calculations this modification will be done numerically using Gaussian elimination. Similarly Eqs. (3.53) and (3.54) must be modified for plane stress.

3.9 Some Remarks on the Creep-Plasticity Interaction

The interaction between creep and plastic deformations in metals is very complex, and is difficult to formulate mathematically within the scope of creep potentials and yield functions.

It has been found that small prior plastic deformations do not harden the material relative to creep at stresses below the proportionality level [42]. Large plastic deformations, however, have significant effect on creep deformations. On the other hand, the creep behavior of a given material is changed substantially when subjected to stresses above the proportionality level. This is observed in tests both for aluminum alloys and steel.

Conversely, previous creep deformations have a significant effect on the instantaneous stress-strain characteristics of most materials. This is illustrated in Fig. 3.5, where a specimen is loaded to a stress level above the proportionality level. The

stress is then kept constant for some time, during which the creep strain ϵ^c is accumulated. Upon instantaneous reloading a new tangent modulus is obtained [42]. This indicates that the effect of creep hardening on the modulus E_t in Eq. (3.60) is of particular interest. Berkovits [96] studied this problem for commercially pure aluminum by subjecting a constant bending creep specimen to a sudden stress change after creep had taken place. In general, the tangent modulus obtained after several hours of creep was approximately equal to the elastic modulus, both for increasing and decreasing stress. Fig. 3.6 shows the variation of the ratio E/E_t as a function of time, as given by Berkovits. As can be seen, recovery has taken place within a very short time (or after a small amount of creep deformation).

This phenomenon can be explained from the changes in the microstructure of the material. Due to dislocation motions and vacancy migration during creep the number of mobile dislocations at the time of the stress change is much lower than when the creep deformation was initiated in the inelastic range. It has been surmised that the number of mobile dislocations after creep has taken place is approximately of the same order as for the initially elastic material. This explains the high tangent modulus that is observed in Figs. 3.5 and 3.6. It should be noted, however, that if the stress increase is large enough dislocation multiplications might take place, resulting in a lower modulus.

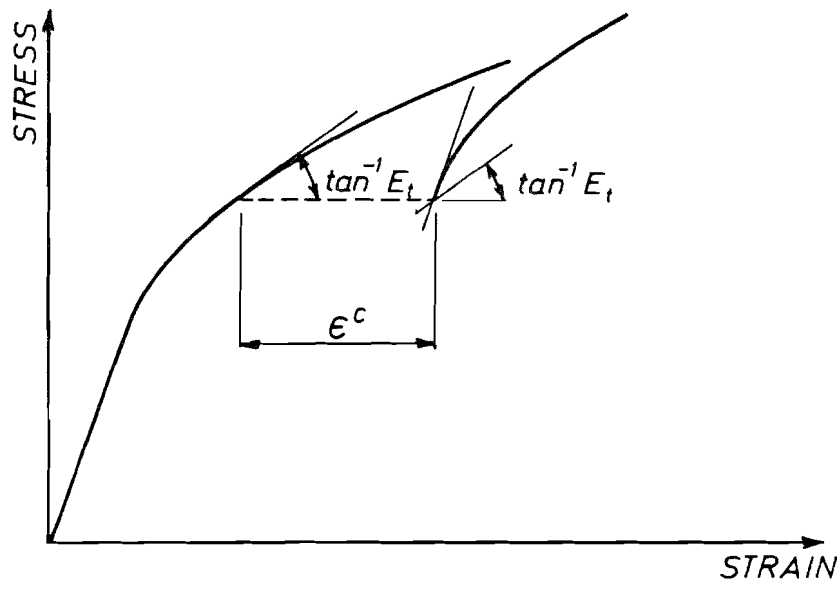

FIG. 3.5 INSTANTANEOUS STRESS-STRAIN CURVE

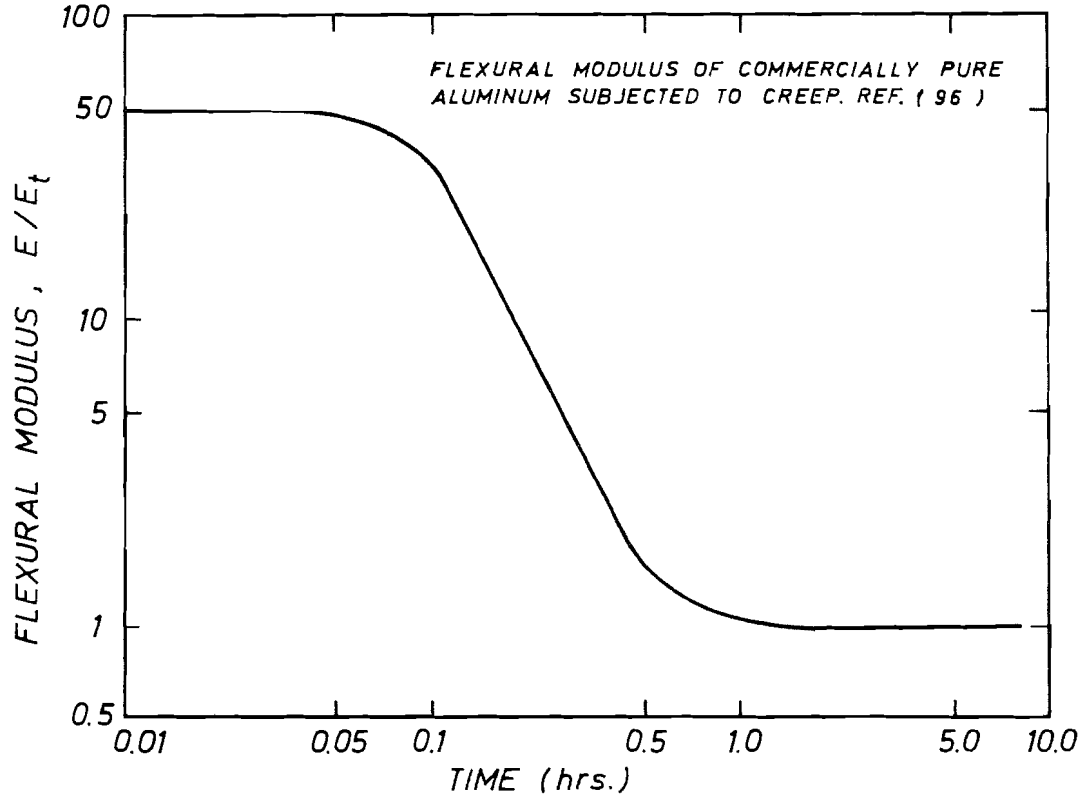

FIG. 3.6 FLEXURAL MODULUS DURING CREEP.

Based on these observations it is clear that the problem of creep-plasticity interaction is very complex. The phenomenon is difficult to describe mathematically, and much work remains to be done before the problem is resolved.

4. AN APPROXIMATE SOLUTION TO PROBLEMS IN FINITE LINEAR VISCOELASTICITY

4.1 Constitutive Equations for Linear and Finite Linear Viscoelasticity

The theory of linear viscoelasticity for infinitesimal deformations is well known, and is presented in a number of texts [97, 98, 99, 100]. A brief review of this theory will be given here, as well as its extensions to geometrically nonlinear applications. The presentation will be restricted to isothermal conditions and quasi-static deformation of isotropic materials.

The basic hypothesis of the classical theory is that the present state of stress σ_{ij} is a function not only of the present state of strain ϵ_{ij}, but also of the past strain history. Mathematically this is expressed by

$$\sigma_{ij}(t) = \underset{s=0}{\overset{t}{\Psi_{ij}}} \left[\epsilon_{kl}(t-s), \epsilon_{kl}(t) \right] \tag{4.1}$$

where Ψ_{ij} is a linear tensor-valued functional that transforms each strain history $\epsilon_{ij}(t)$, $-\infty \le t \le \infty$ into a corresponding stress history. For a continuous strain history Riesz representation theorem may be used to write Equation (4.1) as a Stieltjes integral

$$\sigma_{ij}(t) = \int_0^t G_{ijkl}(t-\tau) \frac{d}{d\tau} \epsilon_{kl}(\tau)\, d\tau \tag{4.2}$$

The integrating function G_{ijkl} is a fourth order tensor, commonly denoted the relaxation function. Equation (4.2) is invariant under time shifts, and is hence restricted to non-aging materials. A discontinuous strain history may be included by integrating the

Dirac delta function.

$$\sigma_{ij}(t) = G_{ijkl}(t)\,\epsilon_{kl}(0) + \int_0^t G_{ijkl}(t-\tau)\,\frac{d}{d\tau}\,\epsilon_{kl}(\tau)\,d\tau \qquad (4.3)$$

The concept of fading memory was defined in a mathematical sense by Truesdell and Noll [4]. From pure physical considerations the concept is based on the postulate that the stress is more strongly dependent on the recent strain history than the distant history. In terms of the integrating function this is expressed by

$$\left| \frac{d}{dt}\, G_{ijkl} \right|_{t=t_1} \leq \left| \frac{d}{d\tau}\, G_{ijkl} \right|_{t=t_2} \quad ; \quad t_1 > t_2 > 0$$

The concept of fading memory is of paramount importance since it reduces the number of past strain histories that must be stored for the evaluation of the convolution integrals in Eqs. (4.2) or (4.3).

It is well known that any isotropic fourth order tensor can be represented by

$$G_{ijkl} = \tfrac{1}{3}\,(G_2 - G_1)\,\delta_{ij}\,\delta_{kl} + \tfrac{1}{2}\,G_1\,(\delta_{ik}\,\delta_{jl} + \delta_{il}\,\delta_{jk})$$

where G_1 and G_2 are independent functions. In the present context they are the shear and bulk relaxation moduli respectively. Using this, Eq. (4.3) may be recast

$$\sigma'_{ij}(t) = G_1(t)\,\epsilon'_{ij}(0) + \int_0^t G_1(t-\tau)\,\frac{d}{d\tau}\,\epsilon'_{ij}(\tau)\,d\tau \qquad (4.4)$$

$$\sigma_{kk}(t) = G_2(t)\,\epsilon_{kk}(0) + \int_0^t G_2(t-\tau)\,\frac{d}{d\tau}\,\epsilon_{kk}(\tau)\,d\tau \qquad (4.5)$$

where the deviatoric tensors are given by

$$\sigma_{ij}' = \sigma_{ij} - \frac{1}{3}\delta_{ij}\sigma_{kk}$$

$$\epsilon_{ij}' = \epsilon_{ij} - \frac{1}{3}\delta_{ij}\epsilon_{kk}$$

This formulation is advantageous for many polymeric materials, where the shear effect is highly viscoelastic while the bulk behavior is almost elastic.

The theory of nonlinear viscoelasticity has many features in common with the infinitesimal theory, the most important one being the memory hypothesis. However, for finite deformations the more stringent definitions of stress and strain must be used, conf. Chapter 2. Furthermore, the formulation should satisfy the principles of determinism, local action and material frame indifference. The latter meaning that the constitutive equations should be invariant under change of frame of reference.

The most general formulation starts from the Clausis-Duhem inequality [99] and gives*)

$$^1S_{IJ} = \rho_0 \frac{\partial\, ^1A}{\partial\, ^1E_{IJ}} \tag{4.6}$$

where the stored energy ^1A per unit mass is a functional of the type

$$^1A = \overset{t}{\underset{s=0}{\Psi}} \left[E_{KL}(t-s),\, E_{KL}(t) \right] \tag{4.7}$$

*) In this chapter all derivations will be made in rectangular Cartesian coordinates.

Assuming the functional to be Fréchet differentiable and continuous in the strain history the proper derivatives may be obtained.

However, Eqs. (4.6) and (4.7) are far too general for practical use. Attempts have therefore been made to obtain integral equations of the form (4.3), that satisfy the general principles listed above. This leads to a constitutive theory commonly denoted finite linear viscoelasticity [4], [101]. Here no restrictions are imposed on the magnitude of deformations.

Truesdell and Noll [4] gave the response as a function of the deformation history measured with respect to the current configuration

$$\underset{\sim}{R}^T \cdot \underset{\sim}{T} \cdot \underset{\sim}{R} = \underset{\sim}{f}(\underset{\sim}{C}) + \sum_{s=0}^{\infty} \underset{\sim}{F} [\underset{\sim}{G}^*(s), \underset{\sim}{C}] \tag{4.8}$$

where

$$\underset{\sim}{G}^*(s) = \underset{\sim}{C}^*_{(t)}(t-s) - \underset{\sim}{I}$$

and

$$\underset{\sim}{C}^*_{(t)}(\tau) = \underset{\sim}{R}^T(t) \cdot \underset{\sim}{C}_{(t)}(\tau) \cdot \underset{\sim}{R}(t)$$

$\underset{\sim}{C}_{(t)}$ is the relative right Cauchy-Green deformation tensor [4].

The polar decomposition theorem gives

$$\underset{\sim}{F} = \underset{\sim}{R} \cdot \underset{\sim}{U}$$

and

$$\underset{\sim}{C} = \underset{\sim}{F}^T \cdot \underset{\sim}{F} = \underset{\sim}{U}^2$$

$$\underset{\sim}{U} = \underset{\sim}{C}^{1/2}$$

where the rotation tensor $\underset{\sim}{R}$ is orthogonal and $\underset{\sim}{U}$ is the symmetric and positive definite stretch tensor. In order to obtain $\underset{\sim}{R}$ the square root of $\underset{\sim}{C}$ must be computed and then inverted numerically. This is a very time consuming operation that makes Eq. (4.8) quite cumbersome in practical applications.

An alternative formulation is used by Fredrickson and Lodge [102], [103], [104], using Eq. (4.3). The stresses σ_{ij} and strains ϵ_{ij} were here referred to convected coordinates. The formulation satisfies the invariance requirements, but the use of convected strain rate is quite inconvenient.

Rivlin [105] suggested the following form

$$ {}^{1}S_{IJ}(t_1) = \overset{t_1}{\underset{s=0}{\Psi_{IJ}}} \left[C_{KL}(t_1 - s), C_{KL}(t_1) \right] \tag{4.9} $$

Equation (4.9) may be considered as a restatement of Eq. (4.6), and indicates kinematical and mathematical variables necessary for an invariant formulation.

Assuming the functional Ψ_{IJ} to be linear and of integral type one may write

$$ {}^{1}S_{IJ}(t_1) = G_{IJKL}(t_1) E_{KL}(0) + \int_0^{t_1} G_{IJKL}(t-\tau) \frac{d}{d\tau} E_{KL}(\tau)\, d\tau \tag{4.10} $$

Equation (4.10) is a direct extension of Eq. (4.3) that satisfies all invariance principles. The equation also reduces to Eq. (4.3) for infinitesimal deformations.

G_{IJKL} should be identified from experimental results of finite strain tests. However, for small strain, large rotation applications the relaxation function G_{IJKL} may be approximated by G_{ijkl} without loss of accuracy. G_{ijkl} is assumed known from infinitesimal strain test for the material at hand.

The integrating function G_{IJKL} and the strain increment E_{KL} are both given with respect to fixed base vectors in configuration $\mathcal{B}_o$. This is a necessity for the evaluation of the integral in Eq. (4.10), since the integral is the limit of a summation process. Any attempt to write an integral constitutive relation of type (4.10) in terms of Cauchy stress and rate-of-deformation is therefore impossible.

4.2 Method of Solution

Solutions to boundary value problems for materials described by the infinitesimal theory of linear viscoelasticity have been given in the literature [106, 49, 107, 51]. The solutions of large displacement problems have been given in reference [64, 65].

For most initial boundary value problems the spatial discretization of the system is most conveniently obtained by the finite element method. This reduces the equilibrium equations to a set of simultaneous integral equations. The size of this set will in most cases prohibit the use of integral transform methods, and a step-forward integration scheme is the only recourse. In this method the kinematic rate quantities must be approximated by some finite difference formula.

The mathematical representation of the relaxation function from the experimental test data will greatly influence the computational effort in the evaluation of the convolution integral. Even for materials possessing a fading memory a finite number of past solutions must be retained. The objective is therefore to obtain a recursive algorithm reducing the number of past solutions needed for the integration process. Such algorithms have been proposed by Chang [49] and Selna [48].

The simplest recursive algorithm available may be formulated for generalized Maxwell type materials where the relaxation moduli may be represented by a Prony series

$$G_\alpha(t) = G_\alpha^0 + \sum_{i=1}^{I} G_\alpha^i e^{-t/\lambda_i} \quad ; \quad \alpha = 1,2 \tag{4.11}$$

where G_1 and G_2 are the shear and bulk moduli respectively. G_α^0 is the equilibrium value obtained when $t \to \infty$, and λ_i may be interpreted as discrete relaxation times. I is the number of generalized Maxwell elements in the representation.

The advantage of this representation is that only the solution from the previous step has to be retained. The algorithm used here was given by Taylor, et al [51], and is shown here for the sake of simplicity for a uniaxial case.

Let the body occupy configuration $\mathcal{B}_n$ at time t_n , at which time the stress and strain are given by σ_n and ϵ_n . Substituting the uniaxial version of Eq. (4.11) into Eq. (4.10) gives

$$\sigma_n = \sigma(t_n) = G_0\,\epsilon(t_n) + \sum_{i=1}^{I} G_i\, e^{-t_n/\lambda_i}\,\epsilon(0) + \int_0^{t_n} \sum_{i=1}^{I} G_i\, e^{-(t_n-\tau)/\lambda_i}\,\frac{d}{d\tau}\epsilon(\tau)\,d\tau \qquad (4.12)$$

The integral may be decomposed by

$$\int_0^{t_n} (\cdots\cdots)\,d\tau = \sum_{k=1}^{n} \int_{t_{k-1}}^{t_k} (\cdots\cdots)\,d\tau$$

Consider one term in this series

$$\int_{t_{j-1}}^{t_j} \sum_{i=1}^{I} G_i\, e^{-(t_n-\tau)/\lambda_i}\,\frac{d}{d\tau}\epsilon(\tau)\,d\tau = \sum_{i=1}^{I} G_i\, e^{-(t_n-t_j)/\lambda_i} \int_{t_{j-1}}^{t_j} e^{-(t_j-\tau)/\lambda_i}\,\frac{d}{d\tau}\epsilon(\tau)\,d\tau \qquad (a)$$

Assuming the strain to vary linearly within the time interval $< t_{j-1}\,,\ t_j >$, the strain rate may be approximated by

$$\frac{d}{d\tau}\epsilon(\tau) = \frac{1}{\Delta t_j}\,d\epsilon(t_j) \qquad (b)$$

with

$$d\epsilon(t_j) = \epsilon(t_j) - \epsilon(t_{j-1})$$

$$\Delta t_j = t_j - t_{j-1}$$

Define

$$h_i(\Delta t_j) = \int_{t_{j-1}}^{t_j} \frac{1}{\Delta t_j}\, e^{-(t_j-\tau)/\lambda_i}\,d\tau = \frac{1}{\Delta t_j}\,(1 - e^{-\Delta t_j/\lambda_i}) \qquad (c)$$

Combining these expressions, Eq. (a) becomes

$$\int_{t_{j-1}}^{t_j} (\cdots\cdots)\,d\tau = \sum_{i=1}^{I} e^{-(t_n-t_j)/\lambda_i}\, h_i(\Delta t_j)\, d\epsilon(t_j) \qquad (d)$$

Equation (4.12) may now be recast into

$$\sigma_n = \left[G_0 + \sum_{i=1}^{I} G_i\, h_i(\Delta t_n) \right] d\epsilon(t_n) + \sum_{i=1}^{I} G_i\, e^{-\Delta t_n/\lambda_i}\, \epsilon(0) + G_0\, \epsilon(t_{n-1}) + \sum_{j=1}^{n-1} \sum_{i=1}^{I} G_i\, e^{-(t_n - t_j)/\lambda_i}\, h_i(\Delta t_j)\, d\epsilon(t_j) \tag{4.13}$$

Further simplifications are possible by defining

$$g_i(t_n) = G_i \left[e^{-t_n/\lambda_i}\, \epsilon(0) + \sum_{j=1}^{n-1} e^{-(t_n - t_j)/\lambda_i}\, h_i(\Delta t_j)\, d\epsilon(t_j) \right] \qquad n \geq 1 \tag{e}$$

or recursively

$$g_i(t_n) = e^{-\Delta t_n/\lambda_i} \left[g_i(t_{n-1}) + G_i\, h_i(\Delta t_{n-1})\, d\epsilon(t_{n-1}) \right] \qquad n \geq 1 \tag{f}$$

Equation (4.13) and (f) gives

$$\sigma_n = \left[G_0 + \sum_{i=1}^{I} G_i\, h_i(\Delta t_n) \right] d\epsilon(t_n) + G_0\, \epsilon(t_{n-1}) + \sum_{i=1}^{I} g_i(t_n) \tag{4.14}$$

Here $d\epsilon(t_n)$ is the strain increment between $\mathcal{B}_{n-1}$ and $\mathcal{B}_n$, and $\epsilon(t_{n-1})$ the total accumulated strain in $\mathcal{B}_{n-1}$

Similarly the stress in configuration $\mathcal{B}_{n-1}$ is given by

$$\sigma_{n-1} = G_0\, \epsilon(t_{n-1}) + \sum_{i=1}^{I} G_i\, h_i(\Delta t_{n-1})\, d\epsilon(t_{n-1}) + \sum_{i=1}^{I} g_i(t_{n-1}) \tag{4.15}$$

The stress increment between $\mathcal{B}_{n-1}$ and $\mathcal{B}_n$ is defined as

$$\sigma = \sigma_n - \sigma_{n-1} = [G_0 + \sum_{i=1}^{I} G_i h_i(\Delta t_n)]\, d\epsilon(t_n) + \tag{4.16}$$
$$+ \sum_{i=1}^{I} (e^{-\Delta t_n/\lambda_i} - 1)[q_i(t_{n-1}) + G_i h_i(\Delta t_{n-1})\, d\epsilon(t_{n-1})]$$

Note that the response is separated into two parts. The first part is an instantaneous response proportional to the strain increment $d\epsilon(t_n)$. For equal time steps this instantaneous modulus is a constant. The second part is the delayed response. In order to calculate the latter the previous strain increment $d\epsilon(t_{n-1})$ and $q_i(t_{n-1})$ must be stored.

The extension of Eq. (4.16) to a multiaxial case is straight forward

$$\{\bar{S}_{IJ}\} = (G_1^0 + \sum_{i=1}^{I} G_1^i h_i(\Delta t_n))\{d\bar{E}_{IJ}(t_n)\} + \tag{4.17}$$
$$+ \sum_{i=1}^{I} (e^{-\Delta t_n/\lambda_i} - 1)(\{q_i^*(t_{n-1})\} + G_1^i h_i(\Delta t_{n-1})\{d\bar{E}_{IJ}(t_{n-1})\})$$

and

$$S_{KK} = (G_2^0 + \sum_{i=1}^{I} G_2^i h_i(\Delta t_n))\, dE_{KK}(t_n) + \tag{4.18}$$
$$+ \sum_{i=1}^{I} (e^{-\Delta t_n/\lambda_i} - 1)(q_i(t_{n-1}) + G_2^i h_i(\Delta t_{n-1})\, dE_{KK}(t_{n-1}))$$

where $\{q_i^*\}$ follows immediately from Eqs. (e) and (f).

Let

$$\alpha_1 = G_1^0 + \sum_{i=1}^{I} G_1^i h_i(\Delta t_n)$$

$$\alpha_2 = G_2^0 + \sum_{i=1}^{I} G_2^i h_i(\Delta t_n)$$

$$\beta = \sum_{i=1}^{I} (e^{-\Delta t_n/\lambda_i} - 1)\left(g_i(t_{n-1}) + G_2^i h_i(\Delta t_{n-1})\, dE_{kk}(t_{n-1}) \right)$$

$$\{b\} = \sum_{i=1}^{I} (e^{-\Delta t_n/\lambda_i} - 1)\left(\{g_i^*(t_{n-1}) + G_1^i h_i(\Delta t_{n-1})\, \{d\bar{E}_{II}(t_{n-1})\}\right)$$

With these abbreviations the response for axisymmetric deformation is

$$\begin{Bmatrix} S_{11} \\ S_{22} \\ S_{33} \\ S_{13} \end{Bmatrix} = \frac{1}{3} \begin{bmatrix} (2\alpha_1+\alpha_2) & (\alpha_2-\alpha_1) & (\alpha_2-\alpha_1) & 0 \\ & (2\alpha_1+\alpha_2) & (\alpha_2-\alpha_1) & 0 \\ & & (2\alpha_1+\alpha_2) & 0 \\ \text{Symmetric} & & & \alpha_1 \end{bmatrix} \begin{Bmatrix} dE_{11} \\ dE_{22} \\ dE_{33} \\ dE_{13} \end{Bmatrix} + \begin{Bmatrix} b_1 + \frac{1}{3}\beta \\ b_2 + \frac{1}{3}\beta \\ b_3 + \frac{1}{3}\beta \\ b_4 \end{Bmatrix} \qquad (4.19)$$

For thin shell applications Eq. (4.19) must be modified due to the generalized plane stress condition $S_{33} = 0$. Due to the appearance of the delayed response this condensation is not as straight forward as given in Chapter 3. Special attention must be given to the definition of b_3 and $d\bar{E}_{33}$ at each step of the integration.

For materials where Poisson's ratio remains constant during the deformation, $\nu(t) \equiv \nu(0)$, the above relationship may be simplified since the Poisson's ratio effect may be kept outside

the integral.

The constitutive relation in matrix form is

$$\{S\} = [C]\{dE\} + \{S^c\} \tag{4.20}$$

where $\{S^c\}$ denotes the delayed stress response and is often called the "creep" stress.

4.3 Some Remarks of the Sources of Errors in the Solution

The accuracy of any numerical method is determined by the approximations made in the initial formulation, and the errors accumulated during the computational process. For the class of viscoelastic boundary value problems discussed here these errors are

(i) Errors associated with the finite element formulation. These originate from the discretization of the system, and from the lack of completeness of the assumed displacement field. Both errors may be reduced by refining the mesh or refining the element.

(ii) Rounding errors in the computation. This error is due to the use of a finite word length in the computer, and may be neglected except for the solution of ill-conditioned systems.

(iii) Errors due to the viscoelastic model. In the present context the assumption

$$G_{IJKL} \equiv G_{ijkl}$$

may introduce errors with the increasing magnitude of the strains. However, for most creep buckling problems the structure will lose stability before the strains reach a level where this becomes important.

Secondly, the strain rate approximation given by Eq. (b) may be too crude. This will occur when the time step is too large and the strain varies significantly with time. For this case the error may be reduced by using a higher order difference approximation to the strain rate.

Another error source may be the inadequacy of the Prony series expansion to model the material behavior of certain materials. If more complicated functions have to be used in the modeling, the simple recursive algorithm used here will break down. For such cases, algorithms that require a larger number of past solution to be stored might be necessary.

Finally, errors may arise from the computational method used in the calculation of the convolution integrals. For isothermal conditions the calculations are exact, but errors will arise for nonisothermal cases [51].

(iv) Errors from the solution of the nonlinear equations. For infinitesimal theory the step-by-step integration of the incremental equilibrium equations does not introduce further errors. For geometrically nonlinear problems, however, the forward integration scheme is known to give solutions that drift away from the exact solution unless equilibrium checks are performed. These equilibrium checks may initiate parasitic oscillations in the solutions, as discussed further in section 5.7.

Concluding, the accuracy of the solutions obtained by the method discussed in this chapter is quite good. The most serious problems are associated with the oscillations in case (iv), and the identification of the material parameters in the Prony series expansion. For creep buckling problems the choice of step length in the forward integration also becomes crucial for the accuracy and economy of the solution.

5. ANALYSIS OF NONLINEAR PROBLEMS

5.1 Characterization of the Nonlinear Problem

A given nonlinear system can be characterized according to the sources of the nonlinearities of the system. For a structural system these sources are:

1. Geometric nonlinearities
2. Physical (material) nonlinearities

For most structural problems both these effects are present, and prominently so in the subject of this study. For better understanding of the nonlinear behavior, the following distinctions should be made:

1. Geometric Nonlinearities

The geometric nonlinearities are due to the finite deformation of the structure, and the necessity of distinguishing between the deformed and undeformed configuration. Two contributions must be considered

(i) The use of the complete nonlinear strain-displacement relations.

(ii) The equilibrium equations are written in the deformed configuration; whereby they become a function of the total deformation.

2. Physical Nonlinearities

The physical (material) nonlinearities are caused by a nonlinear relationship between kinematic and mechanical variables, i.e., through a nonlinear constitutive law. For engineering material this relationship may be of either

(i) Differential form. Stress and strain rates are related through a linear (nonlinear) differential equation. This is the form most commonly used for creep and plasticity of metals, where time and path dependence are given implicitly in the differential equation.

(ii) Functional form. The functional law relates the instantaneous value and past history of the two variables. A special form of this is the hereditary integral law used in linear viscoelasticity. This formulation is extensively used for biological tissues and high polymers.

In the present study material laws of both type (i) and (ii) are applied.

The equilibrium equations, incremental or total, obtained from the field equations will in general result in a system of nonlinear differential or integro-differential equations. For most cases these equations are of such complexity that only numerical solutions are available. For most structural problems the size of this system of equations is such that extensive considerations should be given to what numerical solution method would be most efficient for the problem at hand.

5.2 Numerical Solution Methods for Nonlinear Systems

During the recent years great emphasis has been placed on the development of efficient numerical solution methods for nonlinear equations. A number of authors have characterized and evaluated these methods as related to structural analysis.

Most solution methods can basically be separated into two classes [105, 109].

Class I. Incremental Methods

Class II. Self-correcting Methods

I. Incremental Methods

The most common of these methods are

(i) Pure incremental method

This is essentially a Euler forward integration method, where the solution is obtained through a sequence of linear analysis. The tangent (or instantaneous) stiffness matrix is evaluated at each step, and the total load applied in small increments, Fig. 5.1a. For quasi-static problems the time domain is spanned step-by-step. The method is conceptually extremely simple, and can be applied to nonlinear problems of both types. However, the solution will drift away from the true solution unless extremely small increments are used. The error is of first order in the displacement increment.

(ii) Mid-point Methods

Here the tangent stiffness is replaced by an approximate cord stiffness, $\underset{\sim}{K}_c$, Fig. 5.1b, solving for an approximate displacement increment $\underset{\sim}{\Delta r}^*$ using the tangent stiffness, the approximate $\underset{\sim}{K}_c$ can be evaluated at $\underset{\sim}{r} + \frac{1}{2}\underset{\sim}{\Delta r}^*$. The improved displacement increment is then obtained from $\underset{\sim}{K}_c \cdot \underset{\sim}{\Delta r} = \underset{\sim}{\Delta R}$. This is a second order method, but requires two linear solutions per step. A cruder approximation to $\underset{\sim}{K}_c$ is obtained by

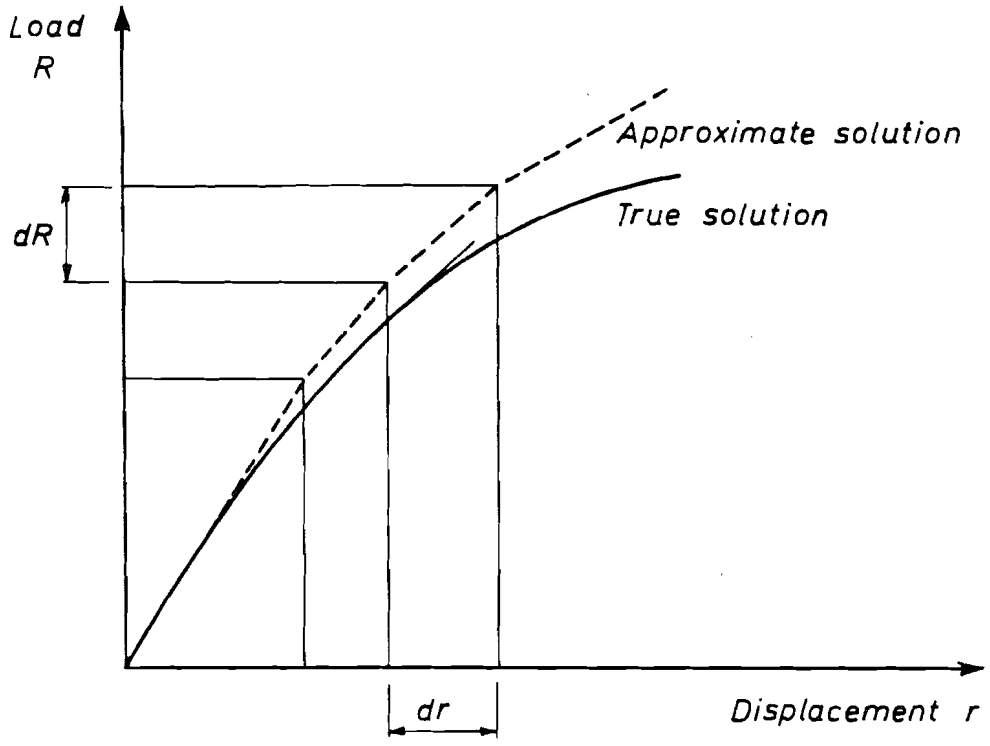

a. PURE INCREMENTAL METHOD.

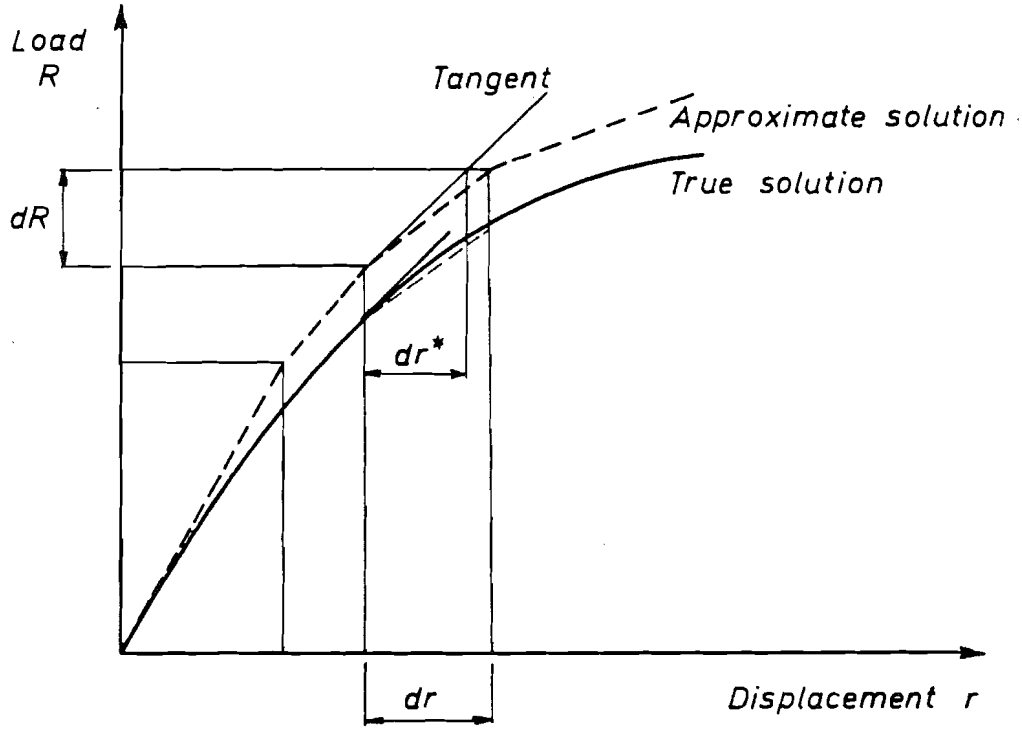

b. MID-POINT METHOD.

FIG. 5.1 CLASS I METHODS FOR NONLINEAR PROBLEMS.

estimating $\underset{\sim}{dr}^*$ directly on the basis of the previous displacement increment, without using the tangent stiffness [110].

(iii) Initial-value methods

The initial-value methods are based on the conversion of the equilibrium equations from nonlinear algebraic equations to ordinary differential equations. The methods are discussed in details by Haisler et al [108].

The characteristic feature of all these methods is that equilibrium is in general violated at all points on the solution path. Hence the solution tends to drift away from the true solution unless extremely small load increments are used. Both (i) and (ii) are applicable to physically nonlinear problems, but some caution should be taken when using (ii).

II. Self-Correcting Methods

(i) Pure iteration

The simplest iteration scheme available is one where the stiffness matrix is kept constant and equal to the initial value during the iteration process, Fig. 5.2a. After each cycle the"out-of-balance" force is computed in the deformed configuration, and applied as a new loading. The computational effort per cycle is small, but convergence is extremely slow.

(ii) "Secant" iteration

The secant stiffness and the load vector are in general dependent of the total deformation. From the initial linear analysis, a first approximation to the displacement is obtained, and the approximate secant stiffness determined. Based on this stiffness a new displacement vector is obtained, and the process is repeated until convergence, Fig. 5.2b. In this approach, convergence is in general slow, and computation of the secant stiffness is relatively time consuming.

(iii) Newton-Raphson iteration

The Newton-Raphson method is a second order method based on a linear Taylor series expansion about a known approximate solution. At each point in the solution path the tangent stiffness and the out-of-balance force are computed, and a new displacement increment determined. Adding this to get a new total displacement, the process is repeated until convergence is achieved, Fig. 5.2c. The method requires the updating and "inversion" of the tangent stiffness matrix for each cycle, but had quadratic convergence.

(iv) Modified Newton-Raphson methods

The necessity of evaluation and triangularization of the tangent stiffness for each cycle makes the Newton-Raphson method relatively slow. In order to speed up the solution a number of schemes have been devised where the stiffness has been kept constant for a certain

number of cycles, and only updated when the rate of convergence has deteriorated [112].

(v) Residual load method

This modified incremental method was originally proposed by Wilson and Murray [15, 16]. At the end of each load increment the "out-of-balance" force $\Delta \underset{\sim}{R}^*$ in the deformed configuration is computed, and added to the load increment $\Delta \underset{\sim}{R}$ for the next step. This is equivalent to a one-cycle iteration on the "out-of-balance" force, without ever formally updating the displacement after the iteration, Fig. 5.2d.

(vi) Self-correcting initial-value methods

This is a modified version of type (iii) in Class I. The method has been found to be extremely efficient for geometrically nonlinear problems [108], but since the stiffness matrix is kept unchanged during the process, it will fall within the initial strain methods for flow theory of plasticity.

All Class II methods are applicable to geometrically nonlinear problems, with (iv), (v) and (vi) being the most efficient. The convergence of the iterative method can be accelerated using extrapolation methods like Richardson's method, etc. [112]. The incremental methods may be improved using the mid-point method as discussed above. For physically nonlinear problems the choice of method is more restricted. For nonlinear elasticity most of the iterative methods may be applied, and method (ii) has been used for deformation (Hencky) type plasticity [111]. Flow theory of

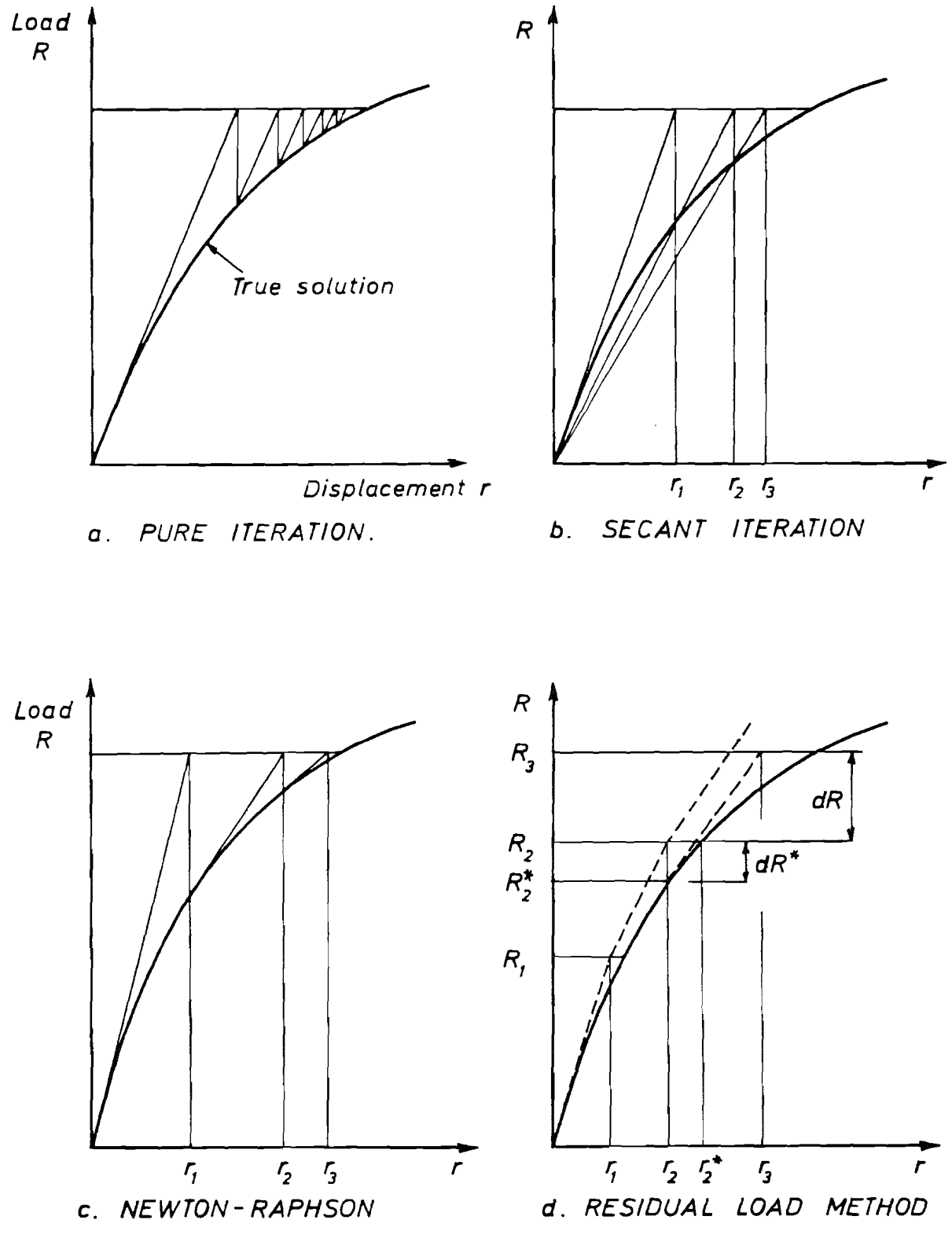

FIG. 5.2 CLASS II METHODS FOR NONLINEAR PROBLEMS.

creep and plasticity, however, is path dependent, and an incremental method is the only recourse.

In the present study the Newton-Raphson and the residual-load method were used for elastic problems, and the latter one for inelastic problems and for elastic snap-through cases where the iterative methods become unstable.

5.3 Post-Buckling Analysis of Structures

The post-buckling behavior of structural elements can be separated into three classes according to the slope of the generalized load-deflection curve in the post-buckling domain, Fig. 5.3a.

I. Positive slope, — plates

II. Approximately zero slope, — columns

III. Negative slope, — arches, shells

In plate-type structures, a stiffening is observed in the post-buckling domain, while columns exhibit almost zero stiffness until the displacements become very large ("Elastica", [113]). Shells and arches, however, show softening with loss of stability, causing large displacement under decreasing loading. The latter phenomenon is commonly called snap-through.

The snap-through problems can be further divided into two cases. Case (a) is characterized by the displacements being multi-valued in the loading, and the loading single-valued in terms of the displacement, Fig. 5.3b. This is typical for spherical shells and arches. Case (b) is common for axially loaded cylindrical shells, where even the loading is multi-valued in the displacements, Fig. 5.3c. In the present study

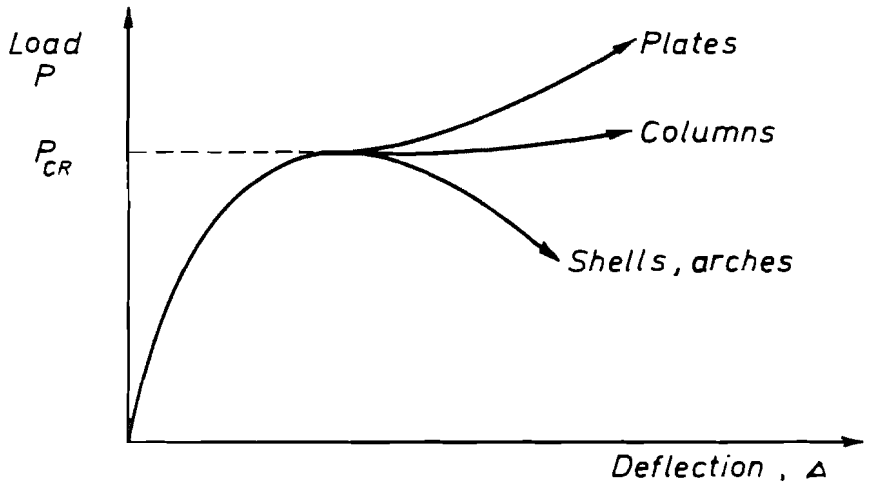

a. CHARACTERIZATION OF STRUCTURAL MEMBERS.

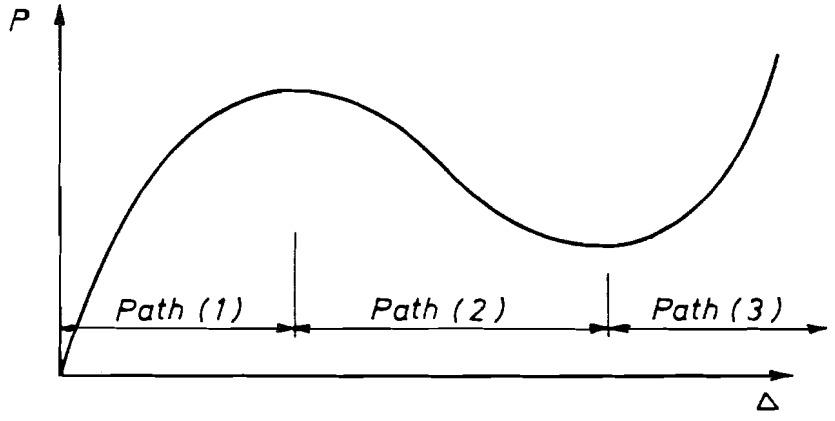

b. SNAP-THROUGH BEHAVIOR, CASE A

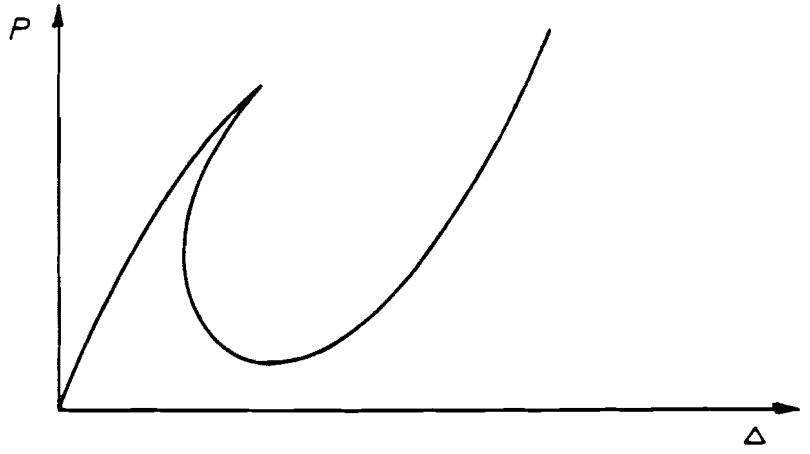

c. SNAP-THROUGH BEHAVIOR, CASE B

FIG. 5.3 POST-BUCKLING BEHAVIOR OF STRUCTURAL MEMBERS.

the attention will be limited to case (a).

The generalized load-deflection curve for snap-through problems is divided into three paths, Fig. 5.3b.

1. Stable ascending path, $\det(\underset{\sim}{K}) > 0$
2. Unstable descending path, $\det(\underset{\sim}{K}) < 0$
3. Stable ascending path, $\det(\underset{\sim}{K}) > 0$

When passing from one path to another the determinant of the stiffness matrix will change sign, causing stability problems in the solution technique. Iterative methods will tend to oscillate while incremental methods will diverge unless the loading is reversed.

The advantage of displacement control is apparent in case (a), where the loading is single-valued in the displacement. This implies that the displacements should be the primary variable instead of loading in the displacement formulation. For multi-degree of freedom system this is quite difficult, but has been obtained for structures subjected to single point loads. Augmenting the structure with a heavy "fictitious" spring under the load renders the combined structure positive definite in the entire displacement domain.

This concept was extended to structures under general loading conditions by Sharifi [114]. Using a linear constraint for each degree of freedom, the constraining force vector was determined as a linear function of the applied load vector $\underset{\sim}{R}$ and a single spring parameter. This gives a modified equilibrium equation

$$(\underset{\sim}{K} + \underset{\sim}{K}_A)\cdot\underset{\sim}{r} = \underset{\sim}{R} \tag{5.1}$$

The augmenting stiffness matrix $\underset{\sim}{K}_A$ is given by

$$\underset{\sim}{K}_A = \alpha \, \underset{\sim}{R} \cdot \underset{\sim}{R}^T \tag{5.2}$$

where α is a proportionality factor given in terms of the spring parameter and trace $\underset{\sim}{K}$.

The major disadvantage of this method is that $\underset{\sim}{K}_A$ will in general be a full matrix, such that the total stiffness matrix will lose its banded form. However, the method has been found to be very valuable in the analysis of elastic-plastic structures near collapse load. Here the load deflection curve is very flat, and the use of displacement control will reduce the error.

A more efficient method for tracing the complete load-deflection curve was used by Wissmann [115] for a simple 2-bar truss. This is an incremental method with load reversal on the unstable path, and does not destroy the banded structure of the stiffness matrix. The major problem in this method is that the local extremum values are not in general known apriori, and hence a simple test must be devised for the load reversal decision. In this study the positive (negative) definiteness of the tangent stiffness matrix was used for this purpose. This test is a direct byproduct of the Gaussian elimination process on the matrix. After transformation to upper triangular form, the determinant is given by the trace of the matrix.

At any point (n) on the loading path the load increment is given by

$$d\underset{\sim}{R}_n = \rho_n \underset{\sim}{R} + d\underset{\sim}{R}^*_n \tag{5.3}$$

where $\underset{\sim}{R}$ is the total applied load, $\Delta\underset{\sim}{R}^{*}_{n}$ is the out-of-balance force vector at point (n) and ρ_n is a load proportionality factor. The problem is then essentially that of assigning the sign and absolute value of ρ_n at each increment.

The basic procedure is as follows:

(i) Compute and assemble the system tangent stiffness matrix at point (n).

(ii) Use Gaussian elimination to transform the matrix to triangular form, and compute the determinant.

(iii) Test the sign of the determinant to determine on which path point (n) is. If on path (1) or (2), write the triangularized matrix on tape.

(iv) Assign the proper sign and value to ρ_n , and compute $\Delta\underset{\sim}{R}_n$. Back-substitute to find $\Delta\underset{\sim}{r}_n$ and compute total displacements and stresses at point $(n+1)$.

(v) Repeat the process.

If going from point (n) to $(n+1)$ the determinant changes sign, the extremum point is passed and the value is given in the interval $< \underset{\sim}{R}_n , \underset{\sim}{R}_{n+1} >$. If a closer interval is needed, backspace to point (n) and read the triangularized matrix from tape. Take $\rho^{*} = 0.2\rho_n$ and use this value for the necessary number of increments until a new sign change is observed. At this point reverse the loading, and proceed according to the basic procedure.

In a pure incremental method $\Delta\underset{\sim}{R}^{*}_{n} = 0$, and no problems were experienced using this procedure. For the residual load method, however, special precautions must be taken at load reversal. Situations will occur where the out-of-balance force

$\Delta \underset{\sim}{R}_n^*$ is positive when passing the local maximum. If ρ_n is chosen negative, but with too small an absolute value, the resulting $\Delta \underset{\sim}{R}_n$ may be positive even when a negative load increment was intended. This problem can be alleviated using large enough values of ρ_n , but this will often lead to large errors in the displacements, due to the small stiffness of the system near the local maximum. Here, this problem was avoided by restricting the generalized displacement increment to 2-5% of the total displacement, and solving for the associated value of ρ_n . This method was used the first 2 to 4 increments after load reversal.

It is the author's experience that the local extremum values can be quite accurately determined by this method. Even when no apriori estimate for the critical load was used, the error in the critical value was about 2-5%, depending on the number of load increments used.

5.4 Determination of Step Size for Time-Integration

For a given creep problem the feasibility of the proposed method is mainly restricted by the computer time needed for the time integration. Of paramount importance here is the choice of step size and integration limit.

Two different problems are considered here.

(i) Determine the "critical time" for a structure subjected to sustained loading during creep.

(ii) Determine the steady state solution for internally pressurized pressure vessels subjected to creep.

In problem (i) the displacement $w \to \infty$ as $t \to t_{cr}$ and in (ii) $w \to w_o$ as $t \to \infty$, where w_o is the steady state solution. The objective is to determine t_{cr} and w_o, and the associated stress and strain fields. In order to obtain a sharp estimate for t_{cr}, problem (i) should be recast to $\frac{1}{w} \to 0$ as $t \to t_{cr}$, which is better conditioned.

Due to lack of computer time only limited attention was paid to the automatic generation of time steps. Most extrapolation methods are difficult to apply since the stiffness matrix is a function of the time step for viscoelastic materials. The following guidelines were used:

(i) From an elastic analysis the equivalent elastic strains due to inplane forces were computed for the sustained load P and the critical load P_{cr}. Let

$$\Delta \bar{\epsilon}_E = \bar{\epsilon}_E(P_{cr}) - \bar{\epsilon}_E(P)$$

be the strain difference at a characteristic node. For a given creep law a crude estimate of the critical time is then obtained by equating

$$\Delta \bar{\epsilon}_E = \epsilon_c(\bar{\sigma}, t_{cr})$$

and solving for t_{cr} assuming the stress, $\bar{\sigma}$, to be constant over the entire time interval. Since the stress increases as $t \to t_{cr}$, this is a conservative estimate. When the total number of increments, N, is chosen, the initial time step is $\Delta t = t_{cr}/N$. During the solution process a given displacement component or displacement norm is recorded at each increment. At time t_i a quadratic polynomial is passed

through these values at t_i, t_{i-1} and t_{i-2}, and the constant curvature computed. Every time the curvature is $(1.1)^n$ times bigger than the initial curvature, the initial time step Δt is reduced by the same factor.

(ii) The initial time increment is determined from the requirement that the initial creep strain increment should not exceed 10% of the effective elastic strain. Subsequent time steps are chosen such that

$$\Delta t_{i+1} = 1.2 \cdot \Delta t_i$$

More extensive studies of step size and convergence for infinitesimal creep problems have been given in references [52, 53].

5.5 Linearized Incremental Equilibrium Equations

A sequence of virtual work expressions for finite deformations were derived in Chapter 2. Eq. (2.51) gives the virtual work done by the internal stress field during the deformation from configuration $\mathcal{B}_1$ to $\mathcal{B}_2$. The virtual work of surface tractions and body forces were derived for different classes of loading, and is given by Eqs. (2.52), (2.57), (2.58), and (2.59).

For the subsequent discussion the residual load approach for nonconservative loading will be considered. The incremental equilibrium equations for this case are obtained by equating Eqs. (2.51) and (2.59).

$$\int_{\mathcal{B}_0} \left(S^{IJ}\delta E_{IJ} + {}^1S^{IJ}\delta\eta_{IJ} \right) dV + \int_{\partial\mathcal{B}_0} {}^2p \frac{\rho_0}{\rho} N^J X^I{}_{|K} X^M{}_{|J} u^K{}_{|M} \delta u_I \, dA$$

$$= -\int_{\partial\mathcal{B}_0} {}^2p \frac{\rho_0}{\rho} N^J X^I{}_{|J} \delta u_I \, dA - \int_{\mathcal{B}_0} \left({}^1S^{IJ}\delta e_{IJ} - \rho_0 f^I \delta u_I \right) dV \tag{5.4}$$

The second integral on the left side of Eq. (5.4) is derived from the loading, but is linear in the displacement increment $\underset{\sim}{u}$ and hence has the form of a stiffness term.

The equilibrium equations of the form above are nonlinear in $\underset{\sim}{u}$, and can only be solved by iteration. This nonlinearity is due to the nonlinear part of the Cauchy-Green strain tensor, which can be decomposed by

$$E_{IJ} = e_{IJ} + \eta_{IJ} \tag{2.50a}$$

where e_{IJ} and η_{IJ} are given by Eqs. (2.50b), (2.50e).

Recalling the incremental stress-strain relations of Chapters 3 and 4, the stress increment is

$$S^{IJ} = C^{IJKL} E_{KL} = C^{IJKL} \left(e_{KL} + \eta_{KL} \right) \tag{5.5}$$

Substitution of Eq. (5.5) into (5.4) gives the incremental equilibrium equations of symbolic form

$$\left(\underset{\sim}{K}_0 + \underset{\sim}{K}_1 + \underset{\sim}{K}_2 + \underset{\sim}{K}_3 + \underset{\sim}{K}_G \right) \cdot \delta\underset{\sim}{u} = \underset{\sim}{R} \cdot \delta\underset{\sim}{u} \tag{5.6}$$

where the following definitions are used:

$$\underset{\sim}{K}_0 \cdot \delta\underset{\sim}{u} = \int_{\mathcal{B}_0} C^{IJKL} e_{KL}\, \delta e_{IJ}\, dV \qquad \text{(a)}$$

$$\underset{\sim}{K}_1(u_i) \cdot \delta\underset{\sim}{u} = \int C^{IJKL} (e_{KL}\, \delta\eta_{IJ} + \eta_{KL}\, \delta e_{IJ})\, dV \qquad \text{(b)}$$

$$\underset{\sim}{K}_2(u_i, u_j) \cdot \delta\underset{\sim}{u} = \int_{\mathcal{B}_0} C^{IJKL} \eta_{KL}\, \delta\eta_{IJ}\, dV \qquad \text{(c)}$$

$$\underset{\sim}{K}_3 \cdot \delta\underset{\sim}{u} = \int_{\partial\mathcal{B}_0} {}^2p\, \frac{\rho_0}{\rho} N^J X^I{}_{/K} X^M{}_{/J}\, u^K{}_{/M}\, \delta u_I\, dA \qquad \text{(d)}$$

$$\underset{\sim}{K}_G \cdot \delta\underset{\sim}{u} = \int_{\mathcal{B}_0} {}^1S^{IJ}\, \delta\eta_{IJ}\, dV \qquad \text{(e)}$$

$$\underset{\sim}{R} \cdot \delta\underset{\sim}{u} = -\int_{\partial\mathcal{B}_0} {}^2p\, \frac{\rho_0}{\rho} N^J X^I{}_{/J}\, \delta u_I\, dA - \int_{\mathcal{B}_0} ({}^1S^{IJ}\delta e_{IJ} - \rho_0 f^I \delta u_I)\, dV \qquad \text{(f)}$$

From Eqs. (a-e) the source of nonlinearity is revealed for each term. $\underset{\sim}{K}_0$ and $\underset{\sim}{K}_G$ are linear in $\underset{\sim}{u}$, and are the infinitesimal strain and geometric stiffness matrix respectively. $\underset{\sim}{K}_3$ is due to the nonconservative loading and is also linear in $\underset{\sim}{u}$. For conservative loading this term vanishes. The remaining stiffness terms are of higher order in $\underset{\sim}{u}$. The load term $\underset{\sim}{R}$ includes both the load increment and the out-of-balance force.

From the discussion of solution methods it is quite clear that the equilibrium requirement is most essential. The degree of accuracy in the tangent stiffness should be of less concern. In view of this the terms $\underset{\sim}{K}_1$ and $\underset{\sim}{K}_2$ can be neglected. Being

quadratic and cubic in $\underset{\sim}{u}$, and restricting $\underset{\sim}{u}$ to be small, these terms are likely to be negligible compared to $\underset{\sim}{K}_0$ and $\underset{\sim}{K}_G$.

The nonconservative loading term $\underset{\sim}{K}_3$ is nonsymmetric, and would give a nonsymmetric system stiffness matrix if included. For most structures this term will be small, and can be neglected in view of the prior discussion. The added accuracy of the tangent stiffness obtained by including $\underset{\sim}{K}_3$ is by far exceeded by the computational effort needed for the solution of the nonsymmetric system of equations, which makes the inclusion of $\underset{\sim}{K}_3$ uneconomical. However, in pneumatic structures where both strains and rotations are large, $\underset{\sim}{K}_3$ should be included.

This leads to the linearized equilibrium equation

$$(\underset{\sim}{K}_0 + \underset{\sim}{K}_G) \cdot \delta\underset{\sim}{u} = \underset{\sim}{R} \cdot \delta\underset{\sim}{u} \tag{5.7}$$

It should be noted here that $\underset{\sim}{K}_0$ is quadratic in ${}^1\underset{\sim}{u}$. The linear strain component is

$$e_{IJ} = \frac{1}{2} \left({}^1F^K_{\ I}\, u_{K/J} + {}^1F^K_{\ J}\, u_{K/I} \right)$$

which substituted in Eq. (a) gives the correct expression for $\underset{\sim}{K}_0$.

The linearization of the tangent stiffness has created some confusion in the evaluation of strain and stress increments. Arguing that the strain computation should be consistent with the above linearization, some authors have neglected the nonlinear term γ_{IJ}. However, in order to avoid "drifting" of the solution, the stresses should at all times be compatible with the kinematics based on the approximate solution obtained at the end of each increment. For iterative methods this is imperative for

convergence, and can only be obtained by including γ_{IJ}. For elastic materials, this is even more clear since the total stress in configuration $\mathcal{B}_1$ is computed from the total strain between $\mathcal{B}_0$ and $\mathcal{B}_1$, and not by adding stress increments along the deformation path. However, since γ_{IJ} is always positive, it will give a positive axial force that may cause oscillation in the solution of problems like the "Elastica" unless small load increments are used.

5.6 Numerical Examples of Solution Methods

The efficiency of the residual load method is illustrated for two simple problems.

(i) Elastic-plastic analysis of beam. Infinitesimal theory. The simply supported, uniformly loaded beam in Fig. 5.4 was analyzed using both the pure incremental and the residual load method. The results are compared to Prager and Hodge's exact solution [116]. From the normalized load-deflection curves in Fig. 5.4 a substantial improvement in the convergence is observed. The explanation for this improvement is as follows.

For each load increment a linear relationship is derived between the increments of stress and strain. The stress increment and the total stress obtained from this series of linear analysis would be in equilibrium with the applied load had not the material yielded in some regions. In these regions the computed stresses are scaled down to the yield stress, whereby the equilibrium between the total applied load

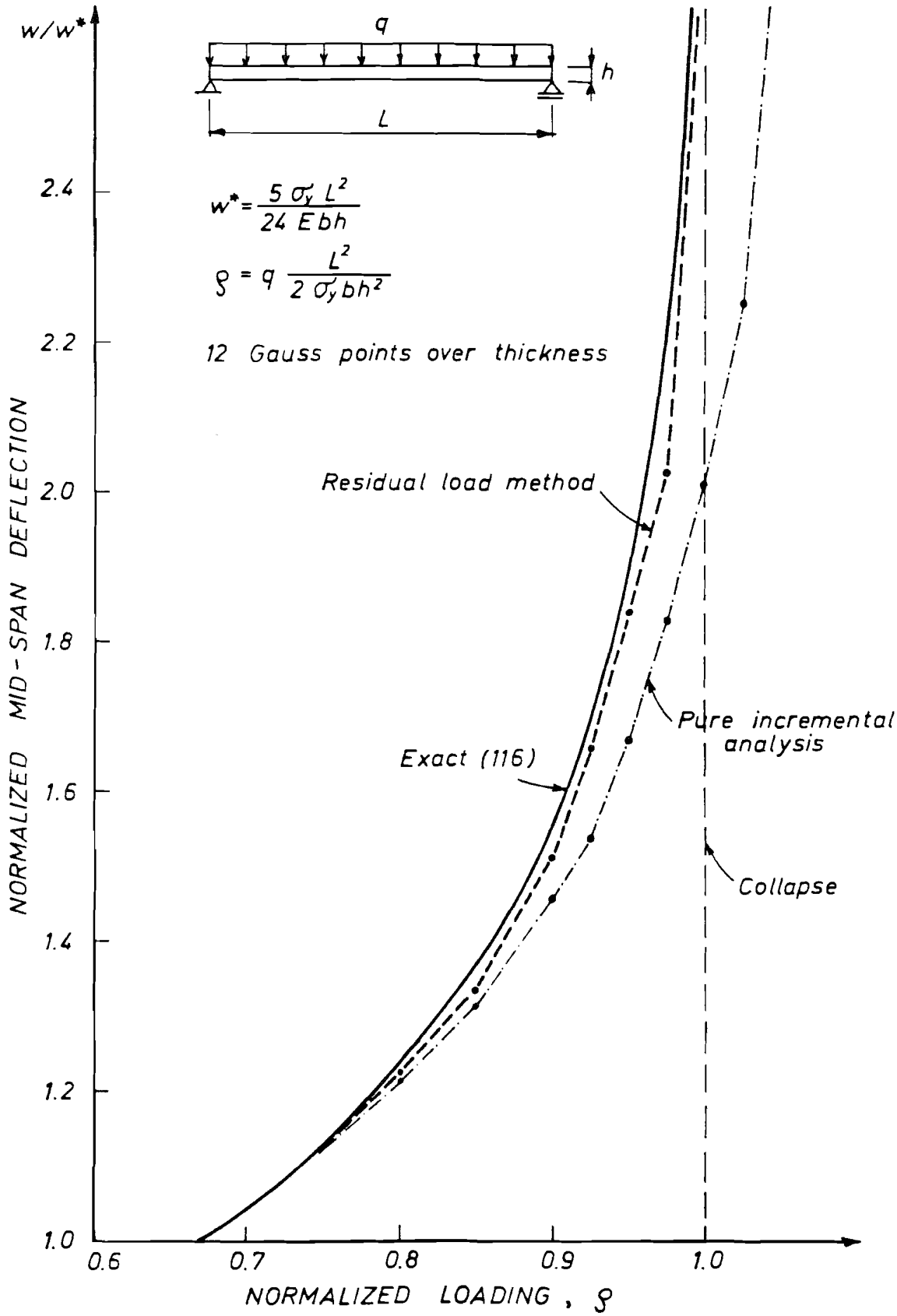

FIG. 5.4 ELASTIC-PLASTIC ANALYSIS OF BEAM.

and the total stress field is destroyed, whereby an "out-of-balance" force is obtained.

(ii) Large displacement analysis of plate strip

A large displacement analysis was made for the infinite plate strip shown in Fig. 5.5. The strip, uniformly loaded and with fixed end supports, was analyzed using the same two methods as above. The step sizes were 10 steps @ 30 psi, and 3 steps @ (50, 100, 150) psi. The results are shown in Fig. 5.5 and Fig. 5.6. The pure incremental method gives results that drift, even for the smallest load increments. The results from the residual load method, however, give very good results even for the largest increments. After increment number one the variation in the axial force N is completely wrong, being zero at the center and having the maximum value at the support. This is due to the nonlinear term in the strain-displacement relationship. However, after the second increment both the value and the variation are very close to the exact one.

5.7 Some Comments on the Residual Load Method

The effectiveness of the residual load method was illustrated for elastic large deformation problems and problems of infinitesimal theory of plasticity in section 5.6. However, the method is not restricted to such problems only, but is equally applicable to large displacement problems in viscoelasticity, plasticity, and viscoplasticity. For the latter classes of problems, the concept

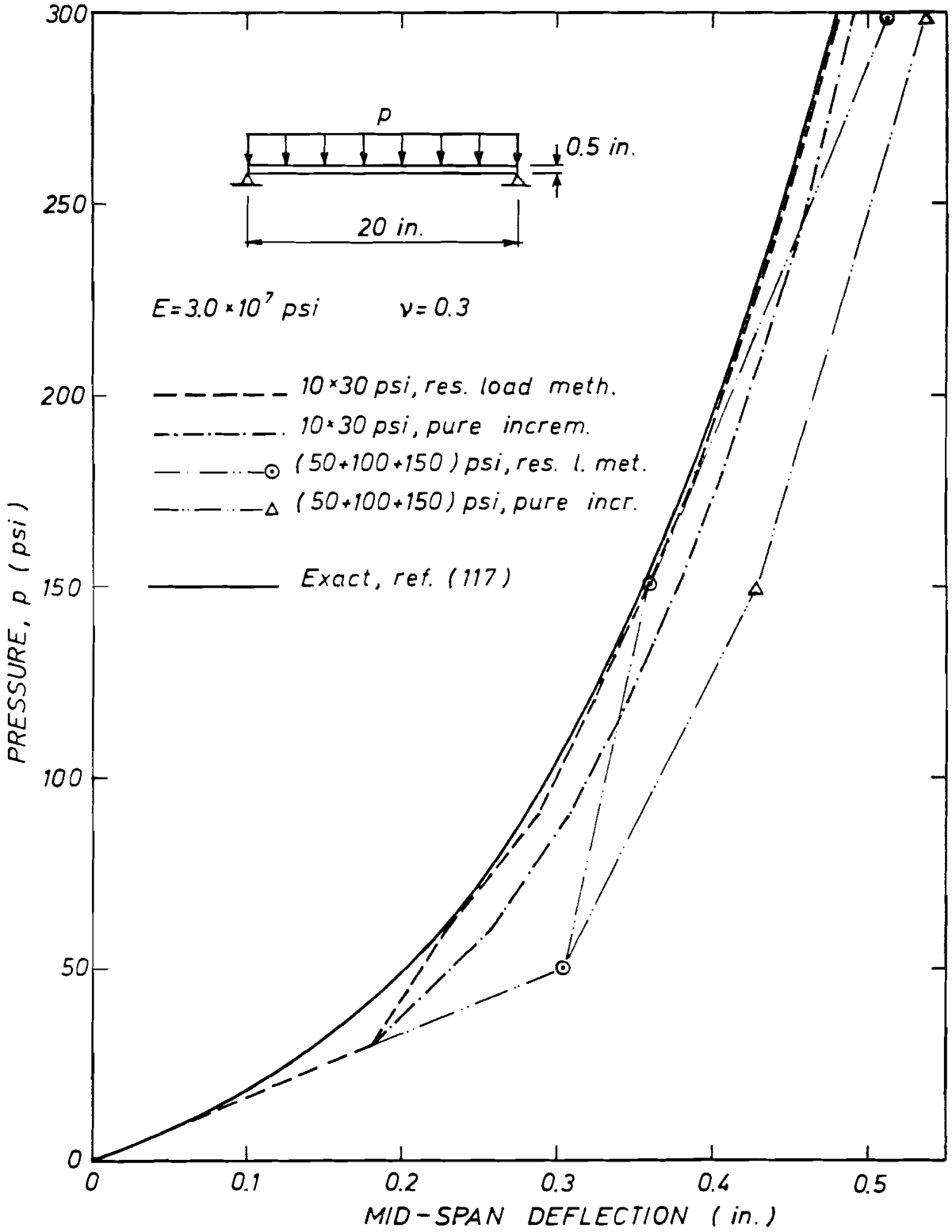

FIG. 5.5 DEFLECTION OF INFINITE PLATE STRIP.

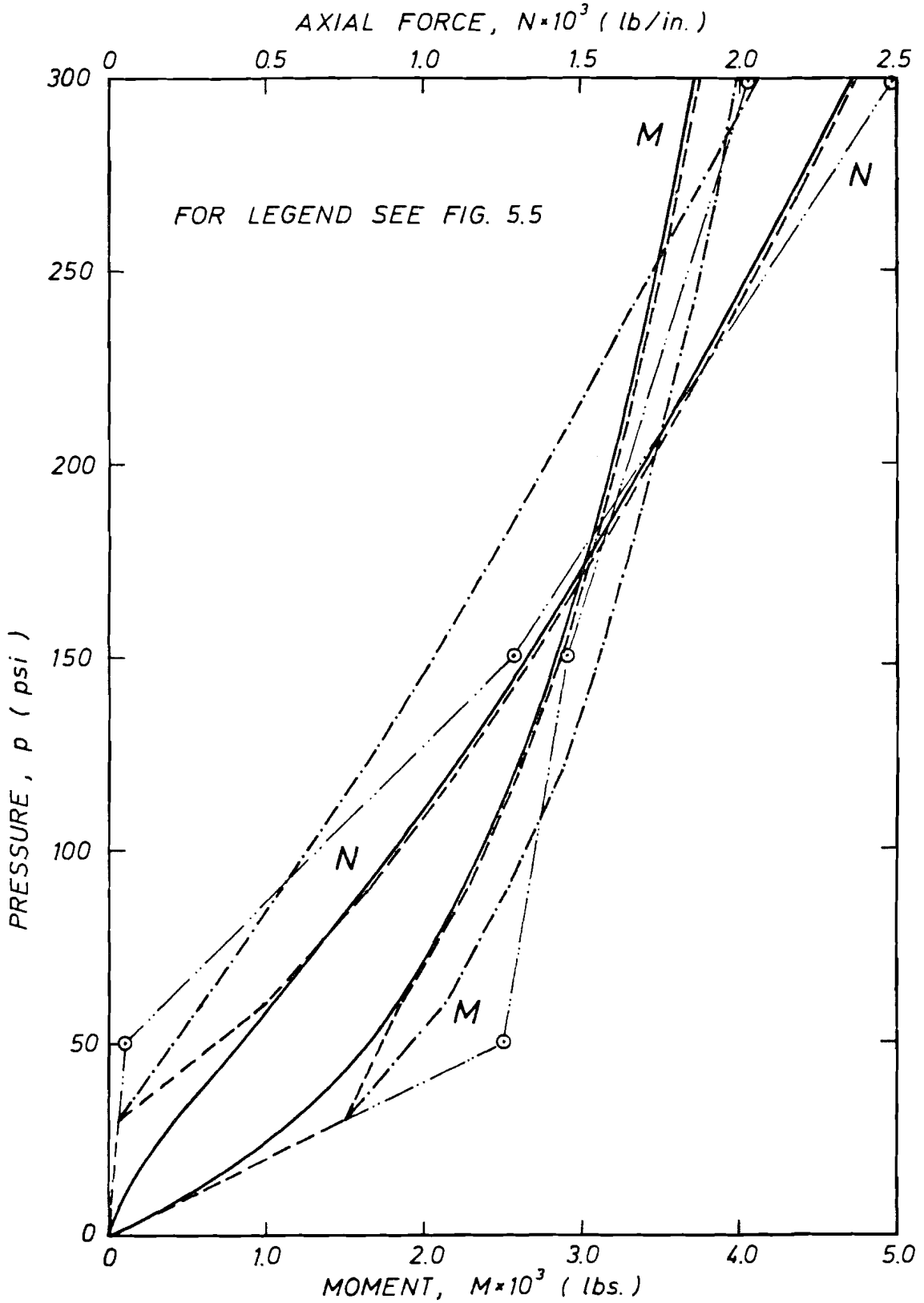

FIG. 5.6 STRESSES IN INFINITE PLATE STRIP.

of unloading is essential which means that certain constraints must be introduced in connection with the residual load method. The problems that must be considered are as follows:

(i) Viscoelasticity

The basic concept in the theory of viscoelasticity is the fading memory hypothesis. This hypothesis implies that the response is more strongly dependent on the recent strain history than the distant history. For large displacement problems in viscoelasticity, this becomes very important, since unloading is possible under constant or monotonically increasing loading.

The cause for this unloading is quite clear. Consider the plate strip in section 5.6, and the load sequence (50+100+150) psi. If this loading sequence was changed to (50+50+....) psi, it can be seen from Fig. 5.5 that the unbalanced (residual) load would be larger than the next load increment. The same thing may happen for a constant loading problem if the time step is chosen such that the creep "pseudo-loading" is smaller than the unbalanced load. In both cases the structure will unload when subjected to the combined loading. Due to the fading memory property of the material, this unloading might cancel out the total previous loading history, and cause a reduction in the stresses also for the next time increment. This reduction in stresses will give new creep "pseudo-loading" that causes further

unloading for this time step. At this time the lack of equilibrium has been overcorrected, and the numerical solution will start to oscillate around the correct solution.

This problem can be avoided by choosing the load or time increments such that unloading will not take place. It should be noted that just reducing the time increments will not be sufficient, and may even increase the amplitude of the oscillations. Furthermore, this is an impractical method since the load-displacement-time relationship is in general not known. Instead the unbalanced load should be applied instantaneously, giving rise to an elastic strain increment. Adding this elastic strain increment to the previous visco-elastic strain increment and proceeding with the time integration will ensure that unloading will not take place. This method was applied to the viscoelastic creep buckling problems in section 7.6.2.

(ii) Plasticity

As in the case of viscoelasticity, unloading might take place if the unbalanced load is greater than the next load increment. This is a situation that is most likely to occur for postbuckling analysis of shells and arches where the load-deflection curve has a negative slope. An example of this is given in Fig. 7.4 for an elastic shallow spherical shell. In this case, however, the oscillations are due to the

fact that Young's modulus will be used for the next load increment when unloading is observed. Since the unloading is due only to our solution procedure and not the physical process in the structure, the lack of equilibrium will again be overcorrected.

Contrary to the viscoelastic case, the problem cannot be avoided by applying the unbalanced force elastically since this will in general give the wrong modulus for the next step. Instead the simplest solution would be to use displacement control where the load steps must be small, and use large enough load step elsewhere.

6. FINITE ELEMENT FORMULATION OF THE NONLINEAR PROBLEM

The linearized equilibrium equations derived in Chapters 2 and 5 will be discretized using the finite element method. This method was first introduced by Turner et al [118], and has later found widespread applications. The method is basically an extension of the classical Ritz method in the sense that the primitive field variables are expanded over a series of subdomains, called finite elements, instead of over the total region. This expansion is commonly obtained by polynomal interpolation, where certain requirements are imposed in order to ensure convergence of the solution. The mathematical background of the method has been discussed in references [119, 120, 121, 122].

The method has been used extensively for problems in linear elastostatics and dynamics, and lately for both geometrically and physically nonlinear problems. Other recent applications have been in the field of mixtures and multiphase materials.

Given the coordinate functions (or interpolation functions) of the field variables, the equilibrium equation can be discretized over each subdomain. Using the direct stiffness method of the displacement formulation the discretized set of equilibrium equations for the total region is then obtained, and solved using Gaussian elimination. The solution process is enhanced by the fact that the coefficient matrix is symmetric, positive definite and banded.

6.1 Isoparametric Finite Elements

Over the years an extensive library of finite elements has been developed. These elements vary from the simplest constant strain triangular element to the highly refined free form shell elements. For most applications the number of feasible elements is quite large, and the choice of the optimum element may be difficult [123].

The isoparametric family of finite elements [124] is among the most effective elements recently developed. This family of elements allows large flexibility in choice of element to fit geometry and continuity requirements. This presentation gives a short review of the theoretical background pertinent to the choice of element for the axisymmetric problem at hand.

On a general quadrelateral in a two-dimensional space any field variable can be approximated by

$$\psi = \sum_{i=1}^{N} \varphi_i(\xi,\eta)\,\hat{\psi}_i = \langle\varphi\rangle\{\hat{\psi}\} \tag{6.1}$$

where φ_i are interpolation polynomials in terms of the natural coordinates ξ and η, and $\hat{\psi}_i$ are the nodal point values of the variable. The number of nodes and the order of the polynomials are determined by the shape of the subdomain and the differentiability requirements on ψ.

The basic concept of the isoparametric element is the choice of the same interpolation formula for both geometry and displacement field.

$$\begin{Bmatrix} r \\ z \end{Bmatrix} = \sum_{i=1}^{N} \varphi_i(\xi,\eta) \begin{Bmatrix} r_i \\ z_i \end{Bmatrix} = [\varphi]\{\hat{r}\} \tag{6.2}$$

$$\begin{Bmatrix} u \\ w \end{Bmatrix} = \sum_{i=1}^{N} \varphi_i(\xi,\eta) \begin{Bmatrix} u_i \\ w_i \end{Bmatrix} = [\varphi]\{\hat{u}\} \tag{6.3}$$

where (r_i, z_i) and (u_i, w_i) are the nodal point coordinates and displacements respectively, Fig. 6.1. This choice completely defines the geometry of the element, and includes the constant straining and rigid body modes. A more general parametric representation would be to use a higher order approximation for the displacements than for geometry [125].

Using this formulation the stiffness matrix must be evaluated using numerical integration. This makes this type of elements quite slow for inelastic analysis of moderately thick shells, since the integration through the thickness cannot be made separately. Furthermore, at least a quadratic variation of displacements over the thickness must be used in order to ensure convergence [126]. The latter problem has been avoided by adding incompatible displacement modes that are condensed before solution [127, 126]. All this implies that an excessive number of degrees of freedom must be used, which makes the elements unfeasible for the non-linear analysis of moderately thick shells.

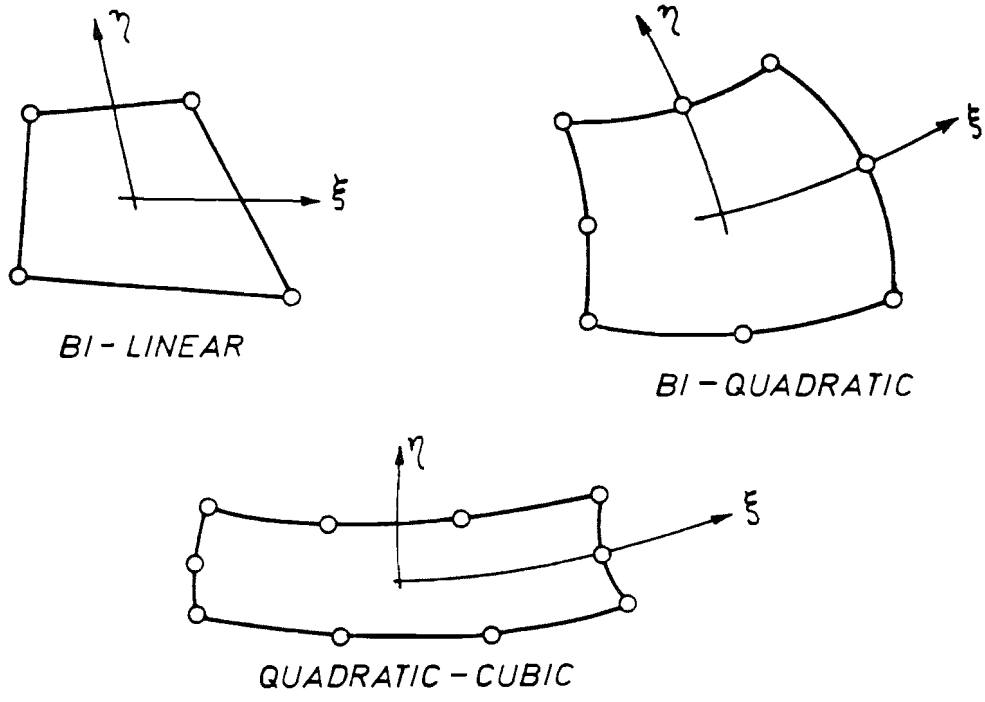

FIG. 6.1 ISOPARAMETRIC FINITE ELEMENTS.

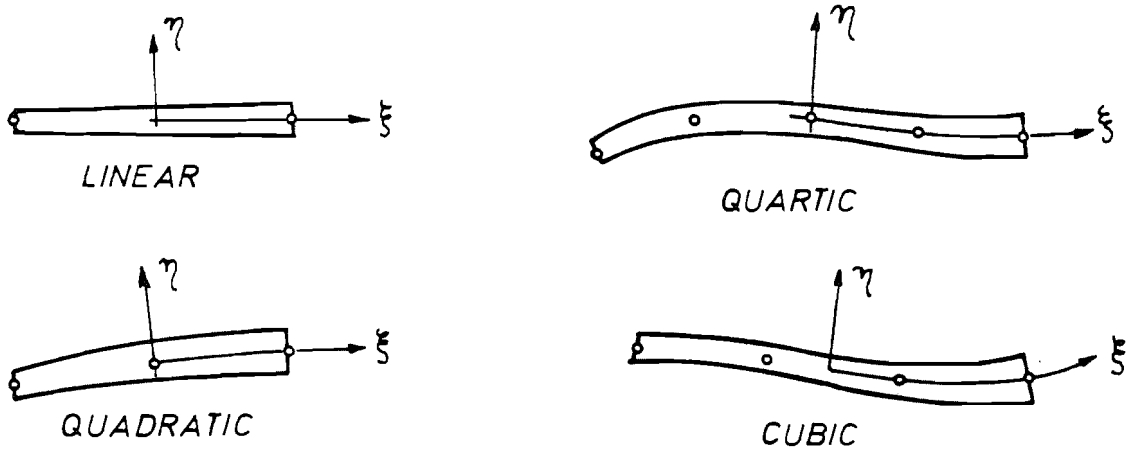

FIG. 6.2 DEGENERATE ISOPARAMETRIC FINITE ELEMENTS.

6.2 Degenerate Isoparametric Shell Elements

The deficiencies of the general isoparametric elements outlined in the previous section were alleviated in the socalled "degenerate" isoparametric shell elements [128]. In these elements different parametric representations are used for geometry and displacement field. The classical Kirchhoff assumption used in thin shell theories is relaxed, permitting shear deformations to be included. This is obtained by prescribing the rotation of the normal to the middle surface independently of the rotation of the tangent to the same surface. Furthermore, the element is considered as part of a solid and not a shell, allowing the use of the strain-displacement relations from the three-dimensional theory of elasticity. The latter implies that the classical problem of the inconsistencies of nonlinear shell theories is redundant.

For moderately thick shells this formulation gives excellent results. However, significant errors occur in applications to thin shells unless special integration schemes are used for the evaluation of the stiffness matrix [129, 130]. The reason for this error is that the relaxation of Kirchhoff's hypothesis allows shear deformations in a pure bending mode. The excessive strain energy due to shear is most dominant for elements with linear and quadratic variation of the displacements. For this reason the cubic element has been chosen for most applications.

6.2.1 Geometric Representation

Following [128] the shell geometry is described by a transformation between two coordinate systems, a global Cartesian system (r,z) and a local natural system (ξ,η). The latter system is in general curvilinear, with

$$-1 \le \xi \le +1$$
$$-1 \le \eta \le +1$$

The ξ-axis describes the middle surface of the shell and bisects the shell thickness. Note that for shells with large curvature the middle surface does not coincide with the neutral surface. The η-axis is not necessarily normal to the middle surface, but is rather defined by $\xi = 0$ along the axis. In this system the outer and inner face of the shell will be described by $\eta = +1$ and $\eta = -1$ respectively, and ends of the element by $\xi = \pm 1$. Finally the "normal" angle θ is defined as the angle between the r-axis and the η-axis, Fig. 6.2.

For later use an auxiliary local orthogonal system (s, t) will be introduced, where the s-axis coincides with the ξ-axis.

The global coordinates of any point (ξ,η) within the element are obtained by the transformation [128]

$$\begin{Bmatrix} r \\ z \end{Bmatrix} = \sum_{i=1}^{M} \varphi_i(\xi) \begin{Bmatrix} r_i \\ z_i \end{Bmatrix} + \eta \sum \tfrac{1}{2} \varphi_i(\xi)\, h_i \begin{Bmatrix} \cos\theta_i \\ \sin\theta_i \end{Bmatrix} \qquad (6.4)$$

where $\varphi_i(\xi)$ are interpolation polynomials, h_i the thickness and θ_i the "normal" angle at node i. The number of nodal points M, and hence the order of the polynomials is determined

by the element type used. In Appendix A the interpolation polynomials are given for linear, quadratic, cubic and quartic elements.

6.2.2 Displacement Field

The following displacement field is used both for the displacement increment $\underset{\sim}{u}$ and the total displacement ${}^{t}\underset{\sim}{u}$.

The kinematics of the element is based on the following assumptions:

(i) Plane sections initially normal to the middle surface remain plane, but not necessarily normal after deformation.

(ii) The displacement normal to the middle surface is constant through the thickness.

This leads to the assumed displacement field, Fig. 6.3.

$$\begin{Bmatrix} u \\ w \end{Bmatrix} = \sum_{i=1}^{N} \varphi_i(\xi) \begin{Bmatrix} u_i \\ w_i \end{Bmatrix} + \eta \sum_{i=1}^{N} \frac{1}{2} \varphi_i(\xi) h_i \begin{Bmatrix} -\sin\theta_i \\ \cos\theta_i \end{Bmatrix} \alpha_i \qquad (6.5)$$

Here the first term represents the displacement of the middle surface and the second the effect of the rotation of the normal. u and w are the global displacements, u_i and w_i the displacements and α_i the rotation of the normal at node i, Fig. 6.3. This gives three DOF at each node. The number of nodes N in the displacement expansion should be equal or greater than M. For reason of convenience M=N in this study.

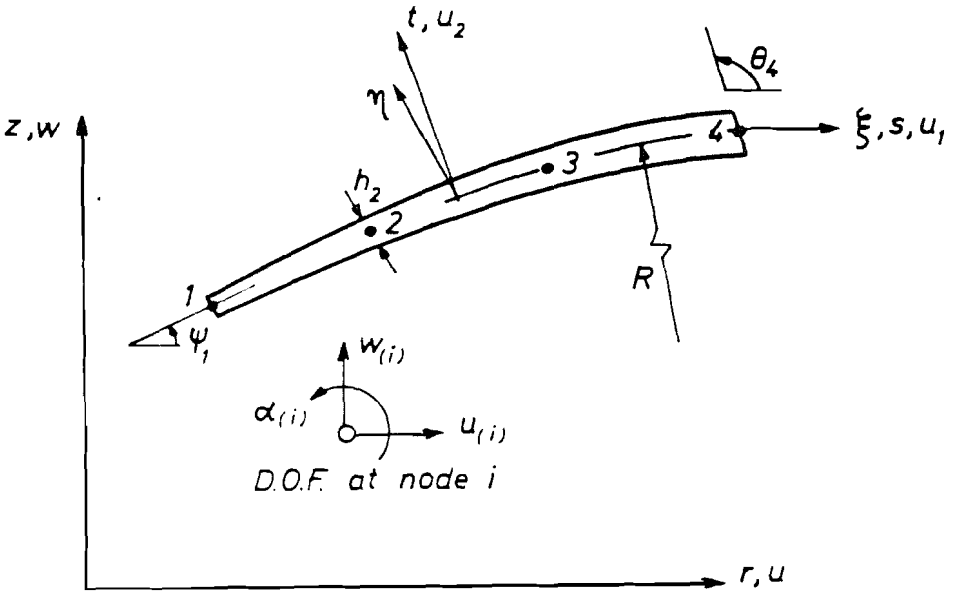

FIG. 6.3 GEOMETRY OF CUBIC ELEMENT.

Symbolically Eq. (6.5) may be written

$$\{u\} = [\varphi_u]\{\hat{u}\} \tag{6.6}$$

where $\{\hat{u}\}$ is the vector of nodal point displacements and rotations.

The displacements relative to the auxiliary coordinate system (s, t) is given by Fig. 6.3

$$\begin{Bmatrix} u_1 \\ u_2 \end{Bmatrix} = \begin{bmatrix} \cos\psi & \sin\psi \\ -\sin\psi & \cos\psi \end{bmatrix} \begin{Bmatrix} u \\ w \end{Bmatrix} \tag{6.7}$$

where $\psi(\xi)$ is defined in Fig. 6.3.

For a straight beam the relationship between the tangent rotation χ, the normal rotation α and the shear deformation γ is given by

$$\alpha(\xi) = \chi(\xi) - \gamma(\xi)$$

The rotation χ of the middle surface for thin shells is given by

$$\chi = \frac{du_1}{ds} - \frac{u_1}{R} \tag{6.8}$$

Let

$$\beta = \left[\left(\frac{\partial r}{\partial \xi}\right)^2 + \left(\frac{\partial z}{\partial \eta}\right)^2 \right]^{1/2}$$

and combine Eqs. (6.5), (6.7) and (6.8) to obtain

$$\chi = \frac{1}{\beta} \varphi_{i,\xi} (u_i \cos\psi + w_i \sin\psi) \tag{6.9}$$

Equation (6.9) shows that the rotation of the tangent to the middle surface can be prescribed independently of the normal rotation α . However, this boundary condition requires modification of the system stiffness matrix, and is not used in this study.

6.3 Strain-Displacement Relations for Axisymmetric Deformations

The increment in Cauchy-Green strain between configuration $\mathcal{B}_1$ and $\mathcal{B}_2$, referred to $\mathcal{B}_0$ is given by

$$E_{IJ} = e_{IJ} + \eta_{IJ} \tag{2.50a}$$

where

$$2\, e_{IJ} = {}^1F^K_{.I}\, u_{K/J} + {}^1F^K_{.J}\, u_{K/I} \tag{2.50c,d}$$

$$2\, \eta_{IJ} = u^K{}_{/I}\, u_{K/J} \tag{2.50e}$$

and e_{IJ} and η_{IJ} are the linear and nonlinear parts respectively.

For axisymmetric deformations the three coordinate axes will be identified with the meridianal (s), hoop and transverse normal (t) direction respectively. Hence

$${}^1F^1_{.2} = {}^1F^2_{.1} = {}^1F^2_{.3} = {}^1F^3_{.2} = 0$$

$$u^1{}_{/2} = u^2{}_{/1} = u^2{}_{/3} = u^3{}_{/2} = 0$$

Furthermore, assumption (ii) in section 6.2.2 implies

$$u_3{}_{/3} = 0 \tag{6.10}$$

$${}^1F^3_{.3} = 1 \tag{6.11}$$

In addition to assumptions (i) and (ii) in section 6.2.2, Love's first thin shell approximation postulates the transverse normal stress to be negligible:

$$S^{33} = {}^{1}S^{33} = 0 \tag{6.12}$$

This postulate is retained also for the moderately thick shells in order to avoid the constraints imposed in the transverse direction by the assumed displacement field. However, since $u_{3/3} = 0$ and $S^{33} = 0$ are mutually exclusive, the well known inconsistency in shell theories must be faced. This inconsistency can be removed by either considering the material to posses a special form of orthotropy [131], or using the generalized plane stress approach. Following the latter approach, the following approximations are made

$$(u_{3/3})^{*} = (E_{33})^{*} \quad (\dagger) \tag{6.13}$$

$$({}^{1}F^{3}_{.3})^{*} = 1 + ({}^{1}E_{33})^{*} \tag{6.14}$$

Equation (6.13) is used for the condensation of the stress-strain transformation matrix in section 3.8, while Eq. (6.14) is imperative in large deformation problems where changes in thickness become important.

It should be noted that E_{33} and ${}^{1}E_{33}$ are not determined from kinematics but from the constitutive relations. Since the constitutive relations are given in terms of physical components,

---

($\dagger$)

$(\ )^{*}$ Denotes physical components

the distinction between tensor and physical components will be dropped in the further development.

The linear part of the strain increment is given in matrix form

$$\{e\} = [\Lambda]\{u_\partial\} \tag{6.15}$$

where

$$\{e\}^T = \langle e_{11} \; e_{22} \; 2e_{13} \rangle$$

and the displacement gradient vector

$$\{u_\partial\}^T = \langle \frac{\partial u_1}{\partial s} \; \frac{u}{r} \; \frac{\partial u_1}{\partial t} \; \frac{\partial u_2}{\partial s} \rangle \tag{6.16}$$

The transformation matrix between strain and displacement gradients is defined by

$$[\Lambda] = \begin{bmatrix} {}^1F^1_{.1} & 0 & 0 & {}^1F^3_{.1} \\ 0 & {}^1F^2_{.2} & 0 & 0 \\ {}^1F^1_{.3} & 0 & {}^1F^1_{.1} & {}^1F^3_{.3} \end{bmatrix} \tag{6.17}$$

Using Eqs. (6.14), this is rewritten in terms of displacements as

$$[\Lambda] = \begin{bmatrix} 1 + \frac{\partial {}^1u_1}{\partial s} & 0 & 0 & \frac{\partial {}^1u_2}{\partial s} \\ 0 & \frac{{}^1u}{r} & 0 & 0 \\ \frac{\partial {}^1u_1}{\partial t} & 0 & 1 + \frac{\partial {}^1u_1}{\partial s} & 1 + {}^1E_{33} \end{bmatrix} \tag{6.18}$$

The displacement gradient vector $\{u_\partial\}$ is given in terms of the displacement increments through the matrix operator [B]

$$\{u_\partial\} = [B]\{u\} \tag{6.19}$$

with

$$\{u\}^T = \langle u \quad w \rangle$$

Similarly for the total displacements

$$\{{}^1u_j\} = [B]\{{}^1u\} \tag{6.20}$$

The mathematical form of [B] is given in Appendix B.

For shell applications the [B] matrix may be decomposed

$$[B(\xi,\eta)] = [B_1(\xi)] + \eta[B_2(\xi)] \tag{6.20a}$$

Combining Eqs. (6.15) and (6.19)

$$\{e\} = [\Lambda][B]\{u\} \tag{6.21}$$

For axisymmetric deformations the nonlinear part of the strain increment is defined by

$$\begin{Bmatrix} \eta_{11} \\ \eta_{22} \\ \eta_{13} \end{Bmatrix} = \frac{1}{2}\begin{Bmatrix} \left(\frac{\partial u_1}{\partial s}\right)^2 + \left(\frac{\partial u_2}{\partial s}\right)^2 \\ \left(\frac{u}{r}\right)^2 \\ \frac{\partial u_1}{\partial s}\frac{\partial u_1}{\partial t} \end{Bmatrix} \tag{6.22}$$

Denoting the i^{th} row of $[B_1]$ and $[B_2]$ by $\langle b_1 \rangle_i$ and $\langle b_2 \rangle_i$ respectively, Eq. (6.22) can be written as

$$\begin{Bmatrix} \eta_{11} \\ \eta_{22} \\ \eta_{13} \end{Bmatrix} = \frac{1}{2}\langle u \rangle \begin{bmatrix} [H_{11}] \\ [H_{22}] \\ [H_{13}] \end{bmatrix} \{u\} \tag{6.23}$$

where

$$[H_{11}] = (\{b_1\}_1 + \eta\{b_2\}_1)(\langle b_1\rangle_1 + \eta\langle b_2\rangle_1) + (\{b_1\}_4 + \eta\{b_2\}_4)(\langle b_1\rangle_4 + \eta\langle b_2\rangle_4)$$

$$[H_{11}] = [\Gamma]_1 + \eta[\pi]_1 + \eta^2[\Omega]_1$$

$$[H_{22}] = (\{b_1\}_2 + \eta\{b_2\}_2)(\langle b_1\rangle_2 + \eta\langle b_2\rangle_2)$$

$$= [\Gamma]_2 + \eta[\pi]_2 + \eta^2[\Omega]_2$$

$$[H_{13}] = (\{b_1\}_1 + \eta\{b_2\}_1)(\langle b_1\rangle_3 + \eta\langle b_2\rangle_3)$$

$$= [\Gamma]_3 + \eta[\pi]_3 + \eta^2[\Omega]_3$$

and

$$[\Gamma]_1 = \{b_1\}_1\langle b_1\rangle_1 + \{b_1\}_4\langle b_1\rangle_4$$

$$[\Gamma]_2 = \{b_1\}_2\langle b_1\rangle_2$$

$$[\Gamma]_3 = \{b_1\}_1\langle b_1\rangle_3$$

$$[\pi]_1 = \{b_1\}_1\langle b_2\rangle_1 + \{b_2\}_1\langle b_1\rangle_1 + \{b_1\}_4\langle b_2\rangle_4 + \{b_2\}_4\langle b_1\rangle_4$$

$$[\pi]_2 = \{b_1\}_2\langle b_2\rangle_2 + \{b_2\}_2\langle b_1\rangle_2$$

$$[\pi]_3 = \{b_1\}_1\langle b_2\rangle_3 + \{b_2\}_1\langle b_1\rangle_3$$

$$[\Omega]_1 = \{b_2\}_1\langle b_2\rangle_1 + \{b_2\}_4\langle b_2\rangle_4$$

$$[\Omega]_2 = \{b_2\}_2\langle b_2\rangle_2$$

$$[\Omega]_3 = \{b_2\}_1\langle b_2\rangle_3$$

It should be noted that $[\Omega]_i$ are of the order $(\frac{h}{R})^2$, where h is the shell thickness and R is the radius of curvature. These terms are retained here even though they are commonly neglected in classical thin shell solutions.

The singularity of e_{22} at the apex (r=0) can be removed using L'Hopital's rule

$$e_{22} = \frac{u}{r} = \lim_{r \to 0} \frac{\frac{\partial u}{\partial r}}{\frac{\partial r}{\partial r}} = \left.\frac{\partial u}{\partial r}\right|_{r=0}$$

If at the apex the tangent to the middle surface is horizontal, we have

$$e_{22} = e_{11} \quad \text{for } r = 0$$

6.4 Element Stiffness Matrix

The linearized incremental equilibrium equations previously derived will, when discretized by the finite element method give rise to the element stiffness matrix [K].

The element stiffness matrix can be decomposed thus:

$$[K] = [K_0] + [K_G]$$

where $[K_0]$ includes the classical infinitesimal strain stiffness and the initial strain matrix as defined by Marcal [27]. $[K_G]$ is the geometric (or initial stress) stiffness matrix.

In the following sections these matrices will be derived. In order to simplify the presentation the radius and the determinant of the Jacobian of Eq. (6.4)are assumed to be independent of η :

$$r = r(\xi)$$

$$|J| = |J(\xi)|$$

This restriction is relaxed in Appendix B, where the detailed derivations are presented.

All volume integrals in the equations for the stiffness matrices are evaluated using Gaussian quadrature. For the integration along the meridional direction no problems appear.

However, both the stress field and the constitutive matrix [C] may possess a discontinuous first derivative in the transverse normal direction during elastic-plastic deformations. For these cases a composite integration scheme will normally give more accurate results than Gaussian quadrature. The improvement experienced in this study using a 13-point Simpson integration compared to a 12-point Gaussian quadrature was of the order of 1% of the total displacement for a simply supported beam under uniform loading. More extreme conditions may occur but it is the opinion of the author that Gaussian quadrature is quite satisfactory for most cases of elastic-plastic deformation.

6.4.1 Incremental Element Stiffness Matrix $[K_o]$

The element stiffness $[K_o]$ is defined by Eq. (5.6a)

$$\underset{\sim}{K_o} \cdot \underset{\sim}{\delta u} = \int_{\mathcal{B}_o} C^{IJKL} e_{IJ}\, \delta e_{KL}\, dV$$

From Appendix B, we have

$$dV = 2\pi r\, dA = 2\pi r |J|\, d\eta\, d\xi$$

Combining this with Eq. (6.21) gives

$$[K_o] = 2\pi \int_{-1}^{+1}\int_{-1}^{+1} [B]^T [\Lambda]^T [C][\Lambda][B]\, r\, |J|\, d\eta\, d\xi \qquad (6.24)$$

Let

$$[D] = [\Lambda]^T [C][\Lambda] \qquad (6.25)$$

and define

$$[D_1(\xi)] = \int_{-1}^{+1} [D]\,|J|\,d\eta$$

$$[D_2(\xi)] = \int_{-1}^{+1} \eta\,[D]\,|J|\,d\eta \qquad (6.26)$$

$$[D_3(\xi)] = \int_{-1}^{+1} \eta^2\,[D]\,|J|\,d\eta$$

Combining Eqs. (6.20a), (6.24) and (6.26) leads to

$$[K_0] = 2\pi \int_{-1}^{+1} \left([B_1]^T[D_1][B_1] + [B_1]^T[D_2][B_2] + \right. \qquad (6.27)$$

$$\left. + [B_2]^T[D_2][B_1] + [B_2]^T[D_3][B_2] \right) r(\xi)\,d\xi$$

Here the first term represents the membrane action, the second and third are coupling terms between membrane and bending action, while the last term is due to bending alone.

For flat plates and shallow shells subjected to small deformations in the elastic range, $[D_2]$ will vanish and no coupling takes place. For inelastic materials and in large displacement theory [D] will be a function of both η and ξ, and $[D_i]$ must be evaluated numerically.

6.4.2 Geometric Stiffness Matrix, $[K_G]$

The geometric stiffness matrix is defined by Eq. (5.6e)

$$\underset{\sim}{K}_G \cdot \delta\underset{\sim}{u} = \int_{\mathcal{B}_0} {}^1S^{IJ}\,\delta\eta_{IJ}\,dV \qquad (5.6e)$$

Let

$$\{{}^1S\}^T = \langle {}^1S^{11}\ {}^1S^{22}\ 2\,{}^1S^{13} \rangle$$

and

$$\{\delta\eta\}^T = \langle \delta\eta_{11}\ \delta\eta_{22}\ \delta\eta_{13} \rangle$$

$\{\delta\eta\}$ is obtained taking the variation of Eq. (6.23) which gives

$$\begin{Bmatrix} \delta\eta_{11} \\ \delta\eta_{22} \\ \delta\eta_{13} \end{Bmatrix} = \langle \delta u \rangle \begin{bmatrix} [H_{11}] \\ [H_{22}] \\ \frac{1}{2}([H_{13}]^T + [H_{13}]) \end{bmatrix} \{u\} \tag{6.28}$$

where $[H_{11}]$, $[H_{22}]$ and $[H_{13}]$ are defined in section 6.3.

Define the following vectors:

$$\begin{aligned} \{M_0\} &= \int_{-1}^{+1} \{1 \; \zeta\} \, |J| \, d\eta \\ \{M_1\} &= \int_{-1}^{+1} \eta \{1 \; \zeta\} \, |J| \, d\eta \\ \{M_2\} &= \int_{-1}^{+1} \eta^2 \{1 \; \zeta\} \, |J| \, d\eta \end{aligned} \tag{6.29}$$

Combining Eqs. (5.6e), (6.28) and (6.29) the final form becomes

$$[K_G] = 2\pi \int_{-1}^{+1} \sum_{i=1}^{3} \left(\{M_0\}_i [\Gamma]_i^* + \{M_1\}_i [\Pi]_i^* + \{M_2\}_i [\Omega]_i^* \right) r(\xi) \, d\xi \tag{6.30}$$

where

$$[\Gamma]_i^* = [\Gamma]_i \quad \text{for } i = 1,2$$

$$[\Gamma]_3^* = \frac{1}{2}([\Gamma]_3^T + [\Gamma]_3)$$

and similarly for $[\Pi]_i^*$ and $[\Omega]_i^*$. Note also that $\{M_0\}_i$ means the i^{th} component of the vector $\{M_0\}$, and that $[\Gamma]_i^*$ is a square matrix.

In classical shell theory, the second moment $\{M_2\}$ is commonly neglected, but can be retained here without significant computational efforts.

6.5 Consistent Nodal Loads

6.5.1 Equilibrium Nodal Forces

Using the Green-Gauss theorem the virtual work equation expressing the equilibrium between the total stress field and the generalized equilibrium nodal forces is obtained

$$\underset{\sim}{R}_E \cdot \underset{\sim}{\delta y} = \int_{\mathcal{B}_o} {}^1S^{IJ}\, \delta e_{IJ}\, dV \tag{5.6f}$$

Combining Eqs. (6.20a), (6.21) and (5.6f), the equilibrium nodal forces are given by

$$\{R_E\}^T = 2\pi \int_{-1}^{+1} \left(\langle N_0 \rangle [B_1] + \langle N_1 \rangle [B_2] \right) r(\xi)\, d\xi \tag{6.31}$$

where

$$\langle N_0 \rangle = \int_{-1}^{+1} \langle {}^1S \rangle [\Lambda]\, |J|\, d\eta$$

$$\langle N_1 \rangle = \int_{-1}^{+1} \eta \langle {}^1S \rangle [\Lambda]\, |J|\, d\eta$$

Here the integration in both ξ and η direction is performed numerically using Gaussian quadrature. Here it should be pointed out that $\langle N_0 \rangle$ and $\langle N_1 \rangle$ are different from the stress resultants defined in section 6.4.2.

6.5.2 Creep Pseudo Loading

The pseudo loading due to creep is constructed similarly to the equilibrium nodal loads

$$\underset{\sim}{R}_c \cdot \underset{\sim}{\delta y} = \int_{\mathcal{B}_o} S_c^{IJ}\, \delta e_{IJ}\, dV \tag{5.6f}$$

where S_c^{IJ} is the time-dependent increment in Piola stress between B_1 and B_2. S_c^{IJ} may be given directly from the stress-strain law as in linear viscoelasticity or by Eq. (2.68e), in flow theory of creep.

Let

$$\langle S_c \rangle = \langle S_c^{11} \quad S_c^{22} \quad 2S_c^{13} \rangle$$

and

$$\langle Q_0 \rangle = \int_{-1}^{+1} \langle S_c \rangle [\Lambda] |J| \, d\eta$$

$$\langle Q_1 \rangle = \int_{-1}^{+1} \eta \langle S_c \rangle [\Lambda] |J| \, d\eta$$

which finally leads to

$$\{R_c\}^T = 2\pi \int_{-1}^{+1} \left(\langle Q_0 \rangle [B_1] + \langle Q_1 \rangle [B_2] \right) r(\xi_1) \, d\xi \qquad (6.32)$$

6.5.3 Traction Type Loading

As indicated in section 2.6, distinction must be made between conservative and nonconservative traction type loading. The conservative loading is derivable from a potential, as for example gravity loads, while hydrostatic pressure is a typical example of nonconservative loading.

For conservative loading the nodal load vector is given by

$$\underset{\sim}{R} \cdot \delta \underset{\sim}{u} = \int_{\partial B_0} \bar{t}^I \delta u_I \, dA \tag{2.52}$$

where $\bar{\underset{\sim}{t}}$ is the prescribed traction vector.

The load intensity at any point on the loading surface is given by

$$\begin{Bmatrix} p_1 \\ p_2 \end{Bmatrix} = \left[\begin{array}{c|c} \langle \varphi \rangle & 0 \\ \hline 0 & \langle \varphi \rangle \end{array}\right] \begin{Bmatrix} \hat{p}_1 \\ \hline \hat{p}_2 \end{Bmatrix} \tag{6.33}$$

with p_1 and p_2 being the load intensities in direction s and t respectively. $\langle \varphi \rangle$ is a vector consisting of the interpolation polynomials $\varphi_i(\xi)$ and $\hat{p}_1$ and $\hat{p}_2$ are vectors of load intensities at nodal points. The number of interpolation polynomials necessary to represent the variation in loading may vary, but in most cases three terms is quite sufficient.

Using Eqs. (6.6) and (6.7)

$$\begin{Bmatrix} u_1 \\ u_2 \end{Bmatrix} = \begin{bmatrix} \cos\psi & \sin\psi \\ -\sin\psi & \cos\psi \end{bmatrix} [\varphi_u] \{\hat{u}\}$$

Further

$$dA = 2\pi r(\xi) \beta \, d\xi$$

where β is defined in section 6.2.2.

Substitution into Eq. (2.52) gives

$$\{R\} = 2\pi \int_{-1}^{+1} \langle \hat{p}_1 \; \hat{p}_2 \rangle \begin{bmatrix} \{\varphi\} & 0 \\ 0 & \{\varphi\} \end{bmatrix} \begin{bmatrix} \cos\psi & \sin\psi \\ -\sin\psi & \cos\psi \end{bmatrix} [\varphi_u] \beta(\xi) r(\xi) \, d\xi \tag{6.34}$$

For nonconservative loading the nodal load vector may be written, Eq. (5.6f) as

$$\underset{\sim}{R}\cdot\delta\underset{\sim}{u} = -\int_{\partial\mathcal{B}_0} p\,\frac{\rho_0}{\rho}\,({}^{t}\underset{\sim}{F}^{-1})^{I}_{\cdot J}\,N^{J}\,\delta u_I\,dA \tag{5.6f}$$

From the requirement of conservation of mass

$$\frac{\rho_0}{\rho} = \det({}^{t}\underset{\sim}{F}) = {}^{t}F^{2}_{\cdot 2}\,({}^{t}F^{1}_{\cdot 1}\,{}^{t}F^{3}_{\cdot 3} - {}^{t}F^{1}_{\cdot 3}\,{}^{t}F^{3}_{\cdot 1}) \tag{6.35}$$

The unit normal to the middle surface may be decomposed as, Fig. 6.2,

$$\{N\}^{T} = \langle -\sin\psi \quad 0 \quad \cos\psi \rangle \tag{6.36}$$

Finally, the inverse of the deformation gradient ${}^{t}\underset{\sim}{F}$ is inverted numerically to yield

$$\{R\} = -2\pi\int_{-1}^{+1} \langle p\rangle\{\varphi\}[\varphi_{,r}][{}^{t}F^{-1}]\{N\}\,r(\xi)\,\beta(\xi)\,d\xi \tag{6.37}$$

where $\langle p\rangle$ is the vector of nodal point values of hydrostatic pressure, and $\{\varphi\}$ is given above.

Equation (6.34) or (6.37) is integrated numerically using Gaussian quadrature, and assembled to give the total load vector.

7. NUMERICAL EXAMPLES

7.1 Description of Computer Programs

Three separate computer programs were written based on the formulation presented in the preceding chapters. All programs were written in FORTRAN IV for use on CDC 6400, using dynamic storage allocation:

i) Program I was written for large displacement analysis of axisymmetric shells with linearly elastic material properties. Post-buckling behavior is included.

ii) Program II treats large displacements of elastic-plastic shells of revolution, and of shells subjected to creep. Both creep and plasticity may occur simultaneously.

iii) Program III analyzes large displacements of shells made on linearly viscoelastic materials. The relaxation modulus of the materials must be given as a Prony series.

All programs basically use in-core storage, except small segments where tape-simulated disc storage is used for displacement gradient matrices and stress-strain matrices. All programs need ca. 40000 (octal) words for the program proper, and additional blank common storage for data and stiffness matrix, etc.

Program I:

This is the basic large displacement program for elastic shells. Large segments of this program are also used in Programs II and III. The program consists of:

MAIN program dynamically assigns the needed storage, and drives the subroutines.

INPUTD subroutine reads geometric and material data and initializes all matrices.

STIFFNS. During the first load increment this subroutine computes all displacement gradient matrices at prescribed integration and nodal points, and stores these on tape-simulated discs. For subsequent increments these matrices are read from tape. Numerical integration of the stiffness matrices is performed using 4 or 6 Gaussian integration points in the meridional direction and 2 points over the thickness. The stress-strain matrix is transformed according to the value of the deformation gradient, and incremental and geometric stiffness matrices are assembled. Finally the equilibrium nodal forces are computed from the stress field.

DISPL. This subroutine triangularizes the system stiffness matrix, and governs the loading sequence for the postbuckling analysis. It calls the load generating subroutine NODLOD and the equation solver BANSOL.

STRESS computes the Piola-Kirchhoff stresses at integration and nodal points, and transforms these to Cauchy stresses. It also computes the deformation gradients at all needed points, and outputs all stress results asked for.

Program II:

Most subroutines are as in Program I, and only those features that are different will be mentioned here.

STIFFNS. For elastic-plastic analysis the stress-strain matrix is read from tape, but computed for creep analysis. The

numerical integration of the stiffness matrix is performed with 2-16 points over the thickness for elastic-plastic cases. For creep analysis the creep pseudo-loading and equilibrium nodal forces are computed.

CREEP. This subroutine computes the creep strain increments and stress increment. Time-hardening or strain-hardening laws may be used for primary creep. Steady state creep is included and also Odquist's inelastic approach.

MATP. Computes stress-strain relationship for elasto-plastic deformations. Checks loading criterion and interpolates material data given in discrete form. If stress exceeds yield stress the total stress or stress increment may be scaled down to yield stress. Stress-strain matrix may be computed using Odquist's modified inelastic theory. All stress-strain matrices are written on tape.

Program III:

This program is identical to Program I in most aspects, except postbuckling capabilities are not included. Only differences are in the STIFFNS subroutine where creep pseudo-loading is computed as in Program II.

VISCO. This subroutine performs the convolution integration using the recursive algorithm given in Chapter 4. Relaxation modulus must be given in terms of an exponential (Prony) series expansion.

7.2 Nonlinear Analysis of Elastic Systems

The program's capability of solving geometrically nonlinear elastic systems has already been illustrated in section 5.6. The infinite plate strip considered there is not a particularly crucial test for the program. Plate structures with fixed supports and normal load are of the stiffening type, where the stiffness increases with increasing loads.

A more representative test would be a softening system, where a small increase in loading will yield a large increase in displacement.

The analysis of highly nonlinear structures will here be illustrated by a torus subjected to external pressure, and the snap-through behavior of a shallow spherical cap. For the latter case instability will occur, and load reversals must be used to solve the problem.

7.2.1 Torus Under External Pressure

The torus shown in Fig. 7.1 is subjected to uniform external pressure. The geometry of the torus is defined by

$L = 150$ in. $\qquad R = 100$ in. $\qquad h = 1$ in.

and the material properties were taken as

$E = 10^7$ psi $\qquad \nu = 0.3$

Due to symmetry only the upper half of the torus is considered. The finite element analysis was carried out using 30 evenly spaced elements. The external pressure was $p = 100$ psi, and a total of 20 load increments were used. Each load increment was 5% of total applied load, and no iterations were performed during the analysis. Equilibrium check using out-of-

balance force method was used to control the convergence.

The numerical results were compared with Kalnins multisegment analysis [132]. The resulting normal displacements, meridional moments and hoop membrane force is given in Figs. 7.1, 7.2 and 7.3. The normal displacement agrees closely with those of Kalnins, while the stress resultants obtained here are slightly smaller than given in [132]. The trend of the results agrees very well, however.

The discrepancies of the stress resultants are only pronounced near the crown of the torus, where the shear stresses are greatest. The inclusion of shear deformations in the present analysis may therefore explain some of the discrepancies. It should also be pointed out that the torus is a quite nonlinear structure, where the nonlinear effects become important even though the normal displacement is only 30% of the wall thickness.

The computer time for the analysis was 0.3 sec. (CP) per element and load step.

7.2.2 Buckling of Shallow Spherical Cap

The large displacement analysis of spherical caps has been the subject of extensive research during the last decade. An excellent bibliography of this work, both closed form solutions and numerical solutions, is given by Yaghmai [31].

It is well known that the nonlinear behavior of this type of structures is highly sensitive to its characteristic geometric parameters. Depending on these parameters the deformation mode

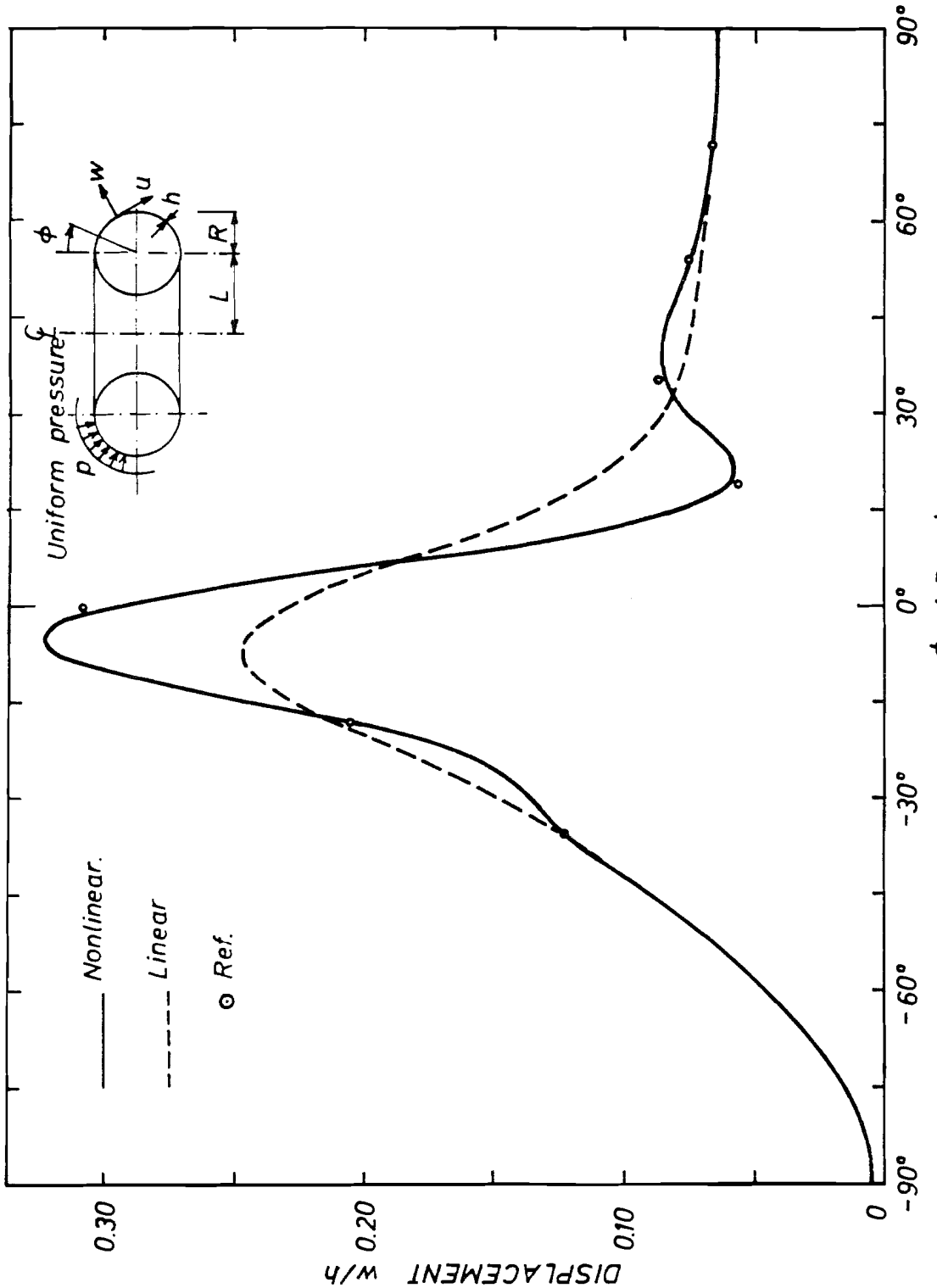

FIG. 7.1 NORMAL DISPLACEMENT OF TORUS.

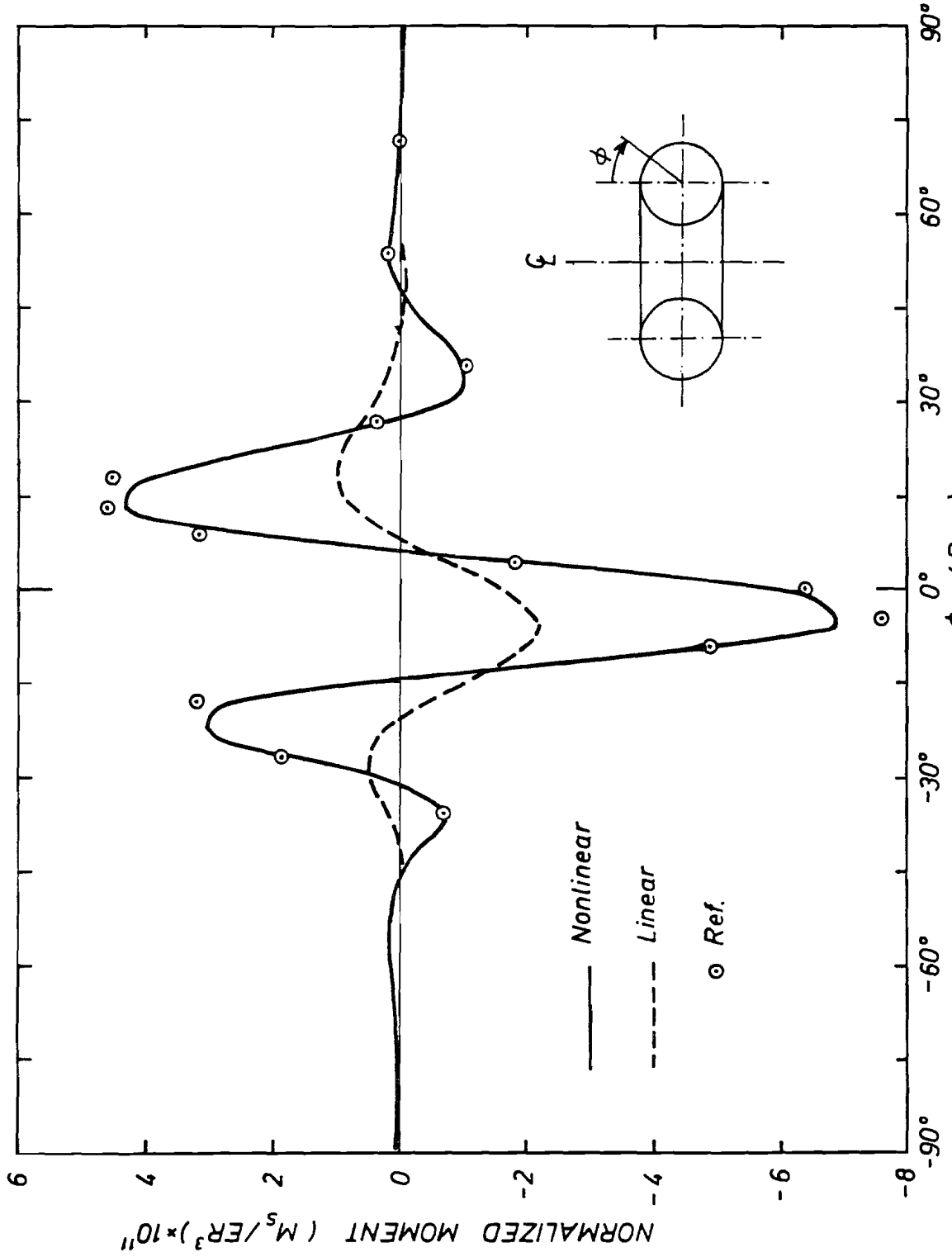

FIG. 7.2 MERIDIONAL MOMENT IN TORUS.

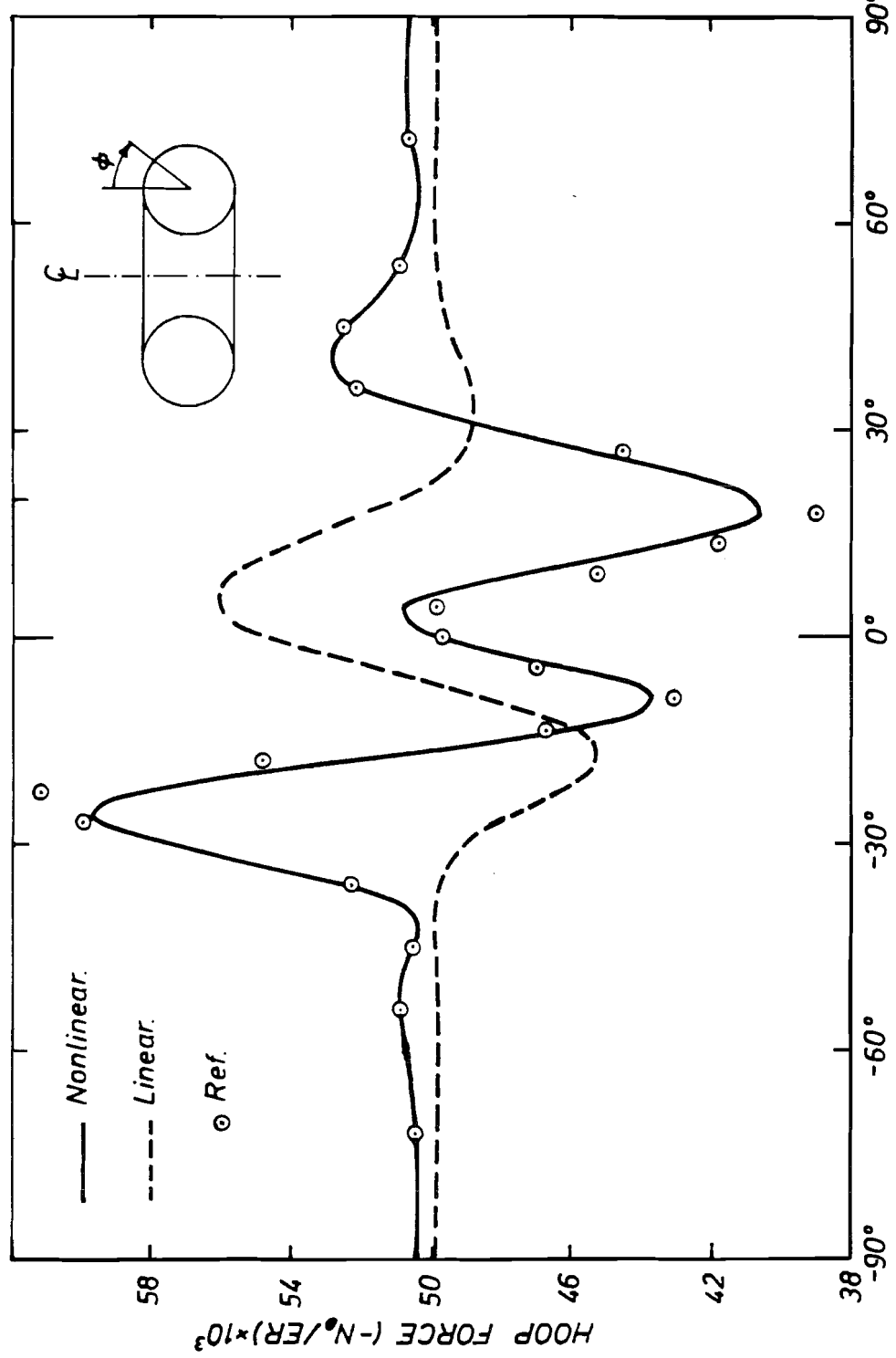

FIG. 7.3 IN-PLANE HOOP FORCE IN TORUS.

will be either axisymmetric or asymmetric, and the stability criterion will be either bifurcation buckling or snap-through.

The characteristic parameter most commonly used is

$$\lambda^2 = (12(1-\nu^2))^{1/2}\, h/t \tag{7.1}$$

where ν is Poisson's ratio, h is the rise and t is the thickness of the shell. Kornishin [133] used the parameter

$$\bar{k} = \frac{a^2}{Rt} \tag{7.2}$$

Here R is the radius of the middle surface of the shell, t the thickness and a the radius of the horizontal projection of the shell.

Finally Weinitschke [134, 135] introduced a slight modification of Eq. (7.1)

$$\mu^2 = m^2 \frac{R}{t} \alpha^2 \tag{7.3}$$

where α is half the opening angle of the shell, R and t as given above, and

$$m^2 = (12(1-\nu^2))^{1/2}$$

Following Weinitschke the following criterion exists for simply supported shells with uniform pressure

i) $2.2 \leq \mu \leq 4.0$

The critical deformation mode is symmetric, and

ii) $\mu > 4.0$

The asymmetric mode becomes governing.

For other boundary conditions these limiting values are modified, for a clamped shell to 3.4 and 5.5.

In order to illustrate the capability of tracing the post-buckling behavior, a shallow cap with an axisymmetric buckling mode was chosen. The geometrical data were as follows, Fig. 7.4.

$R = 50"$ $\quad t = 0.1"$ $\quad \alpha = 4.48^{\circ}$

The material was assumed to be linearly elastic, with Younge's modulus and Poisson's ratio

$E = 10^6$ psi $\quad \nu = 1/3$

This gives a characteristic parameter $\mu^2 = 10$. The shell was fixed at the boundary and loaded by uniform pressure. The normalized load parameter is given by

$$\bar{p} = \frac{\mu^4 m^2}{4E} \left(\frac{R}{t}\right)^2 p$$

and the applied external pressure was 40 psi.

The shell was analyzed using 5 elements, and a total of 36 load increments. Of these, 8 load steps were used to determine the upper critical load, and the remaining steps to trace the complete postbuckling behavior.

The results are compared with Weinitschke's power series solution in Fig. 7.4. The agreement between the two solutions is very good. Even though the load increments used were quite large, both the upper and lower critical value are determined with good accuracy.

The loading sequence was as follows: The ascending part of the load-deflection curve was determined using 5 steps with a load factor of 10%, and then proceeding with steps @ 5% until buckling took place. Then 2 steps with displacement control and 2 steps with load factor equal -1% were used to determine the

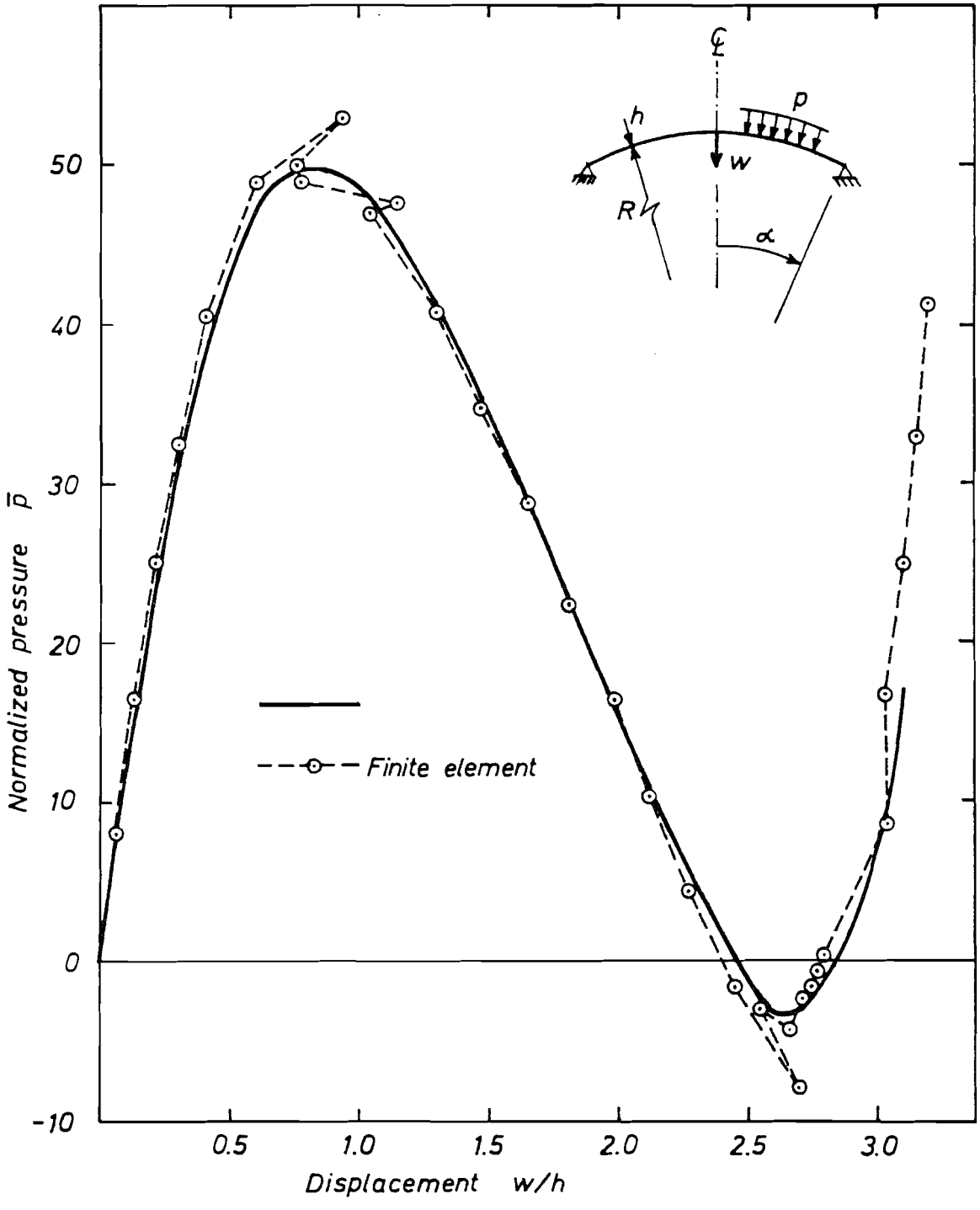

FIG. 7.4 POSTBUCKLING BEHAVIOR OF ELASTIC, SHALLOW SPERICAL SHELL.

start of the descending part of the curve. Thereafter the load was reduced by 7.5% until the lower critical load was reached, and above mentioned procedure was again applied to get onto the final ascending curve.

The computer time needed for the complete analysis of the structure was 0.3 sec. (CP) per element per load step.

7.3 Primary Creep in Pressure Vessels

To demonstrate the application of the method to nonlinear creep problems, a torispherical pressure vessel head under uniform internal pressure is considered. The nonlinear elastic behavior is investigated, and the deformation and stress redistribution under primary creep is studied.

The torispherical head has a skirt diameter, D = 100 in., the radius of the sphere, R = D = 100 in., and the meridional radius of the torus, r = 0.2·D = 20 in. The shell has a uniform thickness h = 0.008·D = 0.8 in. The material is an aluminum alloy 7075-T6, and the temperature T = 600°F. The following material properties were used:

$E = 5.2\ 10^6$ psi $\qquad\qquad \nu = 0.3$

and the creep law was taken in, the form

$$\epsilon_c = A e^{B\sigma} t^k$$

where

$$A = 2.64 \cdot 10^{-5}$$
$$B = 1.92 \cdot 10^{-1}$$
$$k = 0.66$$

Fur use in the analysis the creep law was recast into the strain-hardening form.

The internal pressure was 25 psi.

A total number of 20 elements was used, with 8 equal elements describing both the sphere and the torus, and the remaining 4 representing the cylinder. Eight (8) integration points were used over the thickness to compute the creep "pseudo-loading".

The pressure vessel is only moderately nonlinear at the applied loading range, as indicated in Fig. 7.5. Here the meridional bending moment and in-plane force is plotted for both linear and nonlinear analysis. The nonlinearity can be expected to be more pronounced as the displacements increase due to creep.

For the creep analysis the pressure is applied instantaneously using 6 load steps. A total of 26 time steps were used to trace the behavior up to t = 1000 hours. The step length varied from 0.2 hours to 300 hours.

The normal displacement at the apex is given in Fig. 7.6. It should be noted that the strains here are so small that the reduction of thickness can be neglected. If deflection is used as the controlling factor in design or performance evaluation, the difference between linear and nonlinear analysis may be significant. The variation of normal displacement along the meridian is shown in Fig. 7.7 at various time intervals, and the redistribution of meridional stress due to creep deformation is shown in Fig. 7.8. The reduction of the stress peaks is quite significant.

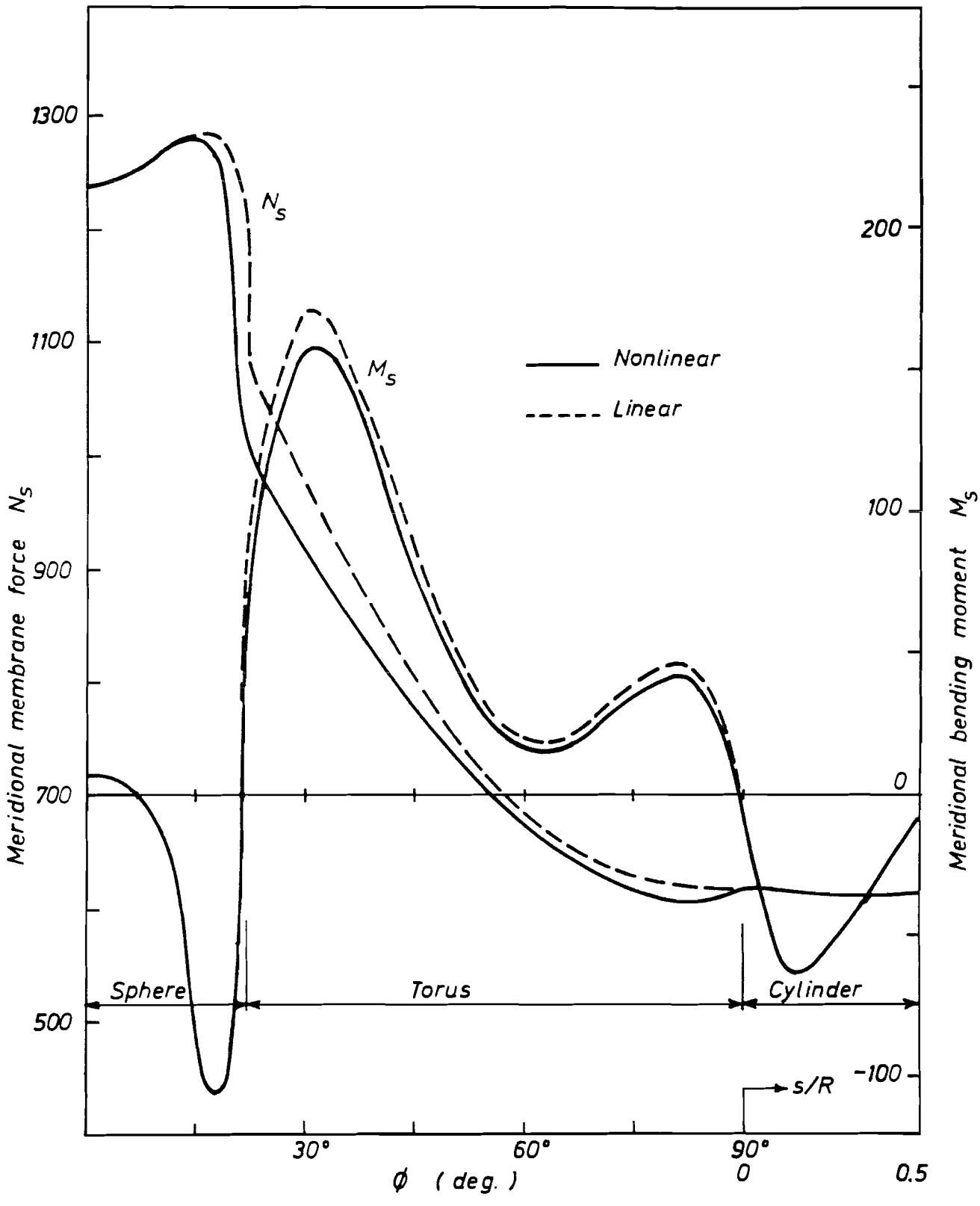

FIG. 7.5 MERIDIONAL MOMENT AND IN-PLANE FORCE IN ELASTIC TORISPHERICAL PRESSURE VESSEL

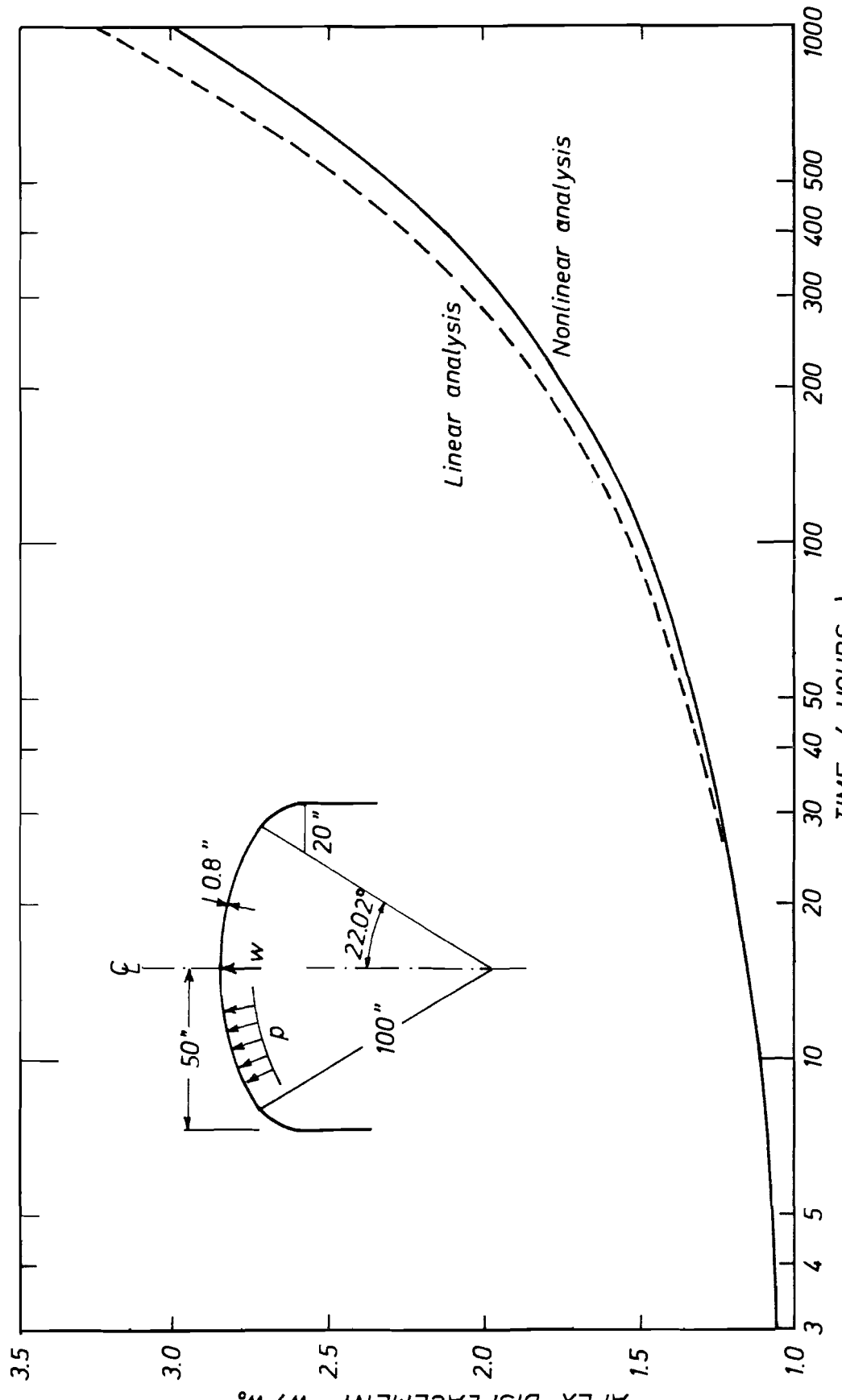

FIG. 7.6 APEX DISPLACEMENT OF TORISPHERICAL HEAD DURING CREEP

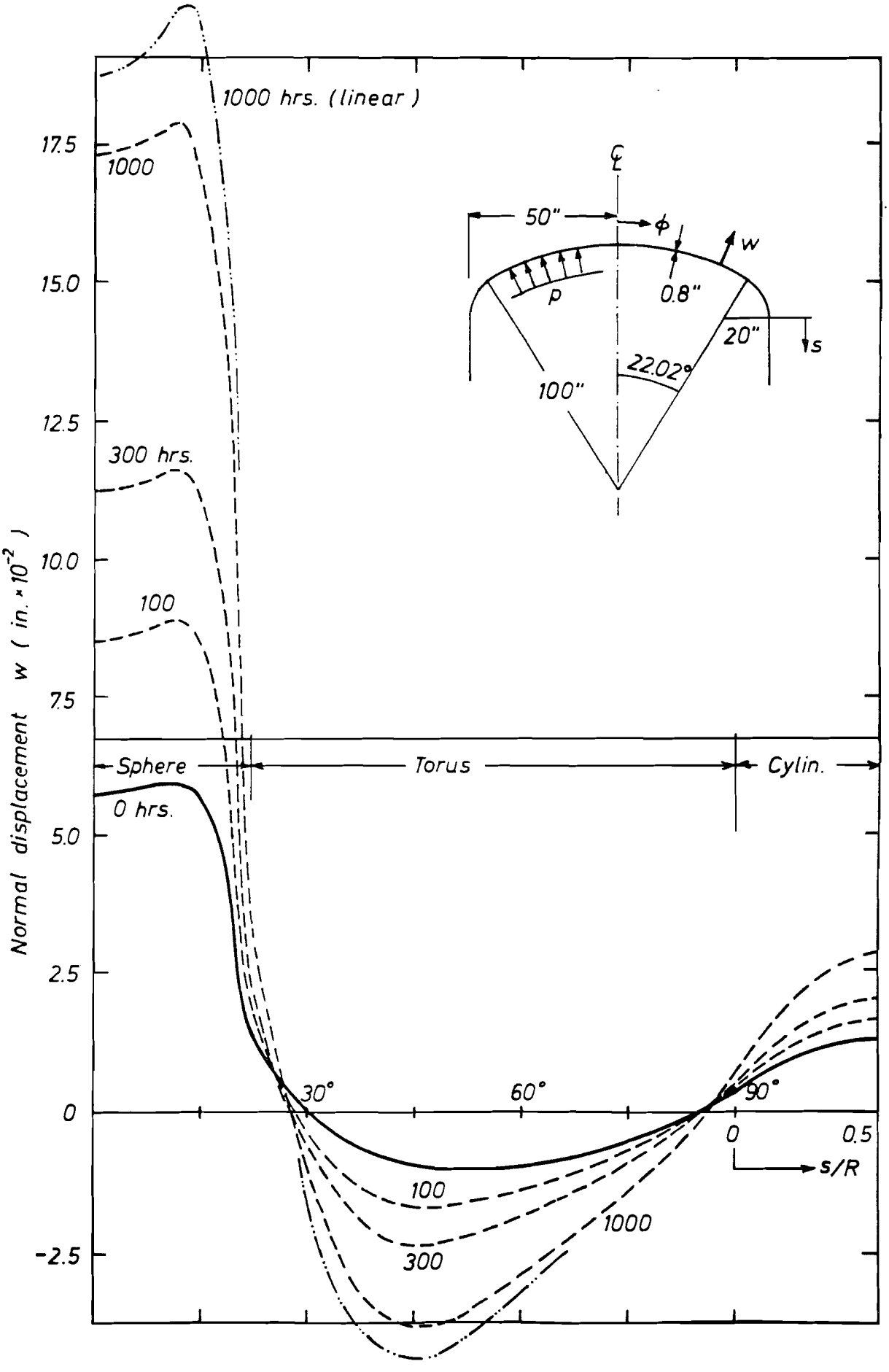

FIG. 7.7 NORMAL DISPLACEMENT OF TORISPHERICAL HEAD

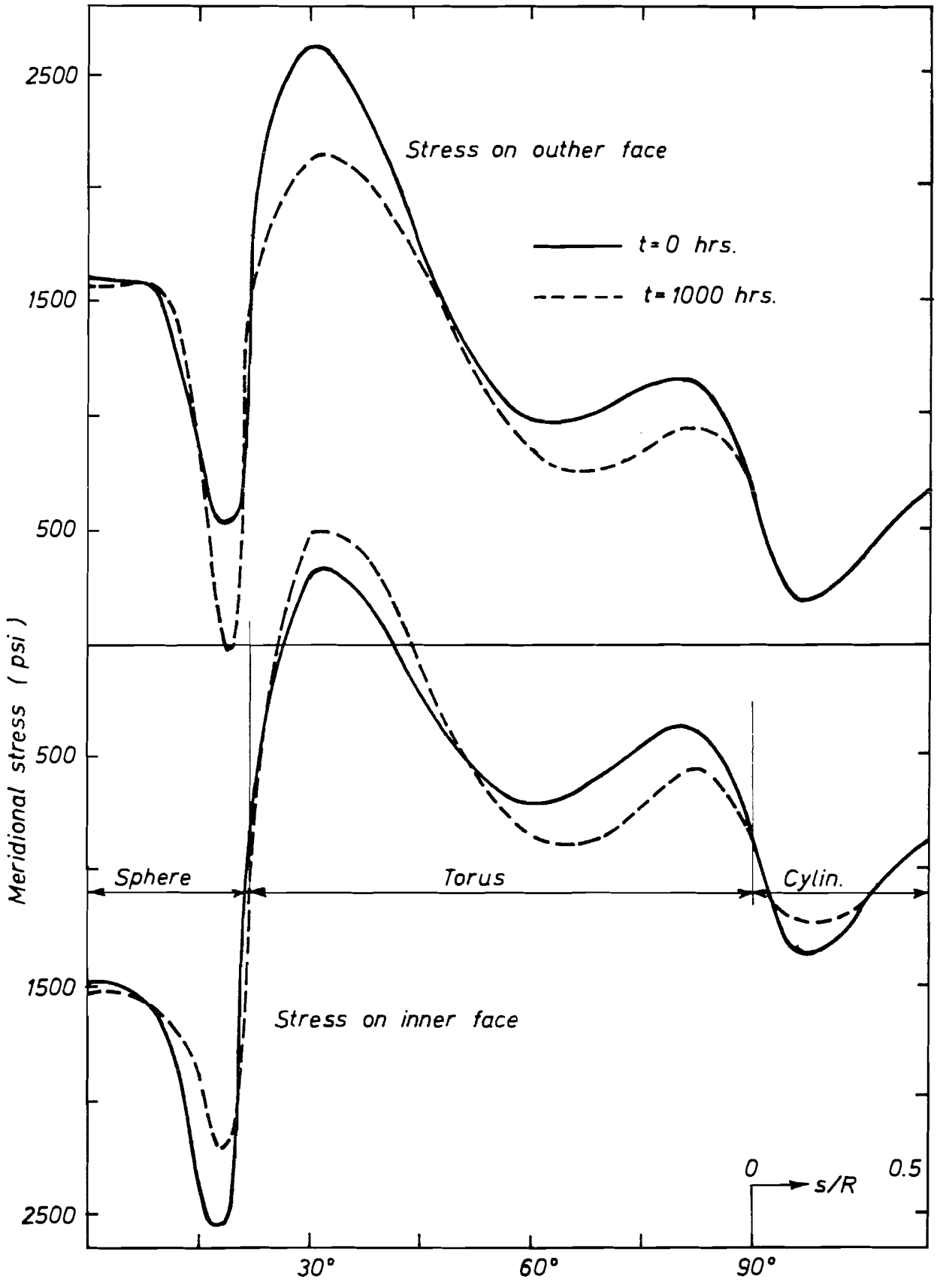

FIG. 7.8 MERIDIONAL STRESS IN TORISPHERICAL HEAD SUBJECTED TO CREEP.

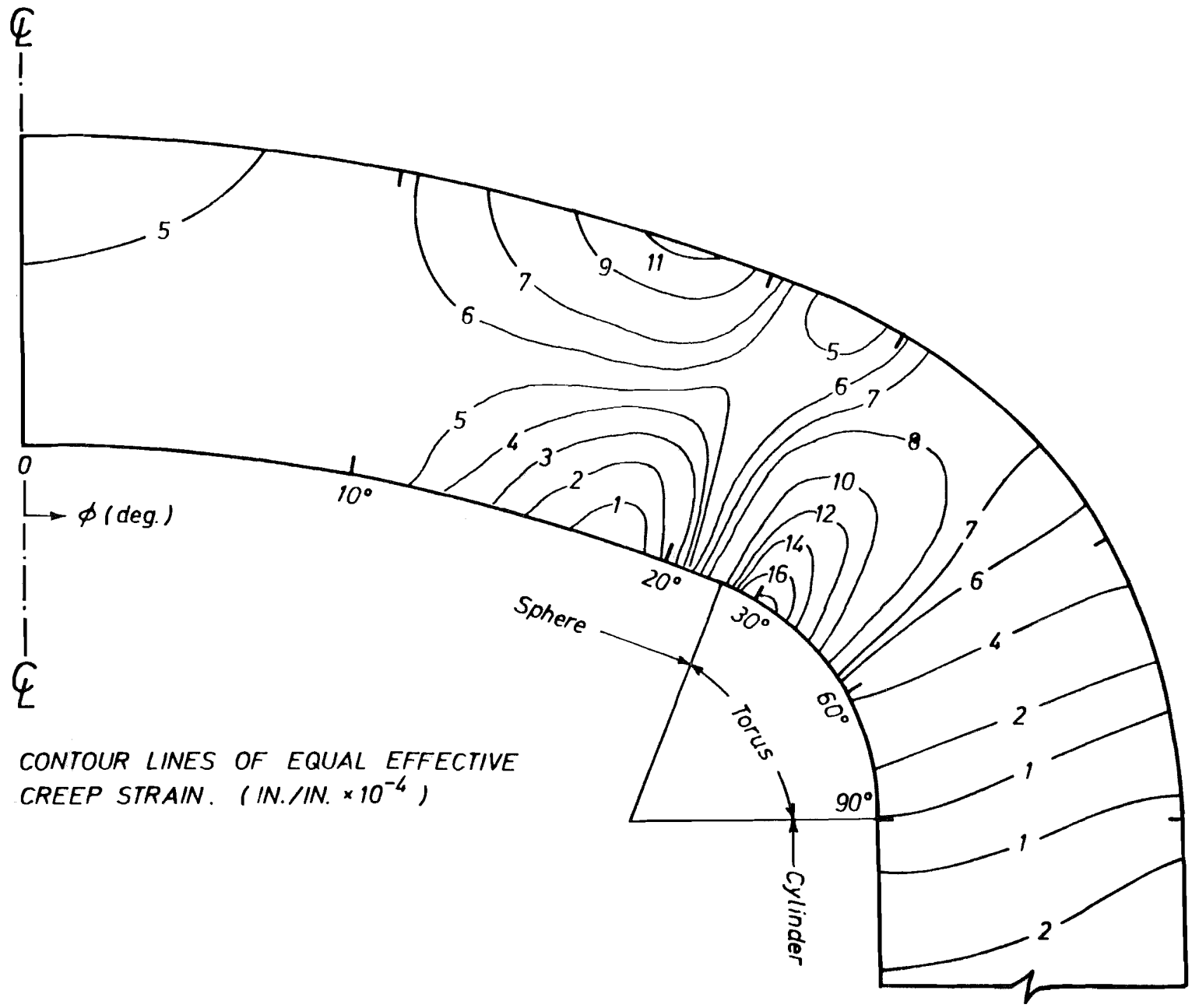

FIG. 7.9 EFFECTIVE CREEP STRAIN IN TORISPHERICAL PRESSURE VESSEL

It should be noted that the analysis was not brought to a point where a steady state solution was obtained, from which the creep rupture load could be determined. The rupture criterions suggested by Kachanov or Rabotnov can, however, easily be incorporated into the program.

Finally the distribution of effective creep strain throughout the pressure vessel is given in Fig. 7.9. The unit used is (in./in. x 10^{-4}). As can be seen, the strains are moderate through most of the shell, except in the torus near the juncture with the sphere.

A total of 312 sec. (CP) computer time was needed for the nonlinear analysis.

7.4 Elastic-Plastic Analysis of Pressure Vessel

The elastic-plastic behavior of a torispherical pressure vessel was studied using Program II. The geometry of the vessel is identical to the vessel analyzed in section 7.3.

$D = 100$ in. $\qquad R = 100$ in.

$r = 20$ in. $\qquad h = 0.8$ in.

The material is assumed to be elastic-perfectly plastic, with yield stress, $\sigma_y = 3.10^4$ psi, Young's modulus $E = 3.10^7$ psi, and Poisson's ratio $\nu = 0.3$.

For the analysis the shell was discretized by 20 finite elements. Eight (8) equal elements were used to describe the sphere and the torus, and 4 elements for the cylinder. The tangent stiffness matrix was integrated using 12 Gaussian integration points over the shell thickness, and 4 points along

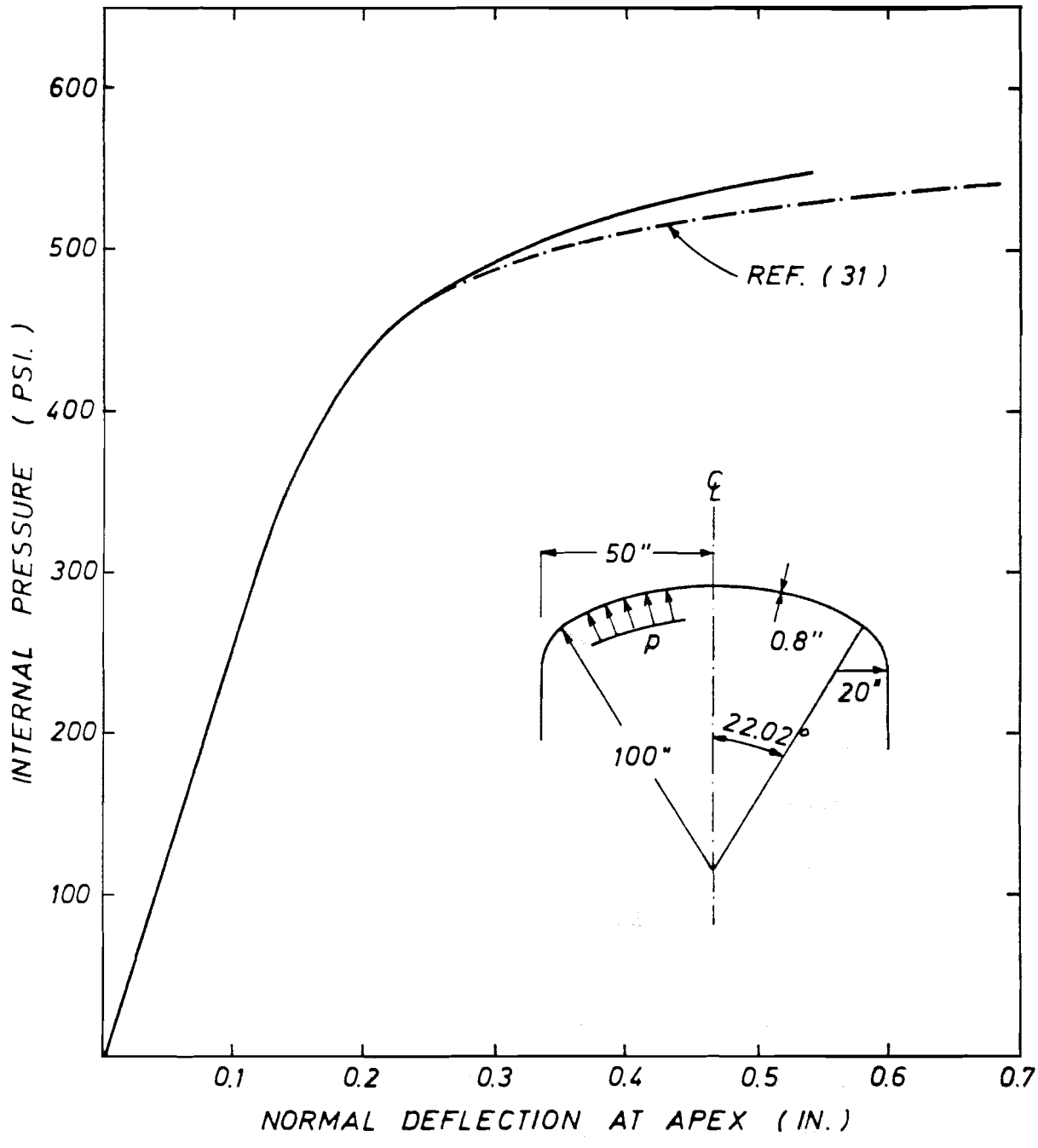

FIG. 7.10 ELASTIC-PLASTIC ANALYSIS OF TORI-SPHERICAL PRESSURE VESSEL.

the meridian of the element. The internal pressure was applied in increments of 50 psi up to a pressure of 400 psi, when the load increment was reduced to 20 psi.

The load-deflection curve for the normal displacement at the apex is plotted in Fig. 7.10, and compared with the results given by Yaghmai [31]. The two analyses give results that agree very well up to a pressure of 480 psi, at which point Yaghmai predicts a more rapid reduction in the stiffness of the shell. The discrepancies between the curves are mostly due to the better representation of the plastic zones in Reference [31]. There 16 integration points were used over the shell thickness and the load applied in increments of 7.5 psi.

In the present study the discretization of the shell and the load sequence were restricted by the limited computer time available for the investigation. For this reason a valid comparison between the two formulations of the elastic-plastic problem was not possible.

7.5 Creep Buckling Problems

7.5.1 Creep Buckling of Imperfect Column

The program's capability for solving creep buckling problems will be verified for an imperfect column with rectangular cross section. This problem has been extensively studied in the literature, and is often used to compare alternative analysis methods [57], [58].

The objective of this analysis is to find the displacement variation with time, and to determine the critical time t_{cr} .

t_{cr} is defined as the time when the column becomes unstable subjected to the given loading, i.e., when the displacements go to infinity. In a large displacement analysis the critical time is reached when the displacements become excessively large.

The column has the following dimensions:

$$L = 8.0 \text{ in.} \qquad h = 0.25 \text{ in.} \qquad b = 1.0 \text{ in.} \qquad w_o = 0.02 \text{ in.}$$

where w_o is the excentricity at midspan. The material used in the analysis was an aluminum alloy 7075-T6, which has the following material properties at 600°F

$$E = 5.2 \cdot 10^6 \text{ psi} \qquad \nu = 0.3 \qquad \sigma_y = 6500 \text{ psi}$$

The creep law was of the time-hardening form

$$\epsilon_c = A e^{B\sigma} t^k \tag{a}$$

with t being the lapsed time. The creep constants were given by Lin [58]

$$A = 2.64 \cdot 10^{-5} \qquad B = 1.92 \cdot 10^{-1} \qquad k = 0.66$$

For the analysis the time-hardening law, Eq. (a), was recast into the strain-hardening form as given by Eq. (3.16).

The Euler load for the column is

$$\sigma_E = \frac{\pi^2 EI}{L^2 bh} = 4170 \text{ psi}$$

An elastic large displacement analysis gave a critical load of 4185 psi.

The finite element analysis was performed using 8 equal elements over half the column length. The numerical integration of the creep pseudo-loading was made using Gaussian quadrature with 4 points in the ξ-direction and 6 points in the η-direction.

For creep analysis where the stress does not exceed the yield stress, increasing the number of points in the η-direction has a negligible effect. An analysis using 12 points gave results that were indistinguishable from those based on 6 points, except immediately before the critical time, when the creep strain rate approached infinity.

The excentricity of the column is so small that the column will buckle elastically, i.e., column will lose stability before the extreme fibers reach the yield stress. This analysis was therefore based on the linearly elastic relationship between increments of stress and strain, without plastic deformations. For other values of the excentricity the column may buckle plastically, and the stress-strain relationship based on the flow theory of plasticity must be used.

The buckling behavior was investigated for three stress levels

i) $\rho = \frac{\sigma}{\sigma_E} = 0.5$; $\sigma = 2085$ psi

ii) $\rho = 0.6$; $\sigma = 2500$ psi

iii) $\rho = 0.7$; $\sigma = 2920$ psi

The results of the analysis for case (ii) are given in Figs. 7.11 and 7.13. The effect of the step length in time integration is illustrated in Fig. 7.11. Doubling the number of steps has reduced the calculated critical time by 10%. For comparison, the results given by Lin [58] are also plotted. Lin used the time-hardening law, Eq. (a), directly. For constant stress the time-hardening and strain-hardening should give the same results, while discrepancies will occur for varying

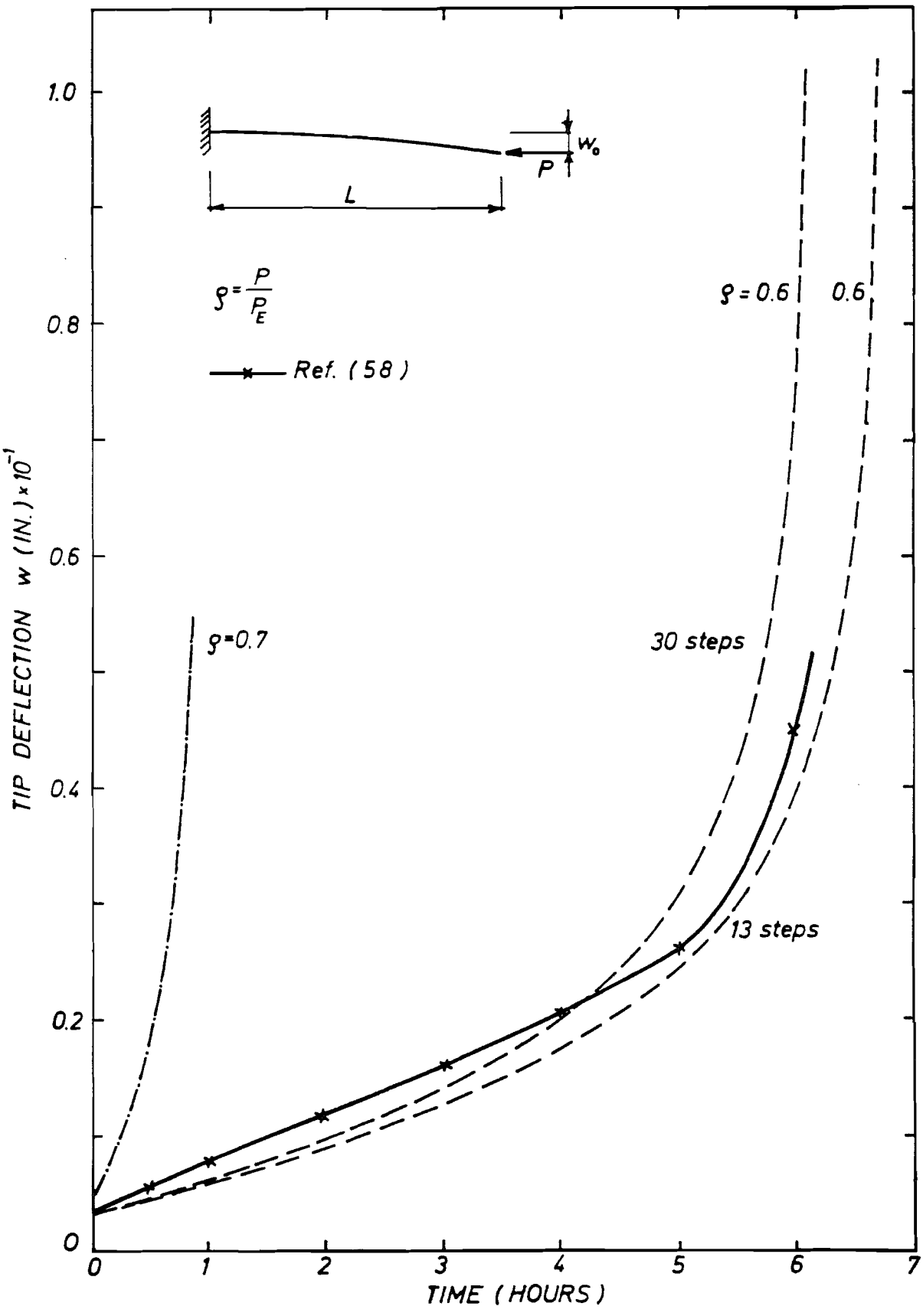

FIG. 7.11 CREEP BUCKLING OF COLUMN.

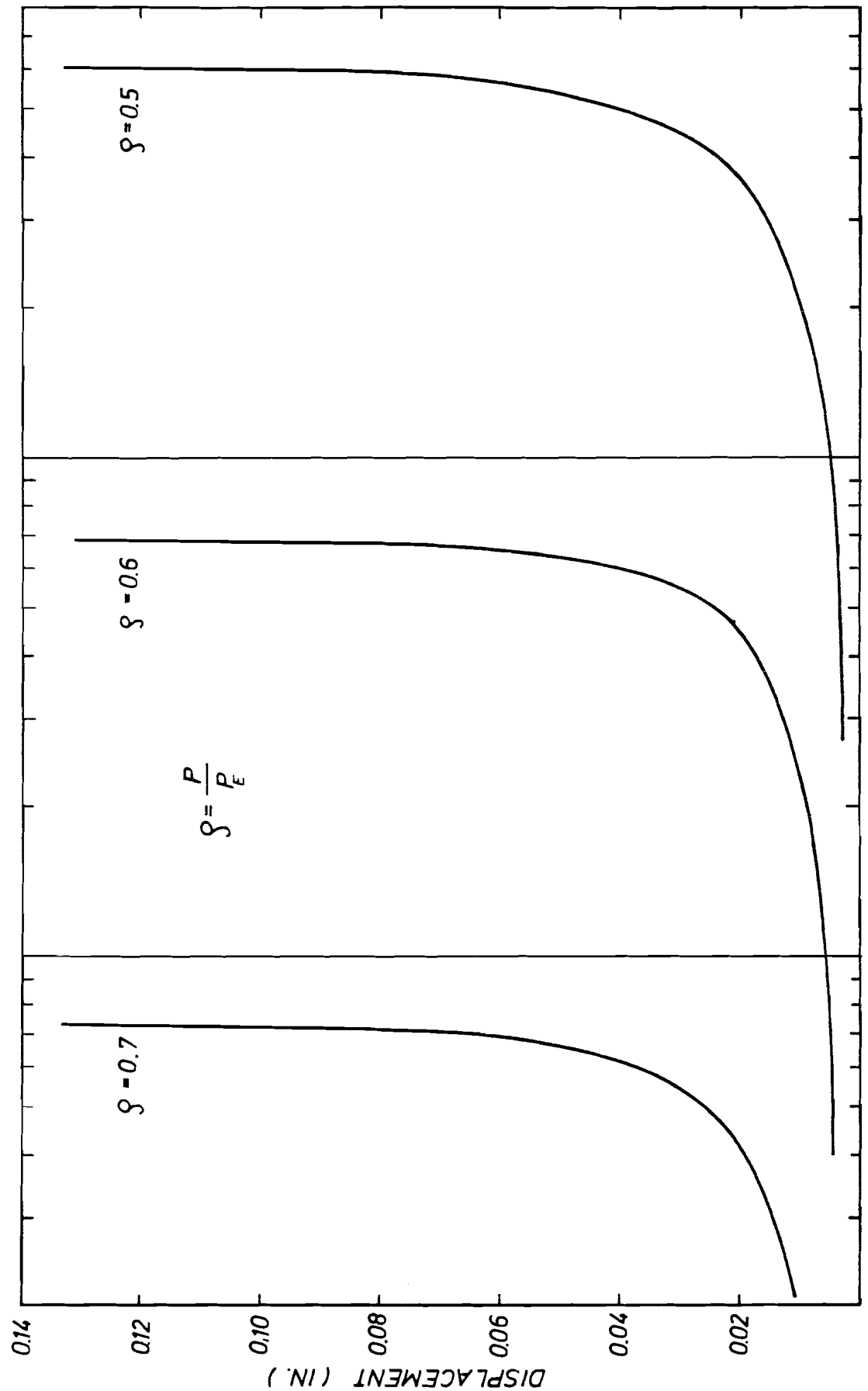

FIG. 7.12 TIME DEPENDENT DISPLACENT IN COLUMN DURING CREEP.

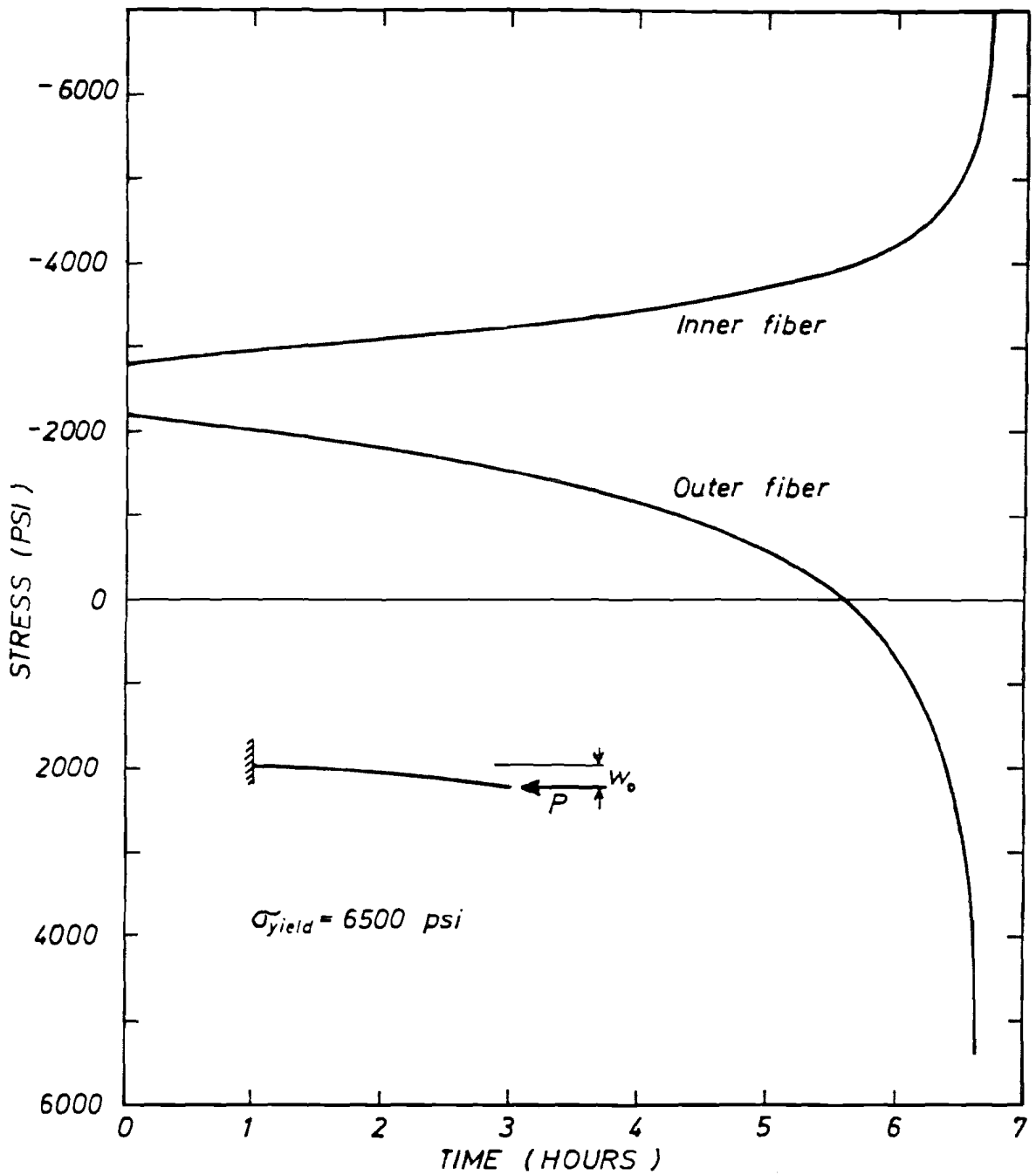

FIG. 7.13 STRESS VARIATION IN COLUMN.

stress. As seen in Fig. 7.13, the stress may be considered constant up to t = 3-4 hrs., and the difference between the solutions is therefore due to the more realistic displacement assumptions used in the finite element solution.

The displacement vs. time relationship for all three cases is given in Fig. 7.12. Here the effect of the stress level, σ , on the critical time is clearly discernible. As seen, the critical times are spaced one decade apart. Since the creep strain depends exponentially on the stress level, an exponential dependence on the stress for the critical time is to be expected. Here an increase in the stress by $0.1 \cdot \sigma_E$ seems to reduce the critical time by one decade.

7.5.2 Creep Buckling of Shallow Spherical Shell

The creep buckling problem of shells of revolution has been given increasing attention during the last few years. Grigoliuk and Lipovtsev [63] and Samuelson [64] treated shells with initial imperfection, the first two authors using Sander's variational principle.

In the present analysis no imperfections are given in the circumferential direction, leading to an axisymmetric deformation mode.

The geometry of the shallow cap is identical to the one treated in section 7.2.2. The characteristic parameter of the shell is

$$\mu^2 = m^2 \frac{R}{t} \alpha^2 = 10$$

The critical external pressure for linearly elastic analysis was determined to be

$$p_{cr} = 12.75 \text{ psi}$$

The material was assumed to be aluminum alloy 7075-T6, subjected to creep at 600°F. The creep law and material data are as given in section 7.5.1. The applied external pressure was taken as

$$p = \beta \cdot p_{cr} = 7.65 \text{ psi}$$

For the finite element analysis of the shell 5 elements were used, and a total of 45 load increments. Of these 10 increments were used to determine the instantaneous elastic response, and 35 steps to solve the quasi-static creep problem. The time steps were chosen as 1 hour up to a lapsed time of 15 hours, and then proceeded with step length 0.5 hours until snap-through occurred. No attempt was made here to trace the postbuckling behavior. The critical time was here taken to be the instant when loss of stability was detected.

The normalized apex displacement, $w(t)/w(o)$, as a function of time is given in Fig. 7.14. It appears that smaller time steps should have been used from t = 20 hours in order to determine the critical time more accurately. The variation in normal displacement and meridional stress with time is given in Figs. 7.15 and 7.16 respectively.

From the stress variation it is quite clear that the shell will buckle elastically. At no time is the yield stress of 6500 psi exceeded, and the flow theory of plasticity is not needed to describe the material behavior.

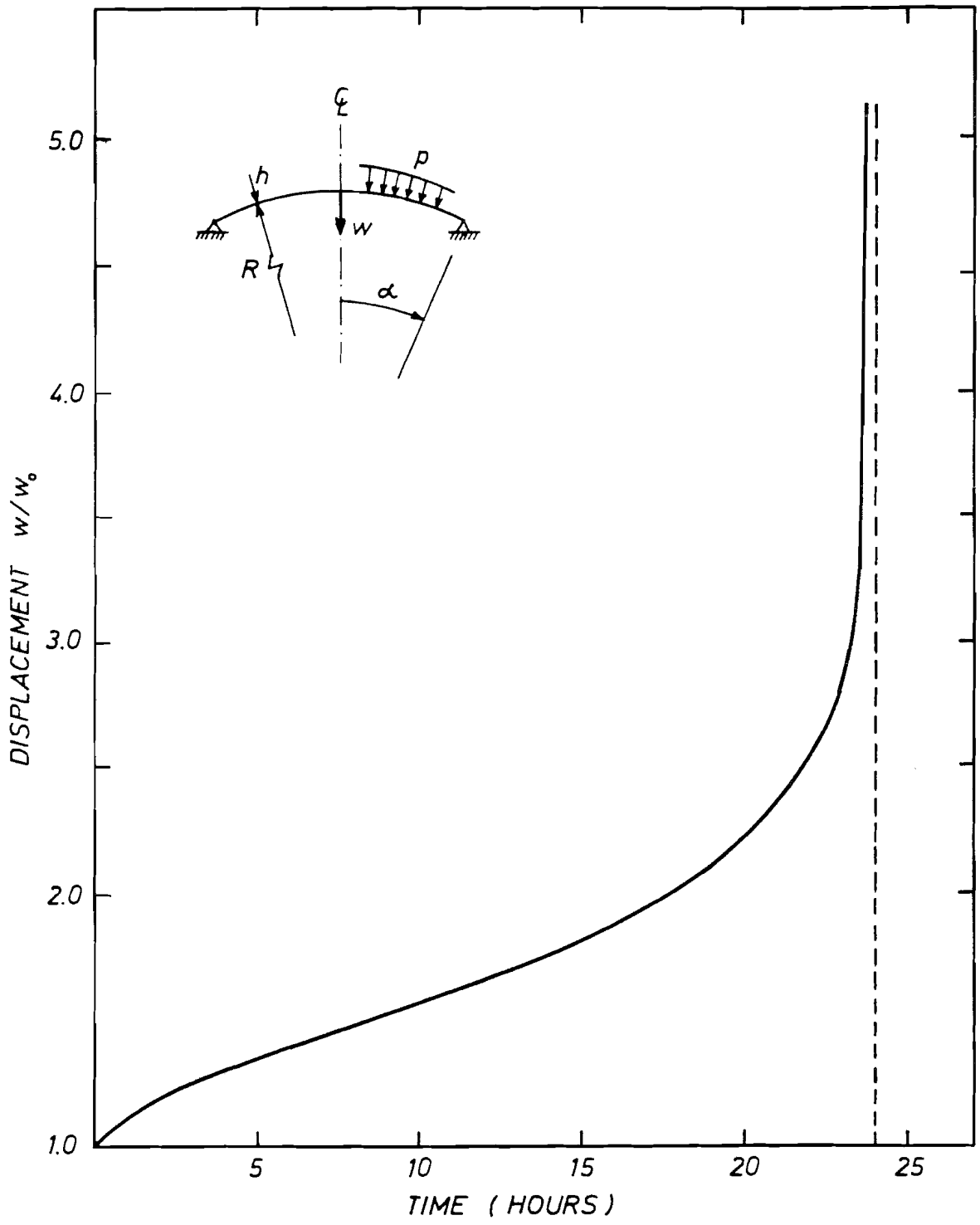

FIG. 7.14 CREEP BUCKLING OF SHALLOW SHELL.

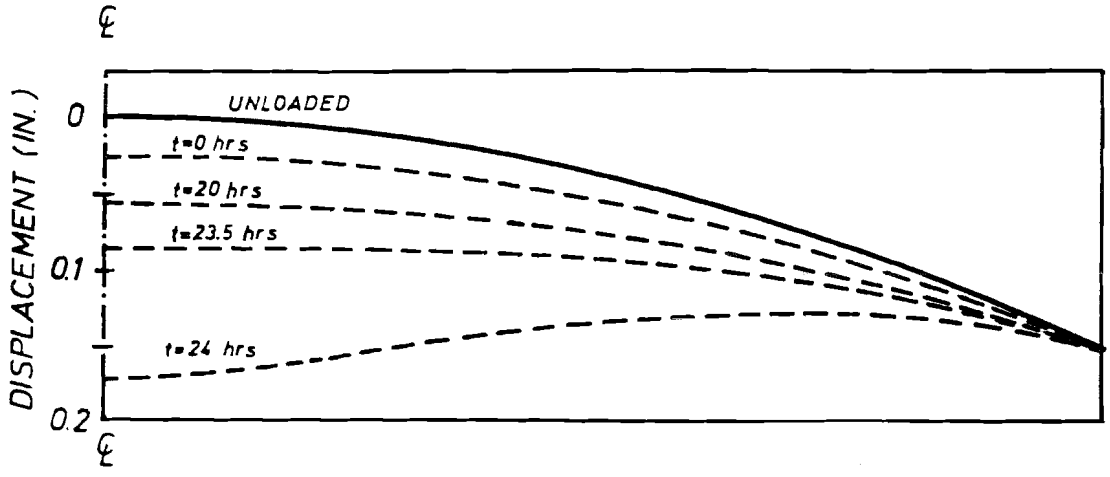

FIG. 7.15 DEFORMED SHAPE OF SHELL.

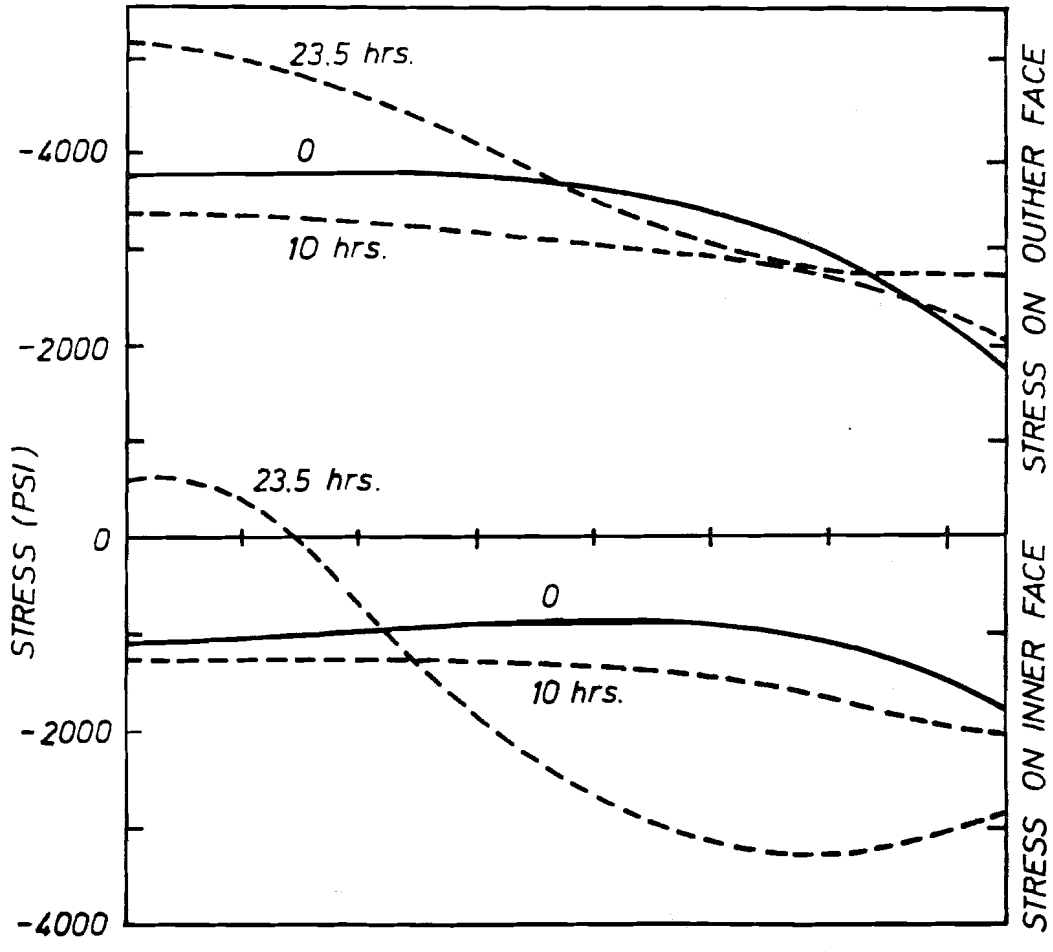

FIG. 7.16 STRESS VARIATION ALONG MERIDIAN.

No attempt was made in this example to determine the post-buckling behavior of the shell, even though such a study is quite feasible using the procedure outlined in section 7.2.2.

The total computer time needed for the complete analysis was 96 sec. (CP).

7.6 Viscoelastic Problems

7.6.1 Identification of Material Parameters

The problem of identification of material parameters in constitutive theories is becoming more important with the increasing use of nonlinear materials and materials with time-dependent behavior. In the present study the objective was to identify the material constants in a Prony series expansion of the relaxation modulus for Plexiglas, using a simple least squares fit to the given data.

The material chosen, Plexiglas grade "G", is produced by Rohm and Haas Corp., and is an acrylic with the generic name PMMA (polymethylmathacrelate). The material was chosen due to its application in the structure analyzed in section 7.6.2.

Relaxation data for Plexiglas obtained from creep tests are given in reference [136]. The data are available only for a stress level of 1000 psi, and the material is therefore assumed to be linear for the purpose of the present study. The discrete values of the relaxation modulus G(t) is given in Table 7.1 for 73°F

Table 7.1

Time (hrs)	0	10	30	100	300	1000
G x 10^5(psi)	4.5	4.1	3.6	3.18	2.8	2.45

The instantaneous Young's modulus and Poisson's ratio are $4.5.10^5$ psi and 0.35 respectively. It has been found that Poisson's ratio remains constant during creep or relaxation for PMMA [107].

A four term Prony series was chosen to represent the relaxation modulus

$$G(t) = G_0 + \sum_{i=1}^{4} G_i e^{-t/\lambda_i}$$

Here both G_0, G_i and λ_i are to be determined from the given data. Hildebrand [137] gives a method where the discrete relaxation times λ_i are determined from the roots of a 4th order polynomial equation, and the discrete moduli from a set of linear algebraic equations. The latter set is usually solved using least squares fit. However, stability problems are often encountered in the solution of the polynomial equation, giving complex roots. For this reason λ_i were chosen one decade apart. This choice is quite arbitrary, but will in most cases give a monotonically decreasing modulus if the discrete moduli G_i are restricted to be positive.

In this case a simple search was made to find the values of λ_i that minimized the root mean square error of the modulus. The results are given in Table 7.2.

Table 7.2

i	$G_i \cdot 10^5$ (psi)	λ_i (hrs)
0	1.25	
1	0.97654	20
2	0.81018	200
3	0.56758	2000
4	0.89394	20000

The relaxation modulus is given in Fig. 7.17, and has a root mean square error of $0.0373.10^5$ psi.

Assuming the creep compliance to be given in the form

$$J(t) = J_0 + \sum_{i=1}^{4} J_i e^{-t/\tau_i}$$

and using the property

$$J(0)\,G(t) + \int_0^t G(t-\tau)\,\frac{dJ(\tau)}{d\tau}\,d\tau = 1 \quad , \; t \geq 0^+$$

the creep compliance parameters were determined.

Table 7.3

i	$J_i.10^{-5}(\text{psi})^{-1}$	τ_i (hrs)
0	0.8	
1	-0.05742	$0.2535.10^2$
2	-0.08266	$0.2594.10^3$
3	-0.09163	$0.2517.10^4$
4	-0.34599	$0.3477.10^5$

The creep compliance is plotted in Fig. 7.18. It is clear from Fig. 7.17 and 7.18 that the compliance is delayed compared to the relaxation modulus. This implies that a structure will continue to deform long after the relaxation modulus has reached its equilibrium value.

In order to test the algorithm used for the computation of the convolution integrals in Chapter 4, a simple bar under uniaxial constant stress was analyzed. By monitoring the displacements the creep compliance can be calculated at discrete times when the relaxation modulus is given as input. This analysis may be used for determining the optimum time step to be used under constant

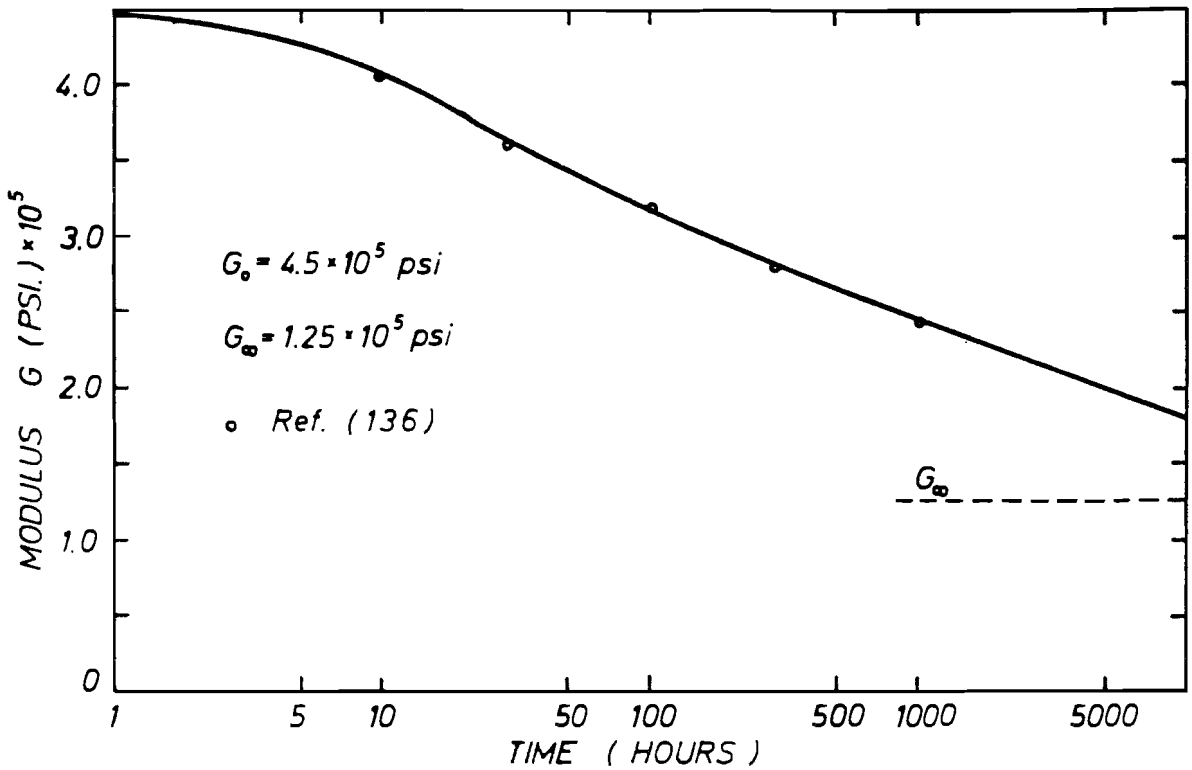

FIG. 7.17 RELAXATION MODULUS FOR PLEXIGLAS.

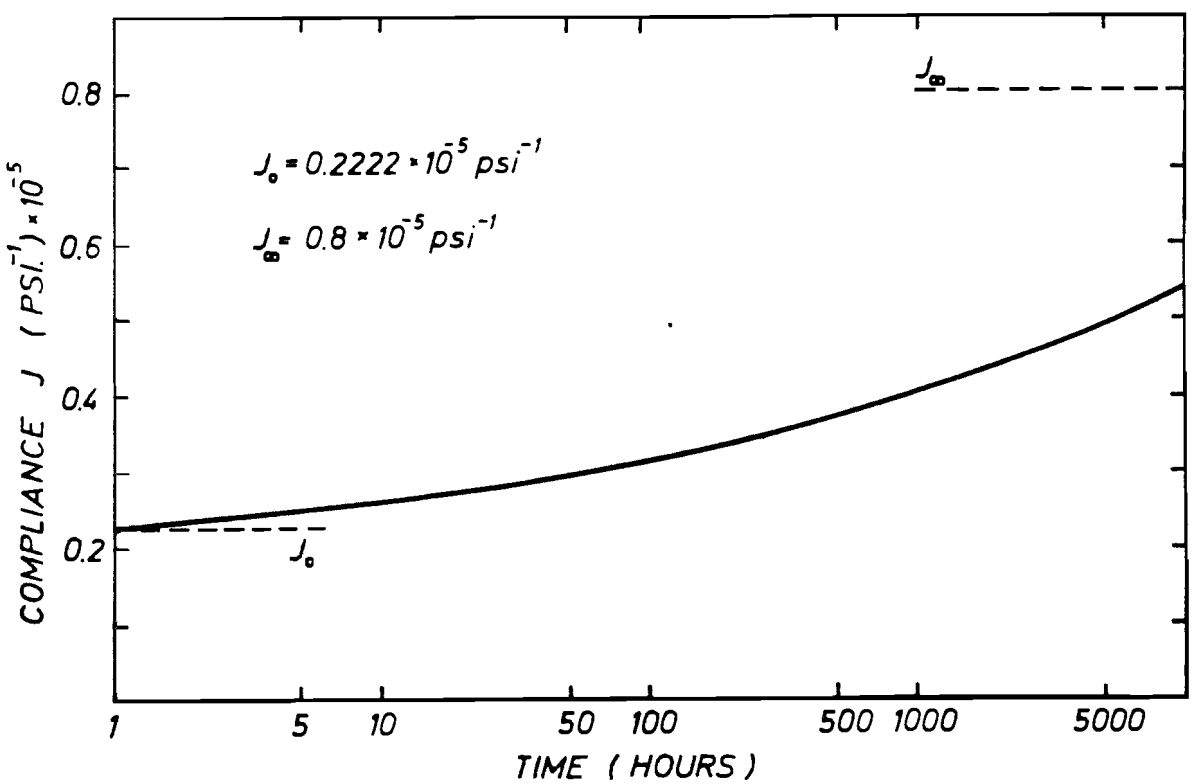

FIG. 7.18 CREEP COMPLIANCE FOR PLEXIGLAS.

stress conditions.

Two analyses were made using time steps of $\Delta t = 200$ and $\Delta t = 500$ hours. The results are given in Table 7.4.

Table 7.4

	Compliance $J(t).10^{-5}$ $(psi)^{-1}$		
Time (hrs)	"Exact"	$\Delta t = 200$	$\Delta t = 500$
1000	0.40148	0.40142	0.39858
2000	0.43325	0.43367	0.43225
3000	0.45613	0.45692	0.45585
4000	0.47409	0.47531	0.47446
5000	0.48877	0.49041	0.48970

Here it is quite clear that $\Delta t = 500$ hours gives sufficient accuracy for constant stress conditions. It should also be noted that even though $\Delta t = 500$ has the largest error at t = 1000 hrs., this is not the case at t = 5000 hrs. This shows that errors do not accumulate in the solution of the integral equation. This is due to the use of the decaying exponential functions in the Prony series, which also implies that the errors will decay with time.

7.6.2 Viscoelastic Creep Buckling of Spherical Shell

The use of polymers as structural material in industrial applications is becoming increasingly more common. The viscoelastic character of these materials require that both instantaneous and sustained loading conditions be considered.

The program's capability of handling nonlinear analysis of linearly viscoelastic shells is illustrated for a spherical shell.

The structure to be considered is the window for a deep-submergence pressure vessel, tested by U.S. Naval Civil Engineering Laboratory [138]. The objective of the present study is to determine the life expectancy of the shell under sustained pressure without the occurrence of implosion.

The radius of the middle surface is R = 31.75 in. and the thickness h = 2.5 in., giving h/R = 0.08. The material considered is an acrylic, Plexiglas grade "G", with instantaneous Young's modulus and Poisson's ratio of $4.5.10^5$ psi and 0.35 respectively. The geometric parameter of the shell $\mu^2 = m^2 \frac{R}{h} \alpha^2 = 16.6$. Relaxation and compliance parameters of the material are given in the previous section.

The Navy tests [138] consisted of spherical shells supported by a rigid frame, where the shells were free to slide against the flange parallel to the shell normal, see insert in Fig. 7.19. Neglecting the friction between shell and flange this is equivalent to a complete sphere subjected to external pressure. The shell was considered to have failed when the deformations became so large that the flange could no longer offer sufficient support, and the shell imploded. The stability of the shell was not considered.

A linear analysis of the sphere subjected to an external sustained pressure of 1000 psi was made; 3 finite elements and a total of 23 time increments were used. The loading was applied instantaneously. The result of the analysis is displayed in Fig. 7.19, where the normal displacement w is plotted vs. time. As can be seen a 80% increase in displacement is obtained after

1000 hours. The computer time needed for the analysis was 23 sec. (CP).

From a structural point of view this is a quite elementary problem, and the structure utilizes the material inefficiently. A shell with clamped edges would be more economical. The basic reason these particular boundary conditions were used is the superior optical properties of this shell. This shell has more uniform optical magnification factors along the meridian, and these remain uniform during deformation. For the clamped shell, the image of an object observed through the window will become more distorted, and the distortion will vary with time.

Without reference to any particular application a clamped window will now be considered, see insert in Fig. 7.20. The post-buckling behavior of the shell under instantaneous external pressure is given in Fig. 7.20. Six (6) finite elements and 23 load increments were used to obtain the load-deflection curve. The upper and lower critical pressures were found to be 1885 psi and 1780 psi respectively, and the shell will exhibit snap-through. However, loss of stability will not take place if a displacement pertubation is imposed on the shell at a pressure below the lower critical pressure.

Three separate analyses were made for the viscoelastic problem, with the external pressure equal to 1510 psi, 1320 psi and 1130 psi respectively. This represents 80%, 70% and 60% of the critical load. The external pressure was applied instantaneously using 12 load increments, and then sustained during the creep process. The displacement of the apex vs. time is plotted in

Fig. 7.21 for all three cases.

The case $\varsigma = P/P_{cr} = 0.8$ exhibited a sudden loss of stability after 70.5 hours, and buckled. The cases $\varsigma = 0.7$ and $\varsigma = 0.6$, however, exhibit a period of gradual softening of the system, followed by a period where the stiffness is small and the displacement increased rapidly. In the third period the stiffness increased rapidly showing a decreasing rate of deflection. The latter two cases show the typical behavior of a shell with a geometric parameter in the domain $8 \leq \mu^2 \leq 10$, [134].

The reason for the snap-through occurring for $\varsigma = 0.8$ is as follows. The relaxation of the stresses at the clamped edge will gradually decrease the degree of rotation constraint. Hence the shell will not behave as a fully clamped shell if subjected to a displacement pertubation. In this respect it should be noted that a simply supported shell will snap-through already for $\mu^2 \geq 5$. For the cases $\varsigma = 0.7$ and $\varsigma = 0.6$, however, the reduction in rotation constraint is not sufficient to give an instability condition, and the shell behaves similarly to a shell with parameter $\mu^2 \leq 9$, [134].

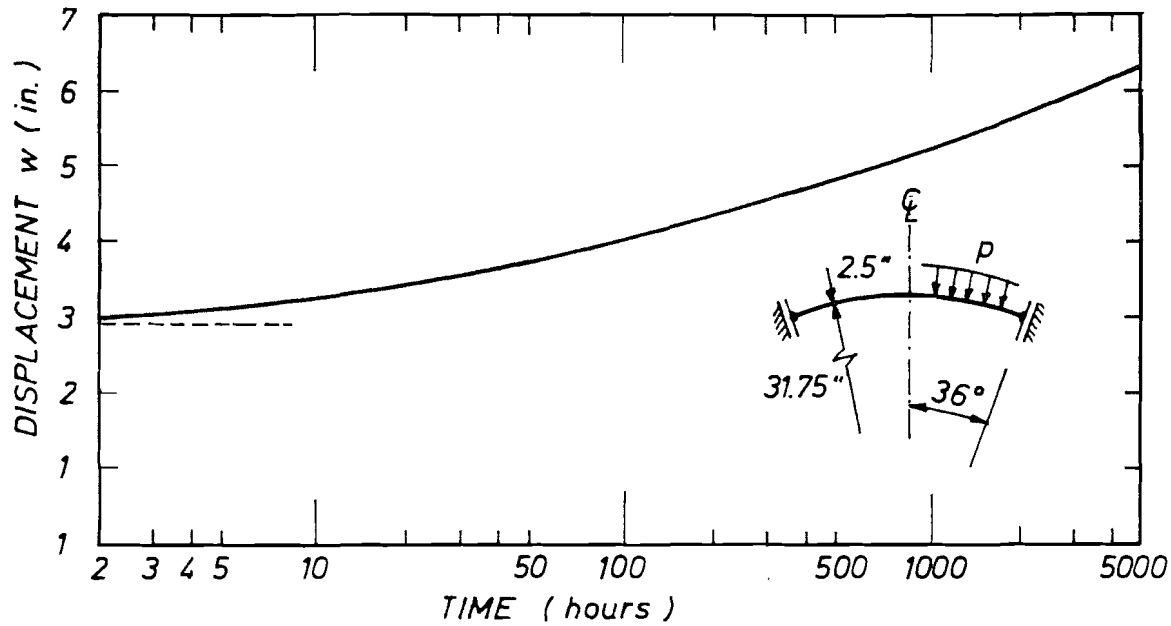

FIG. 7.19 NORMAL DISPLACEMENT OF WINDOW

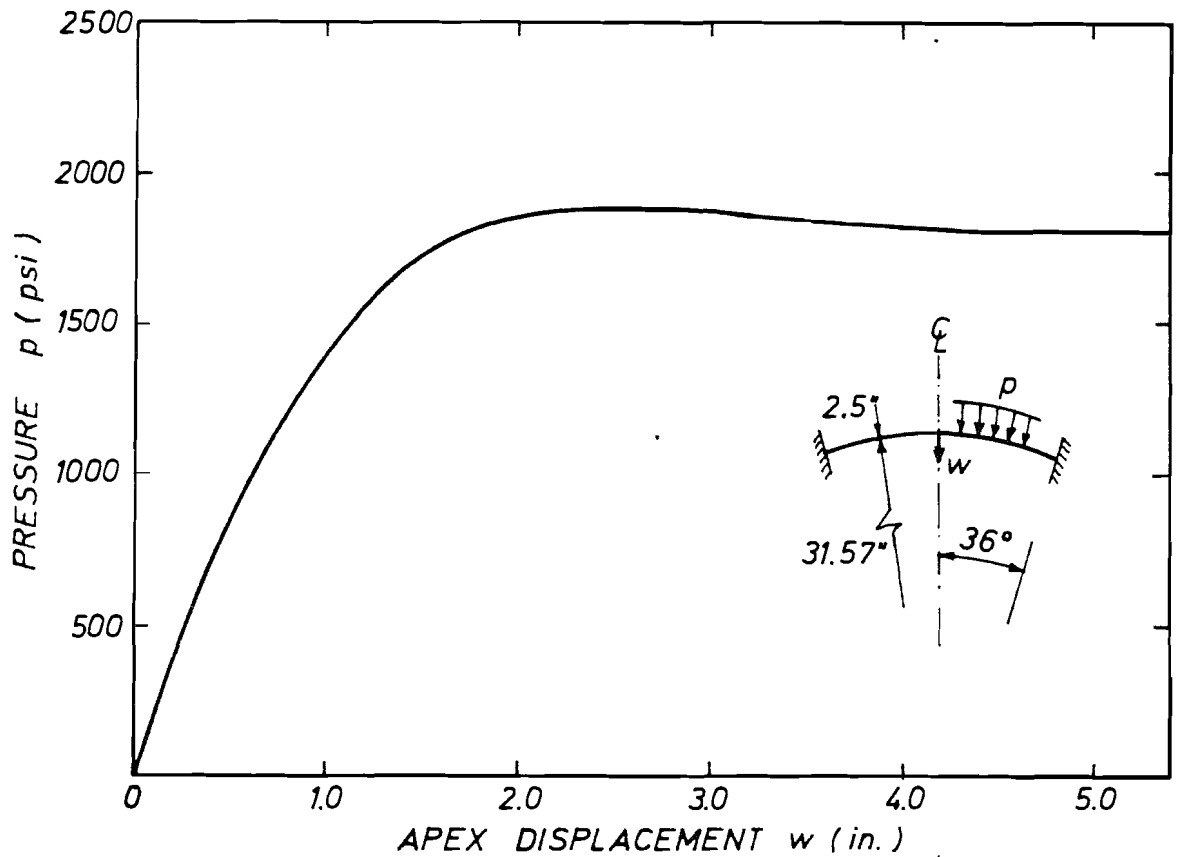

FIG. 7.20 POSTBUCKLING BEHAVIOR OF WINDOW.

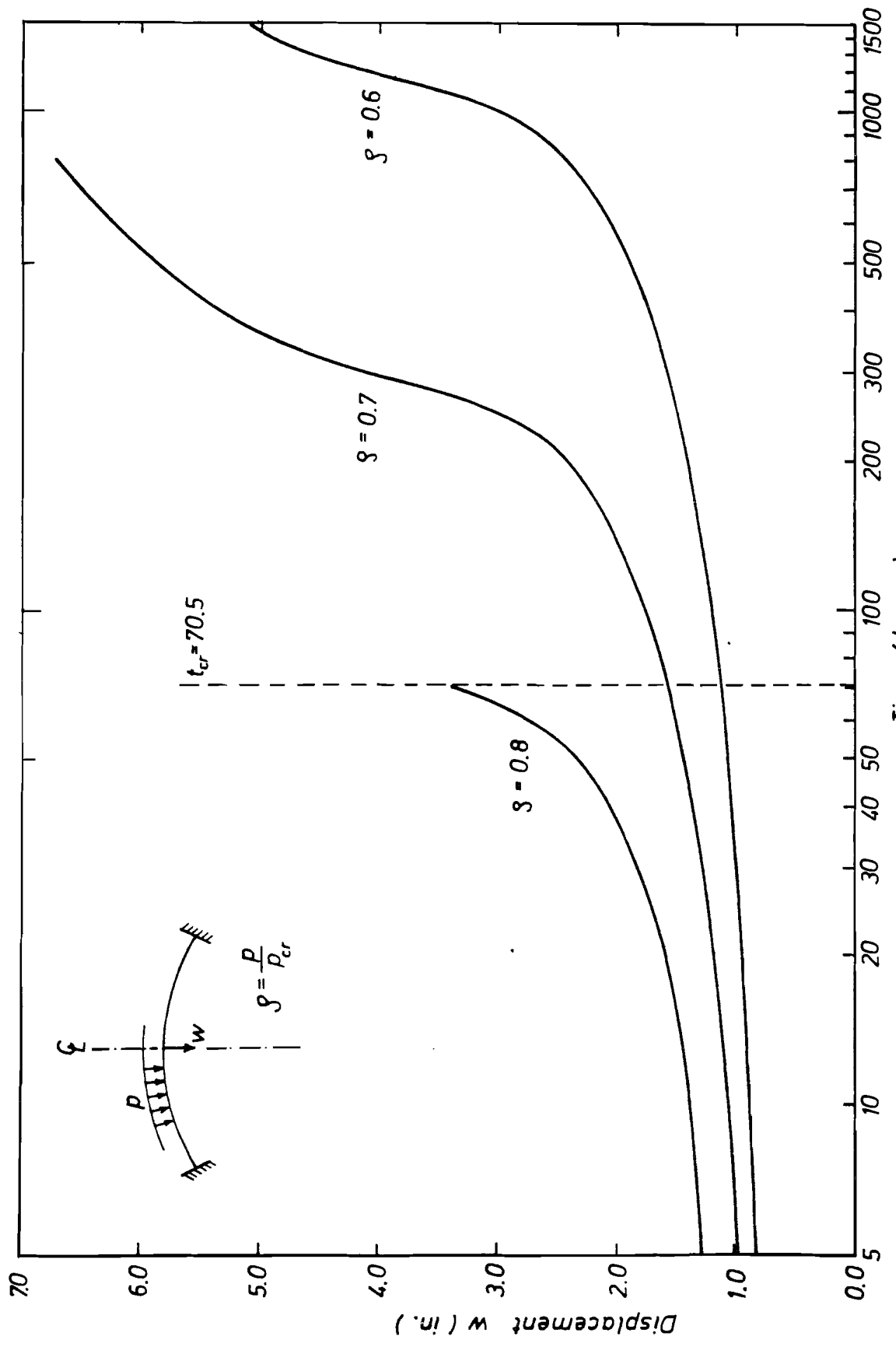

FIG. 7.21 CREEP BUCKLING OF SHALLOW PLEXIGLAS WINDOW.

8. SUMMARY AND CONCLUSIONS

An incremental displacement formulation has been presented for the time dependent nonlinear analysis of structures. Both geometric and material nonlinearities are included. The physical nonlinearities are caused by coupled or uncoupled creep and elastic-plastic deformations in metals. The time dependence of the response arises from creep deformations in metals and from the viscoelastic behavior in polymeric materials. As observed in thin shell applications, the geometric nonlinearities for most cases are restricted to large displacements resulting from finite rotations. No restrictions regarding the magnitude of strains or rotations are imposed on the elastic structures.

Based on a preliminary study of the accuracy and computational efficiency of various modes of descriptions, it was concluded that the Lagrangian formulation was best suited to describe the motion of the body. Using a fixed coordinate system in the reference configuration the appropriate transformations of stresses and strains were introduced. Applying the virtual work principle the incremental equilibrium equations were derived, and modified to account for time effects. The latter was done by decomposing the stress increment into an instantaneous and a delayed part, and deriving the creep "pseudo-loading".

The constitutive relations for creep, plasticity and linear viscoelasticity were written in terms of the symmetric 2nd Piola-Kirchhoff stress tensor and the Lagrangian strain rates. Subsequently the stress response was obtained by transforming the

P-K stress tensor into the Cauchy stress tensor in the current configuration. Both primary and steady state creep were considered; this approach was also used for Odquist's modified "creep-plasticity" formulation. A more fundamental method of coupling creep and plasticity was presented following the theory of viscoplasticity. In this, the flow theory of plasticity, the von Mises yield criterion, and isotropic hardening rule were employed. The complexity of such a formulation was exhibited by showing the time dependence of the flexural modulus of aluminum during creep. Finally, the linear theory of viscoelasticity was extended to large displacement problems, using a Prony series expansion of the relaxation modulus.

Restricting the displacement increments to being small, the incremental equilibrium equations were linearized. The forward integration of these equations were improved using an equilibrium check at each step, and adding the "out-of-balance" load to the next load increment. This method was shown to give excellent results for elastic problems and for problems in the infinitesimal theory of plasticity. However, for finite inelastic and viscoelastic problems, the method gave rise to oscillations unless special modifications or precautions were introduced. This residual load method was shown to give excellent results for postbuckling analysis of a structure when combined with a procedure that controlled the loading sequence based on the positive definiteness of the system stiffness matrix.

Using a degenerate isoparametric shell element, three finite element programs were written for the analysis of axisymmetric deformations of shells of revolution. With these programs the snap-through behavior of a shallow spherical shell was determined, and an elastic analysis of a torus was made. Similarly the creep and elastic-plastic deformations in torispherical pressure vessels were investigated, and the creep buckling behavior of columns and shallow shells was determined. Finally the method was applied to the viscoelastic buckling of a shallow shell made of plexiglas.

For the cases where exact solutions are available favorable agreement was obtained. However, very few experimental data exist for large creep deformations in shells, and the programs could therefore only be verified by inference from simple one- and two-dimensional cases known in the literature.

A number of topics for further research have been pointed out. Much work still has to be done in the field of coupled creep and plasticity in order to determine the material parameters in such constitutive models. Secondly, it is well known that a linear hereditary constitutive law is unsatisfactory for many of the commerically used plastics. Great efforts should therefore be made to obtain nonlinear kernel functions that can be used in efficient recursive algorithms for such materials.

An obvious extension of the present work would be to include the possibility of bifurcation buckling into a nonsymmetric mode during the creep process. This may be done using Fourier series expansion in the circumferential direction or using a general

three-dimensional shell element. In the former case the harmonics will be coupled, and only a very few terms can be used in the series before the computational effort gets out of hand. Another natural extension of the present work is the study of creep buckling of sandwich shells with a soft viscoelastic core. Here the plastic deformations of the metallic facings can be included.

9. REFERENCES

1. Green, A. E. and Zerna, W., Theoretical Elasticity, Oxford University Press, 1954.

2. Green, A. E. and Adkins, J. E., Large Elastic Deformations and Nonlinear Continuum Mechanics, Oxford University Press, 1960.

3. Truesdell, C. and Toupin, R., Classical Field Theories, Handbuch der Physik, Ed. Flugge, S., Vol. III/1, 1960.

4. Truesdell, C. and Noll, W., The Nonlinear Field Theories of Mechanics, Handbuch der Physik, Ed. Flugge, S., Vol. III/3, 1965.

5. Turner, M. J., Dill, E. H., Martin, H. C. and Melosh, R. J., "Large Deflection Analysis of Structures Subjected to Heating and External Loads," Journ. Aerospace Sciences, Vol. 27, No. 2, Feb. 1960, pp 97-106, 127.

6. Martin, H. C., "On the Derivation of Stiffness Matrices for the Analysis of Large Deflection and Stability Problems," Proc. 1st Conf. on Matrix Meth. in Struct. Mech., Wright-Patterson AFB, AFFDL-TR-66-80, 1966, pp 697-715.

7. Gallagher, R. H. and Padlog, J., "Discrete Element Approach to Structural Instability Analysis," AIAA J., Vol. 1, No. 6, 1963, pp 1437-1439.

8. Argyris, J. H., Kelsey, S. and Kamel, H., Matrix Methods in Structural Analysis, AGARD-ograph 72, Pergamon Press, 1964.

9. Argyris, J. H., Recent Advances in Matrix Methods of Structural Analysis, Progress in Aeronautical Sciences, Pergamon Press, 1964.

10. Argyris, J. H., "Continua and Discontinua," Proc. 1st Conf. on Matrix Meth. in Struct. Mech., Wright-Patterson AFB, AFFDL-TR-66-80, 1966, pp 151-170.

11. Argyris, J. H., "Matrix Analysis of Three Dimensional Elastic Media, Small and Large Displacements," AIAA J., Vol. 3, No. 1, 1965, pp 45-51.

12. Hartz, B. J., "Matrix Formulation of Structural Stability Problems," Journ. of the Structural Division, ASCE, Vol. 91, ST6, Dec. 1965, pp 141-157.

13. Kapur, K. K., and Hartz, B. J., "Stability of Plates Using the Finite Element Method," Journ. of the Engineering Mechanics Division, ASCE, Vol. 92, EM2, 1966, pp 177-196.

14. Murray, D. W., "Large Deflection Analysis of Plates," Ph.D. Dissertation, University of California, Berkeley, Report No. SESM 67-44, 1967.

15. Murray, D. W. and Wilson, E. L., "Finite Element Large Deflection Analysis of Plates," Journ. of the Engineering Mechanics Division, ASCE, Vol. 95, EM1, 1969, pp 143-165.

16. Murray, D. W. and Wilson, E. L., "Finite Element Post Buckling Analysis of Thin Elastic Plates", AIAA J., Vol. 7, No. 10, Oct. 1969, pp 1915-20.

17. Gallagher, R. H., Gellatly, R. A., Padlog, J. and Mallet, R. H., "A Discrete Element Procedure for Thin Shell Instability Analysis," AIAA J., Vol. 5, No. 1, 1967, pp 138-45.

18. Gallagher, R. H. and Yang, H. T. Y., "Elastic Instability Predictions for Doubly Curved Shells," Proc. 2nd Conf. on Matrix Meth. in Struct. Mech., Wright-Patterson AFB, AFFDL-TR-68-150, 1968, pp 711-39.

19. Nararatna, D. R., Pian, T. and Witmer, E., "Stability Analysis of Shells of Revolution by the Finite Element Method," AIAA J. Vol. 6, No. 2, Feb. 1968, pp 355-61.

20. Hsueh, T. M. and Wilson, E. L., "Stability Analysis of Axisymmetric Shells", Report No. SESM 69-22, University of California, Berkeley, Sept. 1969.

21. Oden, J. T., "Calculation of Geometric Stiffness Matrices for Complex Structures", AIAA J., Vol. 4, No. 8, Aug. 1966, pp 1480-82.

22. Oden, J. T., "Numerical Formulation of Nonlinear Elasticity Problems," Journ. of the Structural Division, ASCE, Vol. 93, No. ST3, June 1967, pp 235-55.

23. Oden, J. T. and Sato, T., "Finite Strains and Displacement of Elastic Membranes by the Finite Element Method," Int. J. Solids Struct., Vol. 3, 1967, pp 1-18.

24. Oden, J. T., "Finite Element Formulation of Problems of Finite Deformation and Irreversible Thermodynamics of Nonlinear Continua - A Survey and Extension of Recent Developments", Japan-U.S. Seminar on Math. Meth. of Struct. Anal. and Design, Tokyo, Aug. 1969.

25. Oden, J. T. and Key, J. E., "Numerical Analysis of Finite Axisymmetric Deformations of Incompressible Elastic Solids of Revolution, Int. J. Solids Struct., Vol. 6, No. 5, 1970, pp 497-518.

26. Mallet, R. H. and Marcal, P. V., "Finite Element Analysis of Nonlinear Structures," Journ. of the Structural Division, ASCE, Vol. 94, No. ST9, Sept. 1968, pp 2081-2105.

27. Marcal, P. V., "Finite Element Analysis of Combined Problems of Nonlinear Material and Geometric Behavior," Techn. Report No. N00014-0007/1, Brown University, Providence, R.I., 1969.

28. Hibbit, H. D., Marcal, P. V., and Rice, J. R., "A Finite Element Formulation for Problems of Large Strain and Large Displacements," Report No. N00014-0007/2, Brown University, Providence, R.I., 1969.

29. Dupuis, G., "A Lagrangian Formulation for Large Elastic Deformation of Twin Shells," Report No. N00014-0008/2, Brown University, Providence, R.I., 1971.

30. Felippa, C.A., "Refined Finite Element Analysis of Linear and Nonlinear Two-Dimensional Structures," Ph.D. Dissertation, University of California, Berkeley, Report No. SESM 66-22, 1966.

31. Yaghmai, S., "Incremental Analysis of Large Deformations in Mechanics of Solids With Application to Axisymmetric Shells of Revolution," Ph.D. Dissertation, University of California, Berkeley, 1968, NASA, CR-1350, June 1969.

32. Bushnell, D. and Almroth, B. O., "Finite Difference Energy Method for Nonlinear Shell Analysis," Proc. LMSC/AFFDL Shell Conference, Palo Alto, California, Aug. 1970.

33. Popov, E. P., Khojasteh-Bakht, M. and Yaghmai, S., Analysis of Elastic-Plastic Circular Plates, Journ. of the Engineering Mechanics Division, Vol. 93, EM6, ASCE, 1967.

34. Khojasteh-Bakht, M., "Analysis of Elastic-Plastic Shells of Revolution Under Axisymmetric Loading by the Finite Element Method," Ph.D. Dissertation, University of California, Berkeley, Report No. SESM 67-8, 1967.

35. Marcal, P. V. and King, I. P., "Elastic-Plastic Analysis of Two-Dimensional Stress Systems by the Finite Element Method," Int. J. Mech. Sci., Vol. 9, No. 3, 1967, pp 143-45.

36. Zienkiewicz, O. Z., Valliappan, S. and King, I. P., "Elasto-Plastic Solutions of Engineering Problems "Initial Stress" Finite Element Approach," Int. J. for Num. Meth. in Eng., Vol. 1, Jan. 1969, pp 75-100.

37. Armen, H., Pifko, A. and Levine, H. S., "Finite Element Method for the Plastic Bending Analysis of Structures," Proc. 2nd Conf. on Matrix Meth. in Struct. Mech., Wright-Patterson AFB, AFFDL-TR-68-150, 1968.

38. Zudans, Z., "Finite Element Incremental Elastic-Plastic Analysis of Pressure Vessels, Journ. of Eng. for Industry, Trans. of ASME, May 1970, pp 293-302.

39. Odqvist, F.K.G. and Hult, J., Kriechfestigkeit metallischer Werkstoffe, Springer, Berlin, 1962.

40. Finnie, I. and Heller, W. R., Creep of Engineering Materials, McGraw-Hill, 1959.

41. Hult, J., Creep in Engineering Structures, Blaisdell Publ. Co., 1966.

42. Rabotnov, Yu N., Creep Problems in Structural Members, North-Holland Publ. Co., 1969.

43. Odqvist, F.K.G.,"Mathematical Theory of Creep and Creep Rupture," Oxford, Clarendon Press, 1966.

44. Wahl, A. M., "Analysis of Creep in Rotating Disks Based on the Tresca Criterion and Associated Flow Rule," Journ. of Appl. Mech., Vol. 23, June 1956, pp 231-38.

45. Mendelson, A., Hirschberg, M. H. and Manson, S. S., "A General Approach to the Practical Solution of Creep Problems," Journ. of Basic Engineering, ASME, Dec. 1959, pp 585-98.

46. Lin, T. H., "Bending of Plate with Nonlinear Strain Hardening Creep," Creep in Structures, Springer, 1962.

47. King, I. P., "Finite Element Analysis of Two-Dimensional Time-Dependent Stress Problems," Ph.D. Dissertation, University of California, Berkeley, Report No. SESM 65-1, 1965.

48. Selna, L. G., "Time-Dependent Behavior of Reinforced Concrete Structures," Ph.D. Dissertation, University of California, Berkeley, Report No. SESM 67-19, 1967.

49. Chang, T. Y., "Approximate Solutions in Linear Viscoelasticity," University of California, Berkeley, Report No. SESM 66-8, June 1966.

50. Zienkiewicz, O. Z., Watson, M. and King, I. P., "A Numerical Method of Visco-Elastic Stress Analysis," Int. J. Mech. Sci., Vol. 10, 1968, pp 807-827.

51. Taylor, R. L., Pister, K. S. and Goudreau, G. L., "Thermo-mechanical Analysis of Viscoelastic Solids," Report No. SESM 68-7, University of California, Berkeley, 1968.

52. Greenbaum, G. A. and Rubinstein, M. F., "Creep Analysis of Axisymmetric Bodies Using Finite Elements," Nuclear Eng. and Design, Vol. 7, 1968, pp 379-397.

53. Sutherland, W. H., "AXICRP-Finite Element Computer Code for Creep Analysis of Plane Stress, Plane Strain and Axisymmetric Bodies," Nuclear Eng. and Design, Vol. 4, No. 2, 1969, pp 269-285.

54. Rabotnov, G. N. and Shesterikov, S. A., "Creep Stability of Columns and Plates," Journ. of Mech. Phys. Solids, Vol. 6, 1957, pp 27-34.

55. Hoff, N. J., "Buckling of High Temperature," Journ. of the Royal Aeron. Society, Vol. 61, Nov. 1957, pp 756-74.

56. Hoff, N. J., "A Survey of the Theories of Creep Buckling," Proc. of 3rd National Congress of Applied Mechanics, June 1958.

57. Libove, C., "Creep-Buckling Analysis of Rectangular-Section Columns," NACA, Techn. Note 2956, 1953.

58. Lin, T. H., Theory of Inelastic Structures, John Wiley, 1968.

59. Hult, J., "Oil Canning Problems in Creep," Creep in Structures, Springer, 1962, pp 161-73.

60. Hoff, N. J., Jashman, W. E. and Nachbar, W., "A Study of Creep Collapse of a Long Circular Cylindrical Shell Under Uniform External Pressure," Journ. of the Aero/Space Sciences, Vol. 26, Oct. 1959, pp 663-69.

61. Mathauser, E. E. and Berkovits, A., "Determination of Static Strength and Creep Buckling of Unstiffened Circular Cylinders Subjected to Bending at Elevated Temperatures," NASA Memo 6-14-59L, June 1959.

62. Stricklin, J. A., Hsu, P. T. and Pian, T.H.H., "Large Elastic, Plastic, and Creep Deflections of Curved Beams and Axisymmetric Shells," AIAA J., Vol. 2, No. 9, Sept. 1964, pp 1613-1620.

63. Grigoliuk, E. I. and Lipovtsev, Y. V., "On the Creep Buckling of Shells," Int. J. Solids Structures, Vol. 5, 1969, pp 155-73.

64. Samuelson, L. A., "Creep Buckling of a Cylindrical Shell Under Non-Uniform External Loads," Int. J. Solids Structures, Vol. 6, No. 1, 1970, pp 91-116.

65. Bychawski, Z., "Some Problems of Creep Bending and Creep Buckling of Viscoelastic Sheet Panels in the Range of Large Deflections," Non-Classical Shell Problems, Proc. of IASS Symposium, Warsaw, Sept. 1963, North-Holland Publ. Co., 1964.

66. Huang, N. C., "Axisymmetrical Creep Buckling of Clamped Shallow Spherical Shells," Techn. Report No. 145, Division of Engineering Mechanics, Stanford University, Dec. 1963.

67. DeLeeuw, S. L., "Circular Viscoelastic Plates Subjected to In-Plane Loads," AIAA J., Vol. 9, No. 5, May 1971, pp 931-37.

68. Jaunzemis, W., Continuum Mechanics, The Macmillan Co., New York, 1967.

69. Malvern, L. E., Introduction to the Mechanics of a Continuous Medium, Prentice Hall, 1969.

70. Leigh, D. C., Nonlinear Continuum Mechanics, McGraw-Hill, 1968.

71. Lee, E. H., "Elastic-Plastic Deformation at Finite Strain," Journ. of Applied Mech., Trans. of ASME, March 1969, pp 1-6.

72. Toupin, R. A., "The Elastic Dielectric," J. Ratl. Mech. and Anal., Vol. 5, 1956, pp 849-915.

73. Biot, M. A., Mechanics of Incremental Deformation, John Wiley and Sons, 1965.

74. Fung, Y. C., Foundations of Solid Mechanics, Prentice Hall, 1965.

75. Kachanov, L. M., The Theory of Creep, National Lending Library for Science and Technology, 1967.

76. Hill, R., The Mathematical Theory of Plasticity, Oxford, Clarendon Press, 1950.

77. Washizu, K., Variational Methods in Elasticity and Plasticity, Pergamon Press, 1968.

78. Wang, A. J. and Prager, W., "Thermal and Creep Effects in Work-Hardening Elastic-Plastic Solids," J. of Aeronautical Sci., Vol. 21, No. 5, May 1954, pp 343-344.

79. Sanders, J. L., McComb, H. G. and Schlechte, F. R., "A Variational Theorem for Creep with Applications to Plates and Columns," NACA TN 4003, 1957.

80. Pian, T.H.H., "On the Variational Theorem for Creep," J. of Aeronautical Sci., Vol. 24, No. 11, Nov. 1957, pp 846-847.

81. McClintoch, F. A. and Argon, A. S., Mechanical Behavior of Materials, Addison-Wesley, 1966.

82. Sedov, L. I., Foundation of the Nonlinear Mechanics of Continua, Pergamon Press, 1966.

83. Lee, E. H. and Liu, D. T., "Finite Strain Elastic Plastic Theory with Applications to Plane Wave Analysis," J. Appl. Phys., Vol. 38, No. 1, 1967.

84. Green, A. E. and Naghdi, P. M., "A General Theory of an Elastic-Plastic Continuum," Arch. Rat. Mech. Anal., Vol. 18, No. 4, 1965, pp 250-281.

85. Bodner, S. R., "Constitutive Equations for Dynamic Material Behavior," Mechanical Behavior of Materials Under Dynamic Loads, Ed. U. S. Lindholm, Springer-Verlag, New York, 1968.

86. Finnie, I., "Stress Analysis for Creep and Creep-Rupture," Appl. Mech. Review, Oct. 1960, pp 373-387.

87. Pao, Y. H. and Marin, J., "An Analytical Theory of the Creep Deformation of Materials," J. Appl. Mech., Vol. 20, June 1953, pp 245-252.

88. Green, A. E. and Naghdi, P. M., "A Class of Viscoelastic-Plastic Media," Acta Mechanica, Vol. 4, No. 3, 1967, pp 288-295.

89. Rabotnov, Yu. N., "On the Equations of State for Creep," Progress in Applied Mechanics, 1963.

90. Rice, J. R., "On the Structure of Stress-Strain Relations for Time-Dependent Plastic Deformations in Metals," J. Appl. Mech., Sept. 1970.

91. Kratochvil, J. and Dillon, O. W., "Thermodynamics of Crystalline Elastic-Visco-Plastic Materials," J. Appl. Physics, Vol. 41, No. 4, March 1970.

92. Tseng, W., "A General Constitutive Theory for Elastic-Plastic Crystalline Solids," Ph.D. Dissertation, University of California, Berkeley, April 1971.

93. Naghdi, P. M. and Murch, S. A., "On the Mechanical Behavior of Viscoelastic/Plastic Solids," J. Appl. Mech., Vol. 30, Sept. 1963, pp 321-328.

94. Perzyna, P., "Fundamental Problems in Viscoplasticity," Adv. in Appl. Mechanics, Vol. 9, 1966.

95. Naghdi, P. M., "Stress-Strain Relations in Plasticity and Thermoplasticity," Proc. of 2nd Symposium on Naval Structural Mechanics, Pergamon Press, 1960.

96. Berkovits, A., "Primary Creep of Metals due to Varying Stress," Technion-Israel Institute of Technology, TAE Report No. 84, 1968.

97. Bland, D. R., The Theory of Linear Viscoelasticity, Pergamon Press, Oxford, 1960.

98. Flugge, W., Viscoelasticity, Blaisdell Publishing Co., 1967.

99. Christensen, R. M., Theory of Viscoelasticity, Academic Press, 1970.

100. Gurtin, M. E. and Steinberg, E., "On the Linear Theory of Viscoelasticity," Arch. Rat. Mech. Anal., Vol. 11, 1962.

101. Coleman, B. D. and Noll, W., "Foundation of Linear Viscoelasticity," Review of Modern Physics, Vol. 33, No. 2, 1961, pp 239-249.

102. Fredrickson, A. G., Principles and Applications of Rheology, Prentice Hall, 1964.

103. Fredrickson, A. G., "On Stress-Relaxing Solids - I," Chem. Eng. Sci., Vol. 17, 1962, pp 155-166.

104. Lodge, A. S., Elastic Liquids, Academic Press, 1964.

105. Rivlin, R. S., "The Fundamental Equations of Nonlinear Continuum Mechanics," Dynamics of Fluids and Plasmas, Ed. Pai, S. I., Academic Press, 1966.

106. Lee, E. H. and Rogers, T. G., "Solution of Viscoelastic Stress Analysis Problems Using Measured Creep or Relaxation Functions," J. Appl. Mech., Vol. 30, 1963.

107. Muki, R. and Sternberg, E., "On Transient Thermal Stresses in Viscoelastic Materials with Temperature Dependent Properties," J. Appl. Mech., Vol. 29, 1961.

108. Haisler, W. E., Stricklin, J. A. and Stebbins, F. J., "Development and Evaluation of Solution Procedures for Geometrically Nonlinear Structural Analysis by the Direct Stiffness Method," AIAA-ASME 12th Structures, Structural Dynamics, and Materials Conference, Anaheim, California, April 19-21, 1971.

109. Hofmeister, L. D., Greenbaum, G. A. and Evensen, D. A., "Large Strain, Elasto-Plastic Finite Element Analysis," J. Appl. Mech., Vol. 9, No. 7, July 1971, pp 1248-1254.

110. Yeh, C. H., "Large Deflection Dynamic Analysis of Thin Shells Using the Finite Element Method," Ph.D. Dissertation, University of California, Berkeley, Report No. SESM 70-18, Oct. 1970.

111. Jones, L. and Wilson, E. L., Private communication, June 1971.

112. Bergan, P. G., "Nonlinear Analysis of Plates Considering Geometric and Material Effects," Ph.D. Dissertation, University of California, Berkeley, 1971.

113. Timoshenko, S. P. and Gere, J. M., Theory of Elastic Stability, 2nd Edition, McGraw Hill, 1961.

114. Sharifi, P., "Nonlinear Analysis of Sandwich Structures," Ph.D. Dissertation, University of California, Berkeley, 1970.

115. Wissmann, J. M., "Nonlinear Structural Analysis, Tensor Formulation," Proc. 1st Conf. on Matrix Methods in Struct. Mech., AFFDL-TR-66-80, 1966, pp 679-696.

116. Prager, W. and Hodge, P. G., Theory of Perfectly Plastic Solids, Dover, 1968.

117. Timoshenko, S. and Woinowsky-Krieger, S., Theory of Plates and Shells, 2nd Edition, McGraw-Hill, 1959.

118. Turner, M. J., Clough, R. W., Martin, H. C. and Topp, L. J., "Stiffness and Deflection Analysis of Complex Structures," J. Aero. Sci., No. 9, 1956.

119. De Arantes e Oliviera, E. R., "Mathematical Foundation of the Finite Element Method," Lab. Nacional de Engenharia Civil, Lisbon, 1967.

120. Felippa, C. A. and Clough, R. W., "The Finite Element Method in Solid Mechanics," AMS Symposium on Numerical Solution of Field Problems in Continuum Mech., Durham, N.C., 1968.

121. Mikhlin, S. G., Variational Methods in Mathematical Physics, Macmillan Co., 1964.

122. Ciarlet, P. G., Schultz, M. H. and Varga, R. S., "Numerical Methods of High-Order Accuracy for Nonlinear Boundary Value Problems," Numerische Mathematik, No. 9, 1967.

123. Willam, K., "Finite Element Analysis of Cellular Structures," Ph.D. Dissertation, University of California, Berkeley, 1969.

124. Ergatoudis, I., Irons, B. M. and Zienkiewicz, O. C., "Curved, Isoparametric, Quadrilateral Elements for Finite Element Analysis," Int. J. Solids Structures, Vol. 4, 1968.

125. Zienkiewicz, O. C., Irons, B. M., Ergatoudis, I., Ahmad, S. and Scott, F. C., "Iso-parametric and Associated Element Families for Two- and Three-Dimensional Analysis," Finite Element Methods in Stress Analysis, Ed. Holand, I. and Bell, K., Tapir, Theim, Norway, 1969.

126. Larsen, P. K. and Popov, E. P., "Elastic-Plastic Analysis of Axisymmetric Solids Using Isoparametric Finite Elements," Report No. UCSESM 71-2, University of California, Berkeley, 1971.

127. Wilson, E. L., "SAP, A General Structural Analysis Program," Report No. UCSESM 70-20, University of California, Berkeley, 1970.

128. Ahmad, S., Irons, B. M. and Zienkievicz, O. C., "Curved Thick Shell and Membrane Elements with Particular Reference to Axisymmetric Problems," Proc. 2nd Conf. on Matrix Meth. in Struct. Mech., AFFDL-TR-68-150, 1968, pp 539-572.

129. Pawsey, S. F., "The Analysis of Moderately Thick to Thin Shells by the Finite Element Method," Report No. UCSESM 70-12, University of California, Berkeley, 1970.

130. Zienkiewicz, O. C., Taylor, R. L. and Too, J. M., "Reduced Integration Technique in General Analysis of Plates and Shells," Int. J. Num. Meth. Eng., Vol. 3, 1971, pp 275-290.

131. Hildebrand, F. B., Reissner, E. and Thomas, G. B., "Notes on the Foundations of the Theory of Small Displacements of Orthotropic Shells," NACA-TN-1833, 1949.

132. Kalnins, A. and Lestingi, J. F., "On Nonlinear Analysis of Elastic Shells of Revolution," J. Appl. Mech., March 1967, pp 59-64.

133. Kornishin, H. S. and Isanbaeva, F. S., Flexible Plates and Panels, Nauka, Moscow, 1968 (In Russian).

134. Weinitschke, H., "On the Nonlinear Theory of Shallow Spherical Shells," SIAM, Vol. 6, No. 3, Sept. 1958, pp 209-232.

135. Weinitschke, H., "On Asymmetric Buckling of Shallow Spherical Shells," J. Math. and Phys., Vol. 44, No. 2, June 1965, pp 141-163.

136. Encyclopedia of Modern Plastics, 1970.

137. Hildebrand, F. B., Introduction to Numerical Analysis, McGraw-Hill, 1956, pp 378-382.

138. Stachiw, J. D. and Brier, F. W., "Windows for External or Internal Hydrostatic Pressure Vessels - Part III," Tech. Report R-631, U.S. Naval Civil Engineering Laboratory, Port Hueneme, California.

APPENDIX A - INTERPOLATION POLYNOMIALS

The following interpolation polynomials and nodal point coordinates were used:

Linear element:

Nodal points $(-1, +1)$

$$\varphi_1(\xi) = \tfrac{1}{2}(1-\xi)$$

$$\varphi_2(\xi) = \tfrac{1}{2}(1+\xi)$$

Quadratic element:

Nodal points $(-1, 0, +1)$

$$\varphi_1(\xi) = \tfrac{1}{2}\xi(1-\xi)$$

$$\varphi_2(\xi) = (1-\xi)$$

$$\varphi_3(\xi) = \tfrac{1}{2}\xi(1+\xi)$$

Cubic element:

Nodal points $(-1, -\tfrac{1}{3}, +\tfrac{1}{3}, +1)$

$$\varphi_1(\xi) = \tfrac{1}{16}(1-\xi)(-1+9\xi^2)$$

$$\varphi_2(\xi) = \tfrac{9}{16}(1-3\xi)(1-\xi^2)$$

$$\varphi_3(\xi) = \tfrac{9}{16}(1+3\xi)(1-\xi^2)$$

$$\varphi_4(\xi) = \tfrac{1}{16}(1+\xi)(-1+9\xi^2)$$

Quartic element:

Nodal points $(-1, -\tfrac{1}{2}, 0, +\tfrac{1}{2}, +1)$

$$\varphi_1(\xi) = \tfrac{1}{6}\xi(1-\xi)(1-4\xi^2)$$

$$\varphi_2(\xi) = -\tfrac{4}{3}\xi(1-2\xi)(1-\xi^2)$$

$$\varphi_3(\xi) = 1-\xi^2(5-4\xi^2)$$

$$\varphi_4(\xi) = \tfrac{4}{3}\xi(1+2\xi)(1-\xi^2)$$

$$\varphi_5(\xi) = \tfrac{1}{6}\xi(1+\xi)(1-4\xi^2)$$

APPENDIX B - DERIVATION OF DISPLACEMENT GRADIENTS

The equations defining the geometry and assumed displacement field for the degenerate isoparametric elements are given by

$$\begin{Bmatrix} r \\ z \end{Bmatrix} = \sum_{i=1}^{N} \varphi_i(\xi) \begin{Bmatrix} r_i \\ z_i \end{Bmatrix} + \eta \sum_{i=1}^{N} \tfrac{1}{2} \varphi_i(\xi) h_i \begin{Bmatrix} \cos\theta_i \\ \sin\theta_i \end{Bmatrix} \tag{6.4}$$

and

$$\begin{Bmatrix} u \\ w \end{Bmatrix} = \sum_{i=1}^{N} \varphi_i(\xi) \begin{Bmatrix} u_i \\ w_i \end{Bmatrix} + \eta \sum_{i=1}^{N} \tfrac{1}{2} \varphi_i(\xi) h_i \begin{Bmatrix} -\sin\theta_i \\ \cos\theta_i \end{Bmatrix} \alpha_i \tag{6.5}$$

Equations (6.4) and (6.5) are given in terms of the local natural coordinates ξ, η . Before the global displacement gradients can be computed the chain rule differentiation has to be used to give

$$\begin{Bmatrix} \frac{\partial}{\partial r} \\ \frac{\partial}{\partial z} \end{Bmatrix} = \frac{1}{\det J} [J] \begin{Bmatrix} \frac{\partial}{\partial \xi} \\ \frac{\partial}{\partial \eta} \end{Bmatrix} \tag{B.1}$$

where [J] is the Jacobian of transformation (6.4) and is given by

$$[J] = \begin{bmatrix} \frac{\partial z}{\partial \eta} & -\frac{\partial z}{\partial \xi} \\ -\frac{\partial r}{\partial \eta} & \frac{\partial r}{\partial \xi} \end{bmatrix} \tag{B.2}$$

and

$$|J| = \det J = \frac{\partial z}{\partial \eta} \frac{\partial r}{\partial \xi} - \frac{\partial z}{\partial \xi} \frac{\partial r}{\partial \eta} \tag{B.3}$$

Combining Eqs. (6.4), (6.5), (B.1) and (B.2) one gets

$$|J| = \left(\varphi_{i,\xi} r_i + \tfrac{1}{2}\eta \varphi_{i,\xi} h_i \cos\theta_i\right) \tfrac{1}{2} \varphi_j h_j \sin\theta_j -$$
$$- \left(\varphi_{i,\xi} z_i + \tfrac{1}{2}\eta \varphi_{i,\xi} h_i \sin\theta_i\right) \tfrac{1}{2} \varphi_j h_j \cos\theta_j$$

Let

$$P_{ij} = \tfrac{1}{2} \varphi_{i,\xi} \varphi_j \tag{B.4}$$

$$|J| = P_{ij}\left(h_j\left(r_i \sin\theta_j - z_i \cos\theta_j\right) + \eta \tfrac{1}{2} h_i h_j \left(\sin\theta_j \cos\theta_i - \sin\theta_i \cos\theta_j\right)\right)$$

Define

$$J_1(\xi) = P_{ij} h_j \left(r_i \sin\theta_j - z_i \cos\theta_j\right)$$

$$J_2(\xi) = P_{ij} \tfrac{1}{2} h_i h_j \left(\sin\theta_j \cos\theta_i - \sin\theta_i \cos\theta_j\right)$$

The determinant [J] can now be decomposed in one term that is independent of η and one that depends on η .

$$|J| = J_1(\xi) + \eta J_2(\xi) \tag{B.5}$$

Introduce the following notation

$$\begin{aligned}
\{PS\} &= P_{ij} h_j \sin\theta_j \\
\{PC\} &= P_{ij} h_j \cos\theta_j \\
\langle SP\rangle &= P_{ij} h_i \sin\theta_i \\
\langle CP\rangle &= P_{ij} h_i \cos\theta_i \\
\langle RP\rangle &= P_{ij} r_i \\
\langle ZP\rangle &= P_{ij} z_i
\end{aligned} \tag{B.6}$$

This leads to the form

$$J_1(\xi) = \langle r\rangle \{PS\} - \langle z\rangle \{PC\}$$

$$J_2(\xi) = \langle h\cos\theta\rangle \{PS\} - \langle h \sin\theta\rangle \{PC\}$$

The displacement gradients can be derived similarly:

$$\frac{\partial u}{\partial r} = \frac{1}{|J|}\left(\frac{\partial u}{\partial \xi}\frac{\partial z}{\partial \eta} - \frac{\partial u}{\partial \eta}\frac{\partial z}{\partial \xi}\right)$$

$$= \frac{1}{|J|}\left(\tfrac{1}{2}\varphi_j h_j \sin\theta_j \left(\varphi_{i,\xi} u_i - \tfrac{1}{2}\eta \varphi_{i,\xi} h_i \sin\theta_i \alpha_i\right) + \right. \qquad \text{(B.7)}$$

$$\left. + \left(\varphi_{j,\xi} z_j + \tfrac{1}{2}\eta \varphi_{j,\xi} h_j \sin\theta_j\right) \tfrac{1}{2}\varphi_i h_i \sin\theta_i \alpha_i \right)$$

$$\frac{\partial u}{\partial r} = \frac{1}{|J|}\left(\langle u\rangle\{PS\} + \langle EP\rangle\{h\sin\theta\alpha\} + \tfrac{1}{2}\eta\left(\langle SP\rangle\{h\sin\theta\alpha\} - \langle h\sin\theta\alpha\rangle\{PS\}\right)\right)$$

$$\frac{\partial w}{\partial z} = \frac{1}{|J|}\left(\frac{\partial w}{\partial \eta}\frac{\partial r}{\partial \xi} - \frac{\partial w}{\partial \xi}\frac{\partial r}{\partial \eta}\right)$$

$$= \frac{1}{|J|}\left(\tfrac{1}{2}\varphi_i h_i \cos\theta_i \alpha_i \left(\varphi_{j,\xi} r_j + \tfrac{1}{2}\eta \varphi_{j,\xi} h_j \cos\theta_j\right) - \right. \qquad \text{(B.8)}$$

$$\left. - \tfrac{1}{2}\varphi_j h_j \cos\theta_j \left(\varphi_{i,\xi} w_i + \tfrac{1}{2}\eta \varphi_{i,\xi} h_i \cos\theta_i \alpha_i\right)\right)$$

$$\frac{\partial w}{\partial z} = \frac{1}{|J|}\left(-\langle w\rangle\{PC\} + \langle RP\rangle\{h\cos\theta\alpha\} + \eta\left(\langle CP\rangle\{h\cos\theta\alpha\} - \langle h\cos\theta\alpha\rangle\{PC\}\right)\tfrac{1}{2}\right)$$

$$\frac{u}{r} = \frac{1}{r}\left(\varphi_i u_i - \eta \tfrac{1}{2}\varphi_i h_i \sin\theta_i \alpha_i\right) \qquad \text{(B.9)}$$

$$\frac{\partial u}{\partial z} = \frac{1}{|J|}\left(\frac{\partial r}{\partial \xi}\frac{\partial u}{\partial \eta} - \frac{\partial r}{\partial \eta}\frac{\partial u}{\partial \xi}\right)$$

$$= \frac{1}{|J|}\left(-\tfrac{1}{2}\varphi_i h_i \sin\theta_i \alpha_i \left(\varphi_{j,\xi} r_j + \tfrac{1}{2}\eta \varphi_{j,\xi} h_j \cos\theta_j\right) - \right. \qquad \text{(B.10)}$$

$$\left. - \tfrac{1}{2}\varphi_j h_j \cos\theta_j \left(\varphi_{i,\xi} u_i - \tfrac{1}{2}\eta \varphi_{i,\xi} h_i \sin\theta_i \alpha_i\right)\right)$$

$$\frac{\partial u}{\partial z} = \frac{1}{|J|}\left(-\langle u\rangle\{PC\} - \langle RP\rangle\{h\sin\theta\alpha\} - \eta\tfrac{1}{2}\left(\langle CP\rangle\{h\sin\theta\alpha\} - \{h\sin\theta\alpha\}\langle PC\rangle\right)\right)$$

$$\frac{\partial w}{\partial r} = \frac{1}{|J|}\left(\frac{\partial z}{\partial \eta}\frac{\partial w}{\partial \xi} - \frac{\partial z}{\partial \xi}\frac{\partial w}{\partial \eta}\right)$$

$$= \frac{1}{|J|}\Big(\tfrac{1}{2}\varphi_j h_j \sin\theta_j\left(\varphi_{i,\xi} w_i + \tfrac{1}{2}\eta\,\varphi_{i,\xi} h_i \cos\theta_i \alpha_i\right) -$$
$$- \left(\varphi_{j,\xi} z_j + \tfrac{1}{2}\eta\,\varphi_{j,\xi} h_j \sin\theta_j\right)\tfrac{1}{2}\varphi_i h_i \cos\theta_i \alpha_i\Big) \qquad \text{(B.11)}$$

$$\frac{\partial w}{\partial r} = \frac{1}{|J|}\left(\langle w\rangle\{PS\} - \langle zP\rangle\{h\cos\theta\alpha\} + \eta\,\tfrac{1}{2}\left(\langle h\cos\theta\alpha\rangle\{PS\} - \langle SP\rangle\{h\cos\theta\alpha\}\right)\right)$$

Note that

$$|J| = |J(\xi,\eta)|$$

$$r = r(\xi,\eta)$$

Let

$$\frac{\partial u}{\partial r} = \frac{1}{|J|}\left(\langle b_1^*\rangle_1 + \eta\langle b_2^*\rangle_1\right)$$

$$\frac{\partial w}{\partial z} = \frac{1}{|J|}\left(\langle b_1^*\rangle_2 + \eta\langle b_2^*\rangle_2\right)$$

$$\frac{u}{r} = \frac{1}{r}\left(\langle b_1^*\rangle_3 + \eta\langle b_2^*\rangle_3\right) \qquad \text{(B.12)}$$

$$\frac{\partial u}{\partial z} = \frac{1}{|J|}\left(\langle b_1^*\rangle_4 + \eta\langle b_2^*\rangle_4\right)$$

$$\frac{\partial w}{\partial r} = \frac{1}{|J|}\left(\langle b_1^*\rangle_5 + \eta\langle b_2^*\rangle_5\right)$$

Here

$$\underset{(1\times 3N)}{\langle b_1^*\rangle_1} = \langle \{PS\}_1\ 0\ \langle zP\rangle_1 h_1 \sin\theta_1\ \ \{PS\}_2\ 0\ \langle zP\rangle_2 h_2 \sin\theta_2 \cdots\cdots\rangle$$

and

$$\underset{(1\times N)}{\langle b_2^*\rangle_1} = \langle \tfrac{1}{2}\left(\langle SP\rangle_1 - \langle PS\rangle_1\right) h_1 \sin\theta_1\ \ \tfrac{1}{2}\left(\langle SP\rangle_2 - \langle PS\rangle_2\right) h_2 \sin\theta_2 \cdots\cdots\rangle$$

where $\langle b_1^*\rangle_i = (1\times 12)$ and $\langle b_2^*\rangle_i = (1\times 4)$ for the cubic element.

The vectors $\langle b_1^* \rangle_i$ and $\langle b_2^* \rangle_i$, $i \neq 1$ can similarly be determined from Eqs. (B.8 - B.11)

Finally, a simple coordinate transformation from the global (r, z) coordinate system to the local system (ξ, η) yields $\langle b_1 \rangle_i$ and $\langle b_2 \rangle_i$, $i = 1,4$

The displacement gradient matrices $[B_1]$ and $[B_2]$ as defined by Eqs. (6.20) and (6.20a) are then given as

$$[B_1] = \begin{bmatrix} \frac{1}{|J|} & \frac{1}{r} & \frac{1}{|J|} & \frac{1}{|J|} \end{bmatrix} \begin{Bmatrix} \langle b_1 \rangle_1 \\ \langle b_1 \rangle_2 \\ \langle b_1 \rangle_3 \\ \langle b_1 \rangle_4 \end{Bmatrix} \tag{B.13}$$

and

$$[B_2] = \begin{bmatrix} \frac{1}{|J|} & \frac{1}{r} & \frac{1}{|J|} & \frac{1}{|J|} \end{bmatrix} \begin{Bmatrix} \langle b_2 \rangle_1 \\ \langle b_2 \rangle_2 \\ \langle b_2 \rangle_3 \\ \langle b_2 \rangle_4 \end{Bmatrix} \tag{B.14}$$

The dependence on η is here kept as a multiplying factor that is easily included in the numerical integration of Eqs. (6.25) and (6.26). The same procedure is used for the computation of the creep pseudo-loading and for the equilibrium nodal loads.

In the case of the geometric stiffness matrix $[K_G]$ the stress vector $\{s\}$ in Eq. (6.29) must be pre or postmultiplied by the matrix

$$\begin{bmatrix} \frac{1}{|J|^2} & \frac{1}{r^2} & \frac{1}{|J|^2} \end{bmatrix}$$

From this derivation it is quite clear that letting $[J]$ and r vary over the shell thickness does not increase the complexity of the formulation. The additional computational effort is also negligible.